Milestone SPT23MM4:

Completion of Regional Seismic Reflection Profile Reprocessing Part 2: Modeling of Seismic Reflection Profiles from Yucca Mountain

April 3, 1997

WBS 1.2.3.11.2 Surface Geophysics

Principle Investigator - Ernest L. Majer
M. A. Feighner and T. Daley

Earth Sciences Division
Ernest Orlando Lawrence Berkeley National Laboratory
Berkeley, California 94720

9903020129 990223
PDR WASTE
WM-11 PDR

Milestone SPT23MM4:
Completion of Regional Seismic Reflection Profile Reprocessing
Part 2: Modeling of Seismic Reflection Profiles from Yucca Mountain
April 3, 1997

WBS 1.2.3.11.2 Surface Geophysics

Principle Investigator - Ernest L. Majer
M. A. Feighner and T. Daley

Earth Sciences Division
Ernest Orlando Lawrence Berkeley National Laboratory
Berkeley, California 94720

1. INTRODUCTION

During the years 1994 through 1996, a coordinated geophysical effort was made to help address issues related to the characterization of Yucca Mountain as a possible high level nuclear waste repository. The scale and objectives of these studies has varied from detailed small scale studies investigating the suitability of the near surface soils for constructing structures, to investigations of the the deep crust and upper mantle. A summary and combined interpretation of these studies was presented in a synthesis report by Majer et al., (1996). The synthesis report was a compilation and interpretation of the several different types of geophysical data. The vast majority of the data were seismic reflection data. Modeling was performed on gravity and magnetotelluric data, but limited modeling was performed on the seismic data. In addition, the results of the regional seismic lines by Brocher et al., (1996) were mainly interpretive and not based on modeling. Therefore, in an attempt to determine the nature of the varied results from the reflection data, as well as place some confidence intervals on the different interpretations derived from the data sets, a modest modeling effort was undertaken for the repository and regional scale surface seismic profiles. Majer et al. (1996) found that "in general, the geophysical results indicate that the proposed repository volume at Yucca Mountain is a complex overlapping structure of tuffs that vary in physical properties throughout the repository region on a scale not captured in the current geologic model." Because of the variability observed in the surface seismic data sets, even identifying the lithologic units which cause reflections was difficult. The goal of this forward modeling study of surface seismic profiles is to address questions about the variability in seismic reflectivity and the potential of mapping the Paleozoic basement from repository scale surface profiles. To a large degree this modeling effort was in response and related to a review effort of the regional seismic reflection lines. That review (see appendix I) by two independent reviewers, concluded that many of the reflectors, especially over the Yucca Mountain region, may be artifacts of processing and complexity due to the 3-D nature of the structure. Therefore it was desired to model several different structures to determine which, if any, fit the data.

The software used for this study is a commercial package named GX-II produced by GX Technology Corporation. This software is currently not qualified within the Yucca Mountain Project. The field data being modeled, repository lines YMP-3 and YMP-5, are qualified data

and were processed by LBNL with the software package FOCUS-3D which is qualified software. The Regional line 3 data was acquired as qualified data. The processing of Regional line 3 was done by the USGS with the software package ProMAX which is currently not qualified.

2. BACKGROUND

The Yucca Mountain region is typical of many volcanic regions, in that it is very heterogeneous and structurally complex. The general nature of the volcanic stratigraphy (alternating flow properties in vertical and horizontal directions) causes many geophysical anomalies. Faulting further complicates the geophysical signature as does the thick section of partially saturated tuff overlying the area. All of the high resolution reflection seismic surveys in the repository region show a small penetration depth of the seismic signal (several hundred to a thousand meters). Using an accelerated weight drop source, it was typical to only see reflectors within the first hundreds of meters of depth, with reflectivity rarely continuous over a greater lateral distance (Majer et al., 1996). This suggests that 1. inhomogeneities (welding, porosity, lithophysal content, fracture content, faulting, etc.) within the rock formations may be causing variations in travel time and strong attenuation of the seismic signals, or 2. the variability in reflectivity was due to near surface conditions such as poor coupling, noise, severe weathering effects or other factors not related to subsurface conditions. It is important to distinguish between the two effects, if the poor and varied reflectivity is due to subsurface conditions, then the seismic results indicate the nature and location of the heterogeneity.

The complexity observed in the surface reflection profiles from the 1996 synthesis report demonstrated a need for more in-depth modeling; however, this was not possible due to time limitations. In 1997 this study was begun using seismic ray-trace modeling as a tool to further our understanding of how the Yucca Mountain subsurface material properties are expressed in the surface seismic data sets. Our analysis uses forward modeling of the seismic raypaths. Among the specific questions addressed are:

1) Can the reflectivity interpretation used for the repository and regional lines be corroborated by forward modeling using the geologic model and reasonable velocity models?

2) Can a seismic attenuation model explain the weak reflectivity observed on many of the repository lines?

3) What would the seismic signature of a fault zone look like on the repository lines?

4) Can the Paleozoic basement reflector be expected to appear on the repository lines?

5) Can the different interpretations of the Paleozoic basement on the regional lines be corroborated by forward modeling using a reasonable geologic model and reasonable velocity models?

6) Can the steeply dipping coherent events observed on the regional lines be explained?

3. MODELING TECHNIQUE

Ray-tracing analysis begins with the input of a geologic model. The model used for both the repository and regional lines came from the YMP geologic model ISM2.0 (Clayton et al., 1997), using a subset of the identified lithologic horizons. The horizons were chosen because of known variations in velocity or material properties and because of the interpretation of the repository lines (Majer et al., 1996). The repository scale seismic lines were originally interpreted using 4 "marker" horizons which were thought to be key reflectors. These horizons were top of

the Topopah (Tptrv), the region between two reflections from lithophysal zones (Tptpmn) within the Topopah, the crystal poor non-lithophysal vitric zone at the base of the Topopah (Tptpv), and the Prow Pass (Tcp). Each of these horizons is included in the model used here with the exception of Tptrv which is included with the bedded tuffs (Pah Canyon, Yucca Mountain tuffs) to form a relatively thick shallow layer with potential for lateral variability in the model. Additionally, the Paleozoic basement structure estimated from LBNL gravity studies is included in the model.

Each of the selected layers is then assigned material properties, i.e., a seismic velocity and a bulk density. The velocities used for the repository lines (YMP-3 and YMP-5) were taken from VSP data at well UZ-16 from Kaelin and Johnson (1997), as shown in Table 1. (See Appendix II). For the first layer (above Tptrn), the observed stacking velocities from the seismic lines were used: 4000 ft/s for YMP-3 and 6000 ft/s for YMP-5. This was done to better match the moveout observed for the shallowest reflection in the shot gathers. For the deeper portions of the section, namely below the Calico Bedded Tuff, the observed velocity was extrapolated to the basement with a gradient of 0.5 ft/s per foot. The basement was assigned a velocity of 12000 ft/s with a 1 ft/s per foot increase with depth. Comparison tests were done with different velocity structures at depth and were found not to impact the results of the modeling. For REG-3, the velocities from the VSP data from well UE-25 p#1 were used from Brocher et al. (1996), as given in Table 1. The densities used in the modeling were calculated from the P-wave velocities using Gardner's rule, which states that density is proportional to the 1/4 power of the P-wave velocity.

The acquisition geometry of the surface seismic lines is used to define source and receiver locations in the model. We used shot gather geometry to model some of the acquired shot gathers, and we used CDP geometry (normal incidence rays or zero offset rays) to model the CDP stacked sections. For the normal incidence ray or zero offset calculations, the rays were traced from a datum of 5000 feet above sea level with a velocity of 5000 ft/s. This was done to match to observed stacked sections, which also used the same datum. The seismic rays are then traced from the source through the velocity model to the sensors. The rays that arrive at each sensor (including reflected rays) will have an arrival time and a reflection strength. These arrivals define a reflectivity series (also called a 'spike trace') for each sensor. This reflectivity series is convolved with a seismic wavelet to give a wiggle trace display of reflectivity which is band limited and approximates the frequency content of the acquired data. For the modeled shot gathers, a bandpass filter of 6-125 Hertz was used, and for the zero offset rays, a bandpass filter of 6-60 Hertz was used. Additional models were run using random noise to simulate the background noise of field acquisition and using seismic attenuation (Q) models to simulate the affect of scattering and intrinsic attenuation in the field data and using lateral velocity variations to simulate the effect of varying rock properties such as density.

Since no true amplitude processing was done with the original seismic data, none is attempted here. All figures showing the amplitudes of the traces (the blue and red traces) have had an AGC applied with a window of 400 ms. This corresponds with the plots of the observed seismic data, which also have had the same AGC window applied.

It is important to point out that the ray tracing technique used here uses an equivalent media approach. This approach is used widely in the geotechnical and the oil and gas industry. It assumes that the details of the media can be approximated with "equivalent" properties. More advanced theories such as fracture effects and anisotropy are not included in this approach.

4. SIMPLE MODELS OF REPOSITORY SEISMIC LINES YMP-5 AND YMP-3

A. Zero Offset YMP-5 Modeling

The seismic line YMP-5 is a north-south profile located on the ridge of Yucca Mountain (Figure 1). The geologic model for YMP-5 is shown in Figure 2. While the shallow horizons are all from the ISM2.0 geologic model, the Paleozoic basement is taken from gravity modeling done by LBNL (Majer et al., 1996 synthesis report). The velocity model used for YMP-5 is shown in Figure 3 and Table 1. Note that the lower two layers have a linear velocity gradient (i.e., the velocity increases linearly as a function of increasing depth). These layers were assigned a gradient because of their large thickness compared to the shallow layers.

The seismic rays from a zero offset (CDP) geometry were calculated for this velocity model and they are shown in Figure 4. While the shallow layer rays are too densely spaced to be seen in this figure, the Paleozoic basement does show a gap in ray coverage. This gap, approximately between stations 380 and 400, demonstrates that for the YMP-5 location and the proposed basement structure there will be gaps in the Paleozoic reflection image. Figure 5 shows the seismograms calculated from the zero offset rays. The shallow reflections, color coded to match the geologic section, are all continuous across line YMP-5. The basement reflector, colored orange, shows a complex structure with triplications of arrivals. The basement reflections displayed in this zero offset model do not correctly image the input structure. A migration would be needed to restore the correct image, and this would still have gaps from the missing ray coverage. The seismograms shown in Figure 5 have had automatic gain control (AGC) applied, thereby removing relative amplitude information, and the arrivals have been color coded according to the geologic horizon. These two display techniques combine to make reflector identification easy, however the relative amplitude of each reflection is obscured. When displayed without the color coding and wiggle traces, the modeled basement reflector is seen to be very weak (Figure 6). These weak signals are still visible because this numerical model has no noise.

In Figure 7 random noise is added to simulate the natural background noise in field data. The random noise is 36 dB below the maximum signal (a signal-to-noise ratio of 64). At this noise level the basement reflector is no longer visible and even the Calico reflector is partially obscured by noise. The shallow reflectors do have observable and laterally continuous reflections. The amplitude plus noise model of Figure 7 can be compared to the recorded field section of YMP-5 shown in Figure 8. It is apparent that the model is still not capturing the complex structure and variable reflectivity observed in the field data.

B. Zero Offset YMP-3 Modeling

Seismic reflection line YMP-3 is an east-west profile which crosses the Ghost Dance Fault zone and the Imbricate Fault Zone. The east-west orientation gives YMP-3 a different character than YMP-5 since most of the structure(faulting and fracturing) in this area is north-south trending. Figure 9 shows the current geologic model, along with the Paleozoic basement structure estimated from LBNL's gravity modeling. The velocity model used for YMP-3 (Figure 10 and Table 1) is taken from the UZ-16 VSP survey, with a linear gradient used for the 2 deepest formations. The velocities range from 4000 to 15000 ft/s.

Figure 11 shows the zero-offset ray tracing results. While the shallow layers are somewhat obscured by the density of rays, the basement horizon shows a very scattered sampling of the interface. The seismograms generated from these rays (Figure 12) confirm that the Paleozoic

basement is sparsely sampled with the geometry of YMP-3. The shallow reflections do have good sampling across the profile. There are notable fault plane reflections with parabolic moveout from the Imbricate Fault Zone and, to a lesser extent, from the Ghost Dance Fault. An AGC amplitude display of the modeled seismograms without the color reflection identification and wiggle traces (Figure 13) shows that the fault plane reflections are very weak arrivals as are the Paleozoic basement reflections. Figure 14 shows the YMP-3 model results with added noise for comparison to the field data YMP-3 section (Figure 15). The model results have much greater lateral continuity than the field results. As with line YMP-5, a simple model of laterally consistent velocity and attenuation does not capture the variability seen in the field data, even when significant random noise is added.

5. ADDING COMPLEXITY - MODELING SPATIALLY VARYING ATTENUATION AND VELOCITY

A. Spatially Varying Attenuation Within a Layer (YMP-5) Zero Offset and Shot Gather

Because the relatively simple models described above did not capture the variability in reflectivity observed in the field data, we investigated the effects of adding lateral complexity. Our next step in modeling was the addition of an attenuating zone. We observed a lack of reflectivity on YMP-5 approximately between stations 503 and 700 on Figure 8. Figure 16 shows the geologic model surfaces along with the location of an attenuating zone between stations 320 and 460. This zone was assigned a seismic Q of 10. This is a relatively high level of seismic attenuation because we believe the apparent attenuation is a combination of scattering and intrinsic attenuation. Figure 17 shows the calculated zero offset amplitudes for the attenuation zone model of YMP-5. We observe a reduction in amplitude and frequency content and an apparent time delay within the attenuation zone. The addition of random noise, shown in Figure 18, demonstrates that at this level of attenuation the shallow reflectivity becomes nearly lost in the background noise. This gap in reflectivity is similar to the field data. A laterally variable attenuation model would be necessary to more closely match the field data.

To further study the effects of an attenuation zone, a common shot gather with source on the edge of the attenuation zone was modeled. This shot gather model has half the rays in the attenuation zone and half outside. The seismic rays for this shot (number 562) are shown in Figure 19. The seismograms for the modeled shot 562 are shown in Figure 20. The time delay and lowered frequency content are apparent in the attenuation zone (right side). A true amplitude display of this shot gather is shown in Figure 21, and Figure 22 shows the same data with the addition of random noise. The attenuated (right side) and nonattenuated (left side) modeled shot can be compared to a field recording of shot 562 from YMP-5 shown in Figure 23. The frequency content of the attenuated model is closer to the field data. Also the steeply dipping low frequency event seen in the field data is similar to an event seen in the attenuated model shot gather. These attenuation results encourage our belief that some of the character of the field data is caused by laterally varying attenuation.

B. Spatially Varying Velocity Within a Layer (YMP-5) Zero Offset

The next parameter to investigate for lateral variation is velocity. In Figure 24 we show a velocity model for YMP-5 which includes a sinusoidal lateral variation of the top layer velocity between the distances of 5000 and 10000 feet. The velocity was allowed a minimum/maximum variation of 25% of the previous constant velocity. The reflectivity generated from this model is

shown in Figure 25. The effect of the high velocity region is partially obscured by the down dip and thickening of the second layer. We do see a weakening of the second layer reflector since the high velocity in the first layer can nearly match the velocity of the second layer thereby reducing the reflection coefficient. The low velocity region shows a strong effect of down warping the entire section. In Figure 26 random noise is added for comparison to the field data (Figure 8). The modeled low velocity region is similar in appearance to the region near CDP 803 in the field data. It does appear that laterally varying velocities are a factor in the field data.

C. Spatially Varying Attenuation and Velocity Within a Layer (YMP-5) Zero Offset

In an attempt better match physical rock properties, we combined the attenuation and velocity variations. Because high attenuation is generally associated with lower velocities, we assigned the Q=10 zone to the low velocity region of YMP-5 shown in Figure 24. The result from this combined model is shown in Figure 27 and, after adding random noise, in Figure 28. In Figure 28 the low velocity/high attenuation zone (between traces 201 and 260) has attributes similar to those seen in the field data sets. The sequence of reflections between 200 and 400 ms is obscured and only the strong center reflector appears continuous. Even the apparent continuity is an artifact of the time shift aligning different reflectors with similar wavelets, as can be seen by comparing Figures 27 and 28. This result highlights the problems of seismic interpretation in heterogeneous, laterally varying materials.

D. Attenuation Near The Ghost Dance Fault (YMP-3) Shot Gather

To model the effects of a high attenuation zone near a fault, the region around the Ghost Dance Fault was chosen along YMP-3 (Figure 1). The attenuation model is shown in Figure 29 and consists of a high attenuation zone (Q=10) that is 300 feet wide and about 600 feet deep, extending from the surface to the top of Tptpmn. Figure 30 shows the results of the ray tracing of a shot gather with the indicated shot location. This location was chosen to show the difference in character between the two sides of a split shot gather, with the west side containing the fault. Figure 31a shows the color coded arrivals, showing the offsets in the reflectors across the fault. The amplitudes of the reflectors are first shown with no attenuation (Figure 31b) and with attenuation (Figure 31c). The effect of the fault is to disrupt the coherency of the reflectors and the additional effect of the attenuation is to increase this disruption even more and to decrease the frequency content of the reflectors. With the addition of random noise to these two plots (Figure 32a - no attenuation; Figure 32b - attenuation), most of the reflectors on the western half of the split spread have vanished, except for the shallowest event, Tptrn. These may be compared to the observed shot gather given in Figure 33 or the observed stacked section in Figure 15.

6. REGIONAL SEISMIC LINE REG-3

Surface seismic line REG-3 was designed and acquired to image deep regional seismic reflectors, including the Paleozoic basement. The line was roughly east-west crossing Jackass Flats and Yucca Mountain. The results were originally reported in Brocher et al., (1996) and further interpretation was reported in Majer et al., (1996). The interpreted structure of the Paleozoic basement differed in the two reports, and one objective of this modeling is to examine the expected seismograms from each of these interpretations, referred to as the USGS model and LBNL model. Only the portion of REG-3 that lies within the geologic framework model was used. This includes most of the line to CDP 983, so only a small portion of the eastern part of this line is not modeled.

Figure 34 shows the geologic model for REG-3 using the Paleozoic interface from Brocher et al. (1996). Velocities were assigned to this model using results from a VSP in well UE-25 p#1 (Table 1). Figure 35 shows the raypaths for this model. We see in Figure 35 that there is good coverage of the Paleozoic interface, and that there are numerous fault plane reflections including the curved rays near the bottom of the model. Figure 36 shows the color coded identified reflections. The steeply dipping fault plane reflections are apparent. The necessity of migration is also apparent from this model. Of course any migration is very dependent on a-priori knowledge of the true velocity structure including lateral variations. Figure 37 shows the modeled reflections without color coding and wiggle traces.

In Figure 37 we see that the Paleozoic reflector is much more disrupted than the shallower reflectors, due to the sharp offsets in the basement. Figure 38 shows the REG-3 model with random noise added and it can be compared to the field data for REG-3 shown in Figure 39. The Prow Pass reflection appears to correlate with energy on the observed section and the basement generally agrees in the central portion of the line.

Figure 40 shows the geologic model for REG-3 using the Paleozoic interface from Majer et al. (1996). The velocity model is the same as given in Table 1. The raypaths for this model are shown in Figure 41. We can see some deep turning rays from the Prow Pass and the Bullfrog Formations and what appears to be good ray coverage of the Paleozoic interface. The reflections from these rays are shown in Figure 42. Comparing Figures 42 and 36, we see a more complete sampling of the Paleozoic interface in the LBNL model, due to the smoother basement structure. Figure 43, showing the reflections without color coding and wiggle traces, can be compared to Figure 37, again demonstrating a more continuous sampling of the Paleozoic interface in the LBNL model. Figure 44 shows the REG-3 amplitudes with random noise added. Figures 38 and 44 can be compared to Figure 39, the field data from REG-3. The modeled Prow Pass reflector shows fairly good agreement with the field data. It does appear that a reflection at about 1.7 s between CDP's 400 and 700 may be a high in the Paleozoic basement consistent with both USGS and LBNL models.

The observed time section shows strong steeply dipping (down to the east) energy between CDP's 200 and 400 which is not represented by either the USGS or LBNL model. However, this energy does look similar to the steeply dipping fault plane reflections caused by offsets of the Prow Pass and Bullfrog formations, and therefore could be fault planes not present in the geologic model.

7. SUMMARY/CONCLUSIONS

This modest attempt at forward modeling of the Yucca Mountain seismic reflection profiles has been very useful. The simplest models (based on the geologic model of horizontally continuous units) do not capture the lateral variations seen in the seismic data. Addition of random noise can obscure some reflections but it does not change the general appearance of lateral homogeneity. This implies that background noise in the field data is not the main cause of reflectivity variability. The laterally varying attenuation model was able to emulate the field data observation of "gaps" in reflectivity. The combination of laterally varying attenuation and velocity was able to emulate the vertical variability (in time or depth) of many reflections seen in the repository lines.

The variability in shot gathers caused by spatial attenuation variation could explain the difficulty in CDP stacking and velocity analysis observed by Majer et al., (1996). Our ability to

image the Paleozoic basement from the repository scale lines appears quite limited by the geometry (depth of interface, dip of interface, length of surface lines and shot gathers) and by the signal-to-noise ratio of the energy returned from the basement.

To answer the questions specifically posed in section 2:

1) The reflectivity interpretation in Majer et al., (1996), i.e., that changes in reflectivity are due to varying physical properties of the tuffs, is generally corroborated by the modeling of YMP-5 and YMP-3. More accurate modeling would require detailed spatial velocity and attenuation information for each of the repository lines.

2) A seismic attenuation model can explain the gaps in reflectivity observed on the repository lines. Regions of high seismic attenuation may be areas of intense fracturing or high lithophysal zones.

3) The seismic signature of a fault would have weak fault zone reflections and offset of reflectors, both of which could be enhanced by laterally varying attenuation or velocity.

4) The Paleozoic reflector would be quite difficult to observe on the repository lines, based on the modeling of YMP-5 and YMP-3, because of both geometry and signal-to-noise problems.

5) It is still difficult to corroborate an interpretation of the Paleozoic reflection on regional line REG-3. It does appear that an observed reflection at about 1.7 s between CDP's 400 and 700 may be a high in the Paleozoic basement. Both models of the basement dip to the west beneath Yucca Mountain, resulting in a loss of reflected energy on the western portion of the regional line.

6) The steeply dipping events observed on the western part of the regional seismic line may be fault plane reflections from horizons above the basement. Our modeling did not reproduce fault plane reflections in this region, but this may be due to fault planes which are not represented in the geologic model. These events could also be out-of-plane reflections which we cannot model with this software.

The overall results from surface seismic lines were varied. On some lines we were able to image structure within the Tiva Canyon tuff and the Topopah Spring tuff better than any previous seismic studies in the Yucca Mountain area, and better that most of the previous studies in unsaturated volcanic regimes. On other lines we had little seismic reflectivity. Most of the lines demonstrated both of these extremes, with some good reflectors alternating with zones of no reflectivity.

From the modeling effort we have more evidence to believe that the variation in seismic reflectivity is, in large part, due to variation in rock properties. We have demonstrated that porosity can be a controlling factor for seismic velocity and reflectivity in the rock units being studied (Appendix II). Other properties, such as fracture density and fracture stiffness, lithophysal size and distribution, and degree of welding in vitric zones, may be important factors in seismic reflectivity.

We believe that the seismic profiles are mapping these material property variations in the subsurface; however, we can not yet say which property or what depth of interface is controlling each line. Where we have well control, we do see variability in material properties, and we have displayed calculated porosity logs with our interpreted seismic sections. We see large variations in porosity, for example between wells H-3 and H-5 on line YMP-5, where the porosity of the Tpcpv-Tptrv transitions is quite different. Since the interpreted seismic reflectors are bounding thermo-mechanical units, it seems likely that variability in thermo-mechanical units is being

mapped be seismic reflectivity variability.

In the repository region no reflections were identified as a Paleozoic interface on the high resolution lines. As implied in the discussion of the sensitivity of the reflection methods in this area, this is probably due to the combination of the small amount of energy penetrating to depth (high attenuation of the tuffs), and a smaller than expected contrast in the acoustic impedances between the Paleozoic rocks and the overlying tuffs. This would be particularly true in deeper sections where significant compaction has occurred. In the repository region the attenuation is severe, thus making it very difficult for energy to penetrate to depth. Even on the regional lines the highly attenuative properties over Yucca Mountain may be producing artifacts in the data which have been misinterpreted as basement reflectors.

The software used for this study is a commercial package named GX-II produced by GX Technology Corporation. This software is currently not qualified within the Yucca Mountain Project. The field data being modeled, repository lines YMP-3 and YMP-5, are qualified data and were processed by LBNL with the software package FOCUS-3D which is qualified software. The Regional line 3 data was acquired as qualified data. The processing of Regional line 3 was done by the USGS with the software package ProMAX which is currently not qualified.

ACKNOWLEDGEMENTS

This work was supported by the Director, Office of Civilian Radioactive Waste Management, U.S. Department of Energy, through Memorandum Purchase Order EA9013MC5X between TRW Environmental Safety Systems, Inc. and the Ernest Orlando Lawrence Berkeley National Laboratory, under Contract No. DE-AC03-76SF00098. We would like to thank David Okaya and James Rector for their review comments on the regional seismic lines. We would also like to thank Bruno Kaelin for his calculations of the reflectivity. The computations would not have been possible without the continued support of Berkeley Lab's Center for Computational Seismology Center by the Department of Energy's Office of Energy Research Basic Energy Sciences Geoscience Program.

9. REFERENCES

Brocher, T.M., P.E. Hart, W.C. Hunter, and V.E. Langenheim, Hybrid-Source seismic reflection profiling across Yucca Mountain, Nevada: Regional lines 2 and 3, USGS-OFR-96-28, 110 pp., USGS Denver, CO, 1996, DTN: GS960108314211.002 (Q), ACCN:MOL.19970310.0094.

Clayton, R.W., W.P. Zelinski, and C.A. Rautman, ISM2.0: A 3D Geologic Framework and Integrated Site Model of Yucca Mountain, CRWMS M&O, 1997, Document Identifier B00000000-01717-5700-00004, ACCN:MOL.19970122.0053.

Kaelin, B. and L.R. Johnson, Seismic rock properties of partially water saturated tuffs in the Yucca Mountain region derived from well logs and VSP data, submitted, Geophysics, 1997.

Majer, E.L., M. Feighner, L. Johnson, T. Daley, E. Karageorgi, K. H. Lee, K. Williams, and T. McEvilly, 1996, Synthesis of Borehole and Surface Geophysical Studies at Yucca Mountain, Nevada and Vicinity Volume I: Surface Geophysics, Yucca Mountain Project Milestone OB05M, Lawrence Berkeley National Laboratory, Berkeley, CA, 1996, DTN: LB960808314212.001 (Q), LB960808314212.002 (Q), LB960808314212.003 (Q), LB960808314212.004 (Q), ACCN: MOL.19970114.0137.

Appendix I.
Summary of Review Comments of Yucca Mountain Seismic Profiles REG-2 and REG-3.

SUMMARY

A review was made of USGS OFR 96-28 (Brocher et al, 1996) with special focus on the portions of the seismic reflection profiles which cross Yucca Mountain. An attempt was made to identify what types of further efforts should or could be conducted involving these seismic reflection data as well as the level of confidence to be placed on the results of the current processing. The conclusions were:

(A) the original study by the USGS team was conducted in a thorough and scientifically sound manner and the overall interpretations are reasonable;
(B) on a local scale there are a few interpretations which are at the limit of the data and thus other interpretations are allowable;
(C) the seismic data itself are not of high quality and as such there are few new efforts that can be performed beyond what the original team had already conducted.

INTRODUCTION

The reviewers examined the seismic reflection data used in the USGS study as reported in USGS OFR 96-28 ("Hybrid-source seismic reflection profiling across Yucca Mountain, Nevada: regional lines 2 and 3"; Brocher et al, 1996) with attention focussed on the seismic evidence for structures beneath Yucca Mountain. A review of the OFR report indicates that the original study was comprehensive and quite sound. The USGS scientists involved in the study are well-regarded by their peers in the scientific community. The field effort to collect the seismic data was also thorough as is expressed in the types of in-field tests early in the acquisition procedure. The subsequent analysis and integration with other geophysical and geological data was also performed at a high level of proficiency.

USGS INTERPRETATION OF WEST-DIPPING FAULTS UNDER YUCCA MOUNTAIN (REG-2/3)

The USGS interprets west-dipping faults beneath Yucca Mountain which cut the inferred Paleozoic-Tertiary contact. This interpretation is not clear-cut in the seismic profiles. To test this interpretation, the USGS team performed gravity modeling of the Yucca Mountain subsurface with and without these faults. The overall gravity fit along seismic profiles REG-2 and REG-3 is excellent. The wide isostatic gravity low between Steve's Pass and Fortymile Wash indicate an asymmetric basin similar to those present elsewhere in the Basin and Range province. As documented in Figures 19 and 21 of the USGS OFR 96-28, the presense of the west-dipping faults under Yucca Mountain has little expression in the modeled gravity calculations. In essence, the gravity anomaly technique does not have sufficient resolution to detect the presense of faults which have such little offset at the observed depths. Either model presented in these two figures is permissible based on the gravity data and the seismic data.

LINE REG-3 REFLECTION STRUCTURES: INFERRED PALEOZOIC-TERTIARY BOUNDARY

An examination of the Final Stack version of REG-3 suggests an overall trend of eastward-dipping subsurface structures in the upper 2.0 sec of seismic travel-time. These reflections are interpreted by the USGS to be the inferred Paleozoic-Tertiary boundary. Existing geological studies need to be examined to see if these subsurface structures should be deepening under Jackass Flats or should remain sub-horizontal. Due to the use of a seismic floating datum, this eastward dip may be a processing artifact; the Migration Depth Section has almost no noticeable eastward dip. The gravity modeling has produced a good fit using subsurface structures which are largely horizontal and with little eastward dip.

The possible existence of dipping reflections suggested to the reviewer that the original unprocessed seismic field data needed to be examined. In the field data, reflections from dipping horizons will have a different signature than those from horizontal horizons. In a "shot gather", a reflection from a horizontal feature is hyperbolic in "time-offset" with its apex at a source-receiver offset of zero. A reflection from a dipping feature will also be hyperbolic, but its apex will be at a non-zero source-receiver offset located in the updip direction. This difference in apex location is one of the easiest ways to identify if a reflection's horizon is dipping.

The unprocessed Yucca Mountain seismic field data have the following characteristics. The overall data quality is not high. This lack of quality is more likely due to characteristics of the earth rather than to field procedures. Reflections which are known to exist in the Final Stack are not distinct laterally-continuous hyperbolic events in the unprocessed shot gathers but rather are laterally discontinuous. The first arrival refraction which is often a laterally continuous feature is also choppy and broken. These behaviors indicate several shallow geological conditions which are not amenable for seismic reflection acquisition: rapid changes in local elevation, lateral heterogeneity in the acoustic properties of the near surface, and the presense of geological features which act to disrupt or scatter seismic waves. These conditions will alter the seismic propagation sufficiently to degrade the quality of seismic reflections.

Because the near-surface conditions described above affect the quality of the seismic reflections, the subsequent seismic data processing and analysis are made more difficult. Since in the raw data the reflections of the inferred Paleozoic-Tertiary contact are disrupted and choppy, their appearance in the Final Stack is similar. There are few additional computer processing enhancement methods that could improve this.

In addition, this laterally discontinuous, choppy behavior is characteristic of all of the raw seismic data, not just for the raw reflections of the inferred Paleozoic-Tertiary boundary. This behavior is thus also present in both processed seismic profiles. In principle, individual reflections from subhorizontal features should normally be sufficiently laterally continuous to make it difficult for an interpreter to draw a fault through it. As such, it is the termination of a continuous reflection which makes an interpreter suspect the feature is terminated by a fault. As examples, textbook regions of high data quality where confidence in an interpretation can be extremely high are the Permian basin of west Texas or the offshore Gulf of Mexico. However, seismic data whose reflection character is inherently laterally discontinuous and choppy is more difficult to interpret. An interpreter must determine if the lateral terminations of reflections are due to faulting or is just part of the inherent character. In data where the choppy character of the data is strong, the ability to positively identify the presense of faults is difficult and the confidence factor which one may place on the interpretation decreases. Due to the choppy character

of the REG-2/3 seismic data, the identification of faults in these profiles is not easy and the confidence that one may place on any interpretation cannot be high.

Examples of this can be found in the USGS interpretation of the inferred Paleozoic-Tertiary boundary. Under Yucca Mountain in profiles REG-2/3, the USGS has interpreted west-dipping faults to offset this boundary (see above). While the actual reflections of the inferred Paleozoic-Tertiary boundary are laterally discontinuous, suggesting the presense of faults, one may also attribute these terminations in part to the choppy data quality. The true cause of the lateral terminations within these reflections is somewhat ambiguous. Further to the east in REG-3, the reflections of this same boundary have strong amplitudes and do not exhibit distinctly laterally continuous behavior. Even though no faults have been interpreted to exist here by the USGS team, the confidence factor of the interpretation is lowered by the data quality.

As a clarification, the lowered confidence factor of interpreting faults within the REG-2/3 seismic data arises from the quality of the data. It is not a measure of a lowered confidence in the ability of the USGS to interpret data; as stated above, this team has conducted an excellent analysis. The data itself leaves room for unconstrainable alternative interpretations at the local level.

LINE REG-3 REFLECTION STRUCTURES: STEEPLY-DIPPING EVENT UNDER YUCCA MOUNTAIN

Prominent in the Final Stack of REG-3 is a pronounced steeply dipping event under Solitaro Canyon in Yucca Mountain (CDP 250-450 at 1.0 to 2.2 sec TWT in the Final Stack). This event has the appearance of a steeply dipping fault, particularly since it is located at the western edge of the inferred Paleozoic- Tertiary reflections in this profile. The USGS team has indicated that they interpret this event to be an artifact and not a fault.

An examination of the raw data for REG-3 proved unsuccessful in search of the unprocessed reflection which creates this event. If this were a real event, its unprocessed reflection should be a strong reflection whose hyperbola apex is widely offset to the west in the "time-offset" shot gathers. Offset hyperbolic reflections are not to be found. This confirms the USGS interpretation that this is not a real feature.

CONCLUSIONS

(1) The original USGS study of the Yucca Mountain seismic data REG-2/3 was a comprehensive study - little can be done to improve the analysis or results.

(2) The raw seismic data of REG-2/3 are not of high quality. This is not due to improper field technique but rather due to surface and near-surface conditionals which are not well-suited for seismic reflection data acquisition. The USGS team did an excellent job of analysis given what they had to work with.

(3) Of the USGS interpretation of west-dipping faults under Yucca Mountain which cut the inferred Paleozoic-Tertiary boundary, the supporting geophysical data do not have the resolution to confirm or disprove this interpretation. The seismic reflections are sufficiently laterally discontinuous that the interpretation of faulting based on lateral disruption is difficult. The USGS team's own work (Figures 19, 21) indicate that the presense of these faults is not detectable in surface gravity observations. Both types of geophysical data neither prove nor disprove the existence of these faults.

(4) The Final Stack version of seismic profile REG-3 suggests that the inferred Paleozoic-Tertiary reflections dip towards the east. The gravity modeling by the USGS, however, suggests that this boundary is horizontal. The quality of the raw seismic data of REG-3 is not sufficient to indicate if these reflections are dipping or are subhorizontal.

(5) The inherent laterally discontinuous quality of the seismic data lowers the confidence in the presense of any individual fault that may offset the inferred Paleozoic-Tertary boundary. In addition, this data quality negatively affects the ability to interpret the overall seismic profiles and lowers the confidence that any one specific interpretation is a correct one.

(6) The steeply dipping event under Solitaro Canyon in REG-3 has no reflection in the raw seismic data to suggest that it is a real event. The USGS interpretation that this is an artifact seems valid.

(7) Finally, there is little additional seismic data processing or interpretational methods that can be tried with these seismic profiles. The low quality of the data will not allow for traditional seismic reflection processing techniques to be performed.

REFERENCES

Brocher, T.M., P.E. Hart, W.C. Hunter, and V.E. Langenheim, Hybrid-Source seismic reflection profiling across Yucca Mountain, Nevada: Regional lines 2 and 3, USGS-OFR-96-28, 110 pp., USGS Denver, CO, 1996, DTN: GS960108314211.002 (Q), ACCN:MOL.19970310.0094.

Appendix II.
Calculation of Reflectivity (Majer et al., 1996)

All the high resolution reflection seismic surveys in the repository region show a small penetration depth of the seismic signal. Using the weight drop source, only reflectors within the first hundreds of meters of depth are imaged, and are rarely continuous over greater lateral distance. This suggests that inhomogeneities (welding, porosity, lithophysal content, fracture content, faulting, etc.) within the rock formations may be causing variations in travel time and strong attenuation of the seismic signals. In an attempt to provide a quantification of the effect of the attenuation of signals (be it from scattering or intrinsic loss) well logs and the data from the UZ-16 VSP survey were used to determine the seismic properties at this specific site. Using this model the effect of changes in porosity, water saturation and rock matrix composition on seismic waves can be studied in greater detail.

The data from the near offset UZ-16 VSP (103 ft) was used for this analysis. The sensor spacing was 16 ft., starting at 95 ft. and continuing to 1615 ft. depth. For the following analysis only the vertical component was available, which allowed us to study the P-wave only. The well logs cover 40 ft. to 1640 ft. depth with a sample interval of 0.5 ft. Total water saturation, total porosity, bulk density and then analog mineral composition log was used for the analysis.

In general the log data are too noisy to derive the rock properties at every sample depth. Hence the logs were simplified to 21 layers, which allowed us to obtain reliable estimates for the porosity, the water saturation and the bulk density for each layer (Figure II-1a, b and c) The VSP data are used to obtain interval velocities between two adjacent receivers. We assume that the first arrival is the direct wave from the source to the receiver. Only half the period of each arrival was used during the analysis to avoid contamination with refractions and reflections. The general procedure was to compute the Fourier spectrum of the first arrival for each receiver. By dividing two neighboring Fourier spectra all the frequency independent effects like receiver and source coupling are eliminated and we can obtain the phase and modulus difference due to the rock properties between the receivers. For the uppermost receivers frequencies up to 160 Hz are beyond the noise level. Moving further down the borehole the significant frequency range reduces steadily and at the last receiver only frequencies up to 50 Hz can be used for the analysis. Some traces show clear later arrivals almost simultaneously with the first arrival and the arrival time was picked by hand. Figure II-2 shows the interval velocities derived from the VSP survey at UZ 16.

Rock matrix properties

The VSP data provide averaged interval velocities only. To study the effect of porosity and water saturation on the seismic wave we must know the P-wave velocity at every single sample depth, i.e. every 0.5 ft.. Only in this way can dispersion and attenuation effects due to changing porosity and water saturation be studied. The first step is to determine the mineralogy of the rock matrix. The mineralogy log was used to obtain a rough estimate of the volume fraction of the main minerals. Together with porosity, saturation and bulk density, a simplified mineral composition in UZ 16 was then computed. Most of the rock matrix consists roughly of 30 % fused Quartz and 70 % K-Feldspar. Table II-1 shows the mineralogical composition of the rock matrix in UZ 16. The single minerals seismic properties are listed in Table II-1 as well. Taking the mineral compositions and the log data we can then compute the correct mean density for the different units. The matrix velocities however disagree with measurements taken on different samples out

of the Yucca Mountain region. Nelson and Anderson (1992) reported velocities of the rock matrix between 4.5 km/s and 5.3 km/s for all studied lithologies. It seems legitimate to assume that this difference stems from the imperfection of the rock minerals themselves and probably from loose contacts between the different constituents. These two effects can be described with cracks, which are always present at low pressure environments. To study the effect of cracks on the velocity we use the self-consistent approach by O'Connell and Budiansky (1974). With an increasing number of water saturated cracks the compressibility of the rock matrix remains the same, but the shear strength decreases. This leads to an increased Poisson's ratio of the rock matrix.

The last step in matching the velocities derived from the VSP data is to take into account the effect of the pore space. For this purpose we use Berryman's self-consistent approach for spherical inclusions (Berryman, 1980). Using porosity and water saturation from the well logs together with these two theoretical approaches we can match the mean P-wave velocity in almost every unit and obtain the matrix properties for the different layers in UZ-16. Only the velocities for the bedded tuffs and a small portion near the top of the Prow Pass can not be matched. Berryman's theory predicts that the rock loses its shear strength for porosities higher than about 50%. This leads to extremely small P-wave velocities for partially saturated media. This effect has been observed in marine seismology and studied in great detail (e.g. Anderson and Hampton, 1980). Table II-2 lists the rock matrix properties used to match the VSP data.

Synthetic Velocity Profile

The P-wave velocities shown above agree very well with the measurements in the laboratory by Nelson and Anderson (1992). Using the actual log data we are now able to compute a synthetic velocity profile, which shows the actual velocity variation on a scale of 0.5 ft. (Figure II-3). Again, the synthetic velocities at the bedded tuffs and at the top of the Prow Pass Tuff are smaller than the VSP velocities due to the large porosity.

Now we can use the synthetic velocity profile and the density data to compute the synthetic seismogram of a normal incident P-wave on a layered medium. The properties of the different layers are calculated with the rock matrix properties, the porosity and the water saturation. In a first step no anelasticity within the layers is applied. The input signal has a center frequency of 40 Hz with the corners at 10 Hz and 70 Hz respectively. We first compute a seismogram with homogeneous layers (Figure II-4a) and with the actual velocity variation within the layers (Figure II-4b). The first seismogram shows two very strong reflection in the beginning of the seismogram. The first has a positive polarity and originates from the top of the Tiva Canyon Tuff. The second has a negative polarity and comes from the bedded tuffs. All later arrivals are just reverberations within the Tiva Canyon Tuff. No energy can penetrate the low velocity layer at the bedded tuffs and the total penetration depth for the original log data is only about 150 ft. (46 m). The reason for this effect is the very high porosity in the bedded tuffs, which builds a barrier for the seismic waves.

Nevertheless we have already noticed that the VSP data shows a larger P-wave velocity. There are basically two different explanations for this disagreement:

1. The log data overestimate the actual porosity in the bedded tuffs.
2. The large porosity is a local effect and can not be represented with a layered medium.

If only the second argument holds true, the seismic wave will experience a strong reflection at this point and the transmitted wave will only be weak. To match the VSP data in these two

critical zones with a layered medium we have to assume smaller porosities. If we take into account the velocity variations within the layers the interpretation of the seismogram is less obvious. The reverberations are distorted by multiple scattered waves within the alluvial fill and the Tiva Canyon Tuff.

Synthetic Seismograms: Corrected Log Data

The porosities in the bedded tuffs have to be reduced by almost 30% and in the Prow Pass Tuff the porosities are reduced by 10%. With these corrections all the VSP velocities can be matched (Figure II-5). The rock matrix parameters agree now entirely with the laboratory measurements (Table II-3). As before we computed the synthetic seismogram without velocity variation within the layers (Figure II-6a) and with velocity variation within the layers (Figure II-6b). Figure II-6a still shows a strong reflection at the top of the Tiva Canyon Tuff. But now we also receive reflections from almost all the lithologic boundaries.

Synthetic Seismograms: Hypothetical Reflector at the Bottom of the Prow Pass Tuff

The coherent transmitted wave at the bottom of the Prow Pass Tuff has lost about 90% of the original energy. Any reflection from below will therefore show less than 3% of the original seismic energy. In the following we assume a hypothetical layer at 1735 ft. (530 m) depth, which will produce a reflection at exactly 400 ms travel time. We use following material properties for this reflector: Vp = 6.00 km/s, Vs = 3.50 km/s, density = 2.70 g/cc. All the other layers are the same as were used to produce Figure II-6b. Figure II-7 shows the seismogram without a high velocity layer (top) and the seismogram with a hypothetical layer at 1735 ft. depth (bottom). As we have already seen from energy considerations, the reflection is very weak and hidden in all the scattered waves. The overall shape of the seismogram does not change at 400 ms, but we see a slightly stronger amplitude with positive polarity.

VSP data together with well logs are a powerful tool to study and plan seismic reflection surveys. We can show that at UZ-16 there are two extremely critical zones for the seismic wave propagation, at the bedded tuffs and at the Prow Pass Tuff. The log data show at these two zones porosities higher than 50%, which leads to very high seismic contrasts in a partially water saturated medium. If the high porosities are only a local phenomenon the CDP gathers will fail to produce coherent reflections, because of the heterogeneity of the subsurface. The theoretical calculations also reveal that in the vicinity of UZ-16 it is very difficult to get enough energy below the Prow Pass Tuff. The transmitted wave looses about 90% of its energy traveling from the surface to the Prow Pass Tuff due to strong reflections at the different lithologic boundaries. The implications are profound when one realizes that almost all of the seismic energy is confined above the Prow Pass. The modeling for the case just considered implies that the Paleozoic interface can not be imaged with surface seismic methods. We should note, however, that the measured porosity varies between wells and that these computed results for UZ-16 can not be extrapolated to all surface seismic lines. Nonetheless, it does seem that porosity is a material property which causes dramatic variability in seismic reflection data at Yucca Mountain.

REFERENCES

Anderson, A. L. and Hampton, L. D., Acoustics of gas-bearing sediments I. Background: Journal of the Acoustical Society of America, 67 (6) 1865-1889, 1980, ACCN: N/A. DTN: N/A.

Anderson, D. L., Theory of the earth, Blackwell Scientific Publications, Boston, MA, 366 pp., 1989, ACCN: N/A. DTN: N/A.

Berryman, J. G., Long-wavelength propagation in composite elastic media I. Spherical inclusions: Journal of the Acoustical Society of America, 68, 1809-1819, 1980, ACCN: N/A. DTN: N/A.

Carmichael, R. S., Practical handbook of physical properties of rocks and minerals: CRC Press, 1982, ACCN: N/A. DTN: N/A

Johnson, L. J. and Plona, T. J., Acoustic slow waves and the consolidation transition: Journal of the Acoustical Society of America, 72 (2), 556-564, 1982, ACCN N/A. DTN: N/A.

Majer, E.L., M. Feighner, L. Johnson, T. Daley, E. Karageorgi, K. H. Lee, K. Williams, and T. McEvilly, 1996, Synthesis of Borehole and Surface Geophysical Studies at Yucca Mountain, Nevada and Vicinity Volume I: Surface Geophysics, Yucca Mountain Project Milestone OB05M, Lawrence Berkeley National Laboratory, Berkeley, CA, 1996, DTN: LB960808314212.001 (Q), LB960808314212.002 (Q), LB960808314212.003 (Q), LB960808314212.004 (Q), ACCN: MOL.19970114.0137.

Nelson, P. H. and Anderson, L. A., Physical properties of ash flow tuff from Yucca Mountain, Nevada: Journal of Geophysical Research, 97, 6823-6841, 1992, ACCN: NNA.19920707.0061. DTN: GS920608314213.001 (Non-Q)

O'Connel, R. J. and Budiansky, B, B., Seismic velocities in dry and saturated cracked solids: Journal of Geophysical Research, 79, 5412-5426, 1972, ACCN:NNA:19930215.0047. DTN:N/A

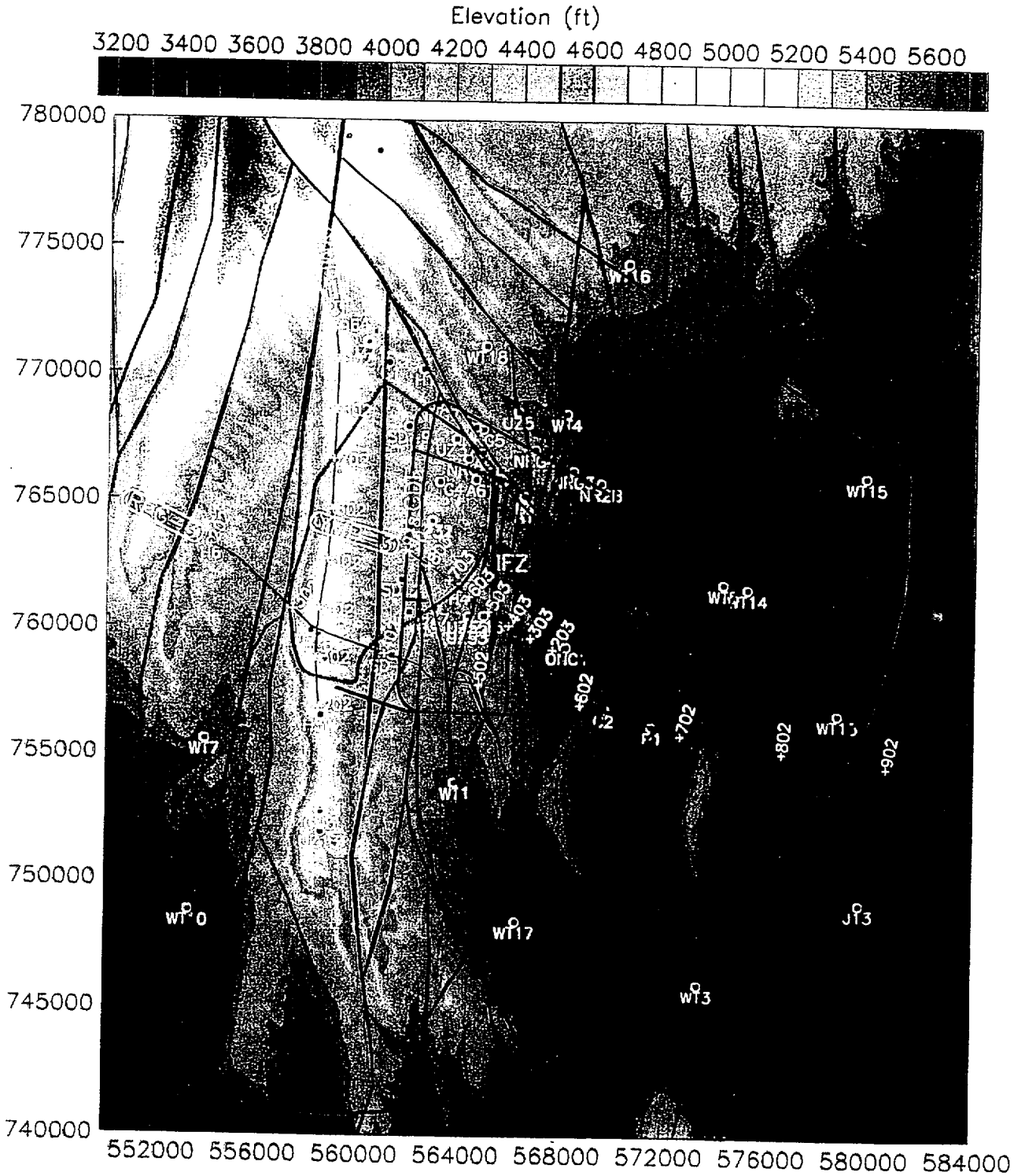

Figure 1 Location map for surface seismic profiles discussed in this report. Topography is shown color coded and some nearby wells are shown as black dots. The seismic lines YMP-5, YMP-3 and REG-3 are shown as white lines with CDP numbers labeled. The red lines are surface faults from the geologic model ISM2.0 (Clayton et al., 1997). The Ghost Dance Fault is labeled GDF and the Imbricate Fault Zone is labeled IFZ. Axis are labeled in Nevada state plane coordinates (feet).

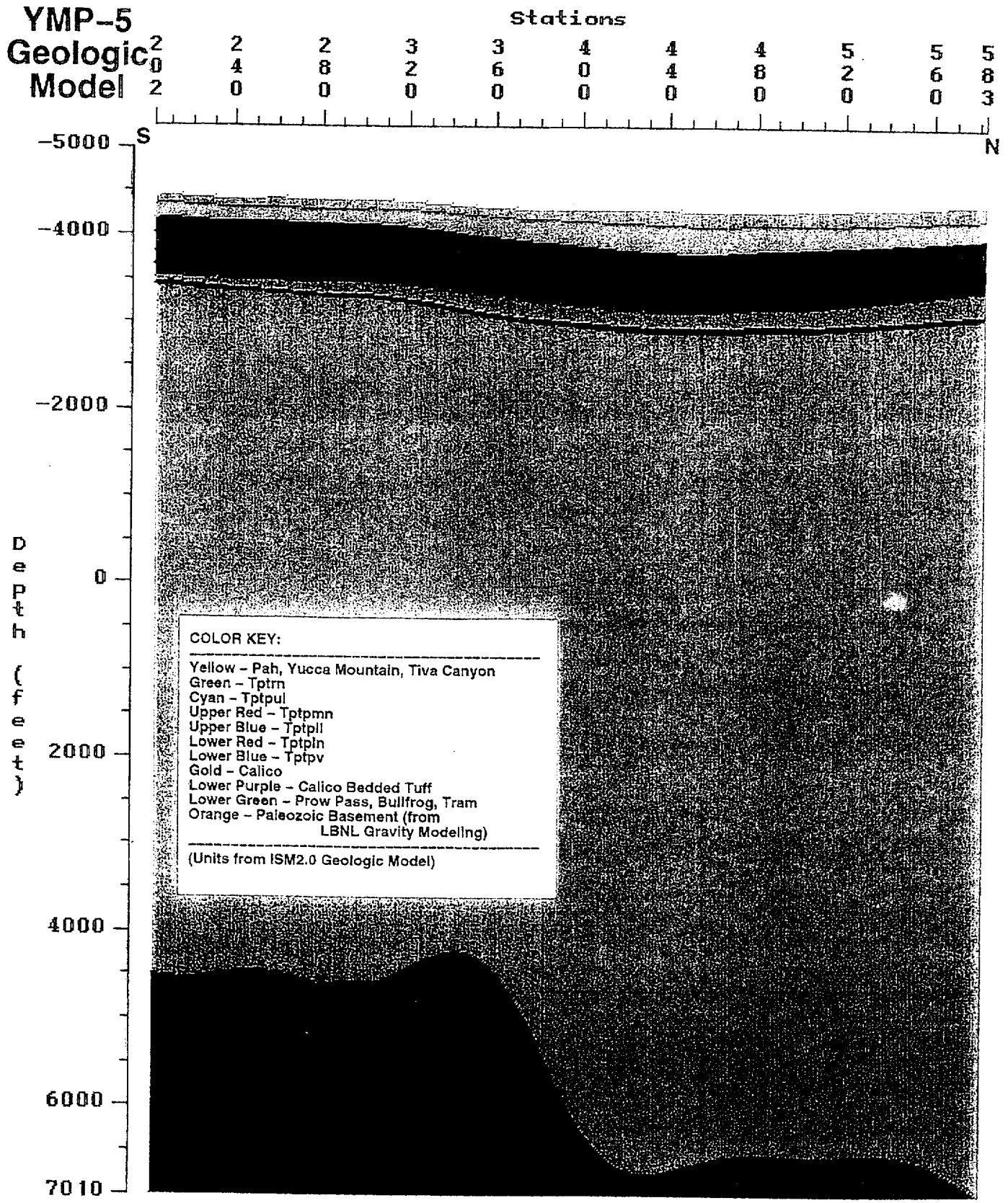

Figure 2 Geologic model for line YMP-5.

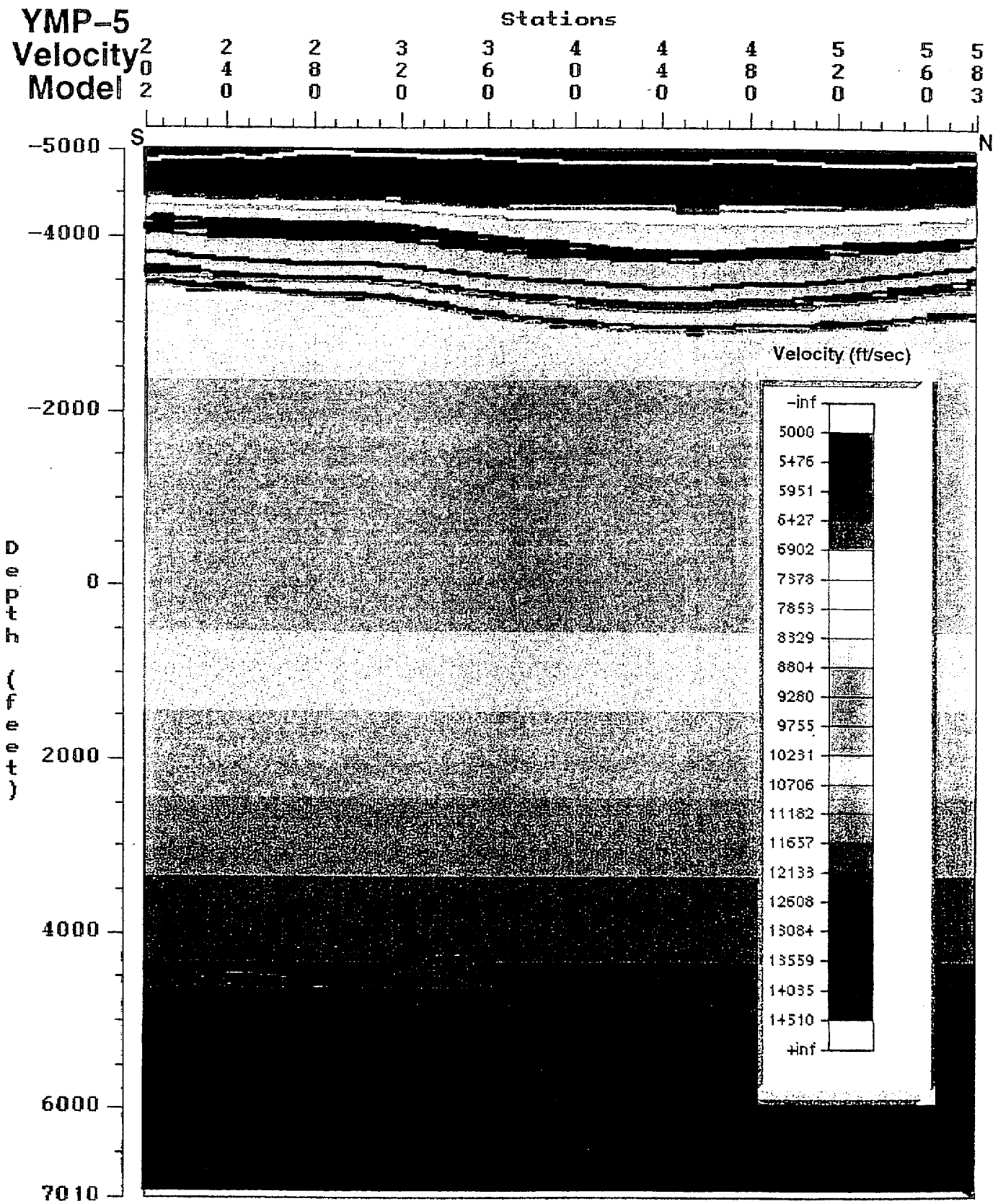

Figure 3 Velocity model for line YMP-5. The bottom two units have a linear vertical velocity gradient.

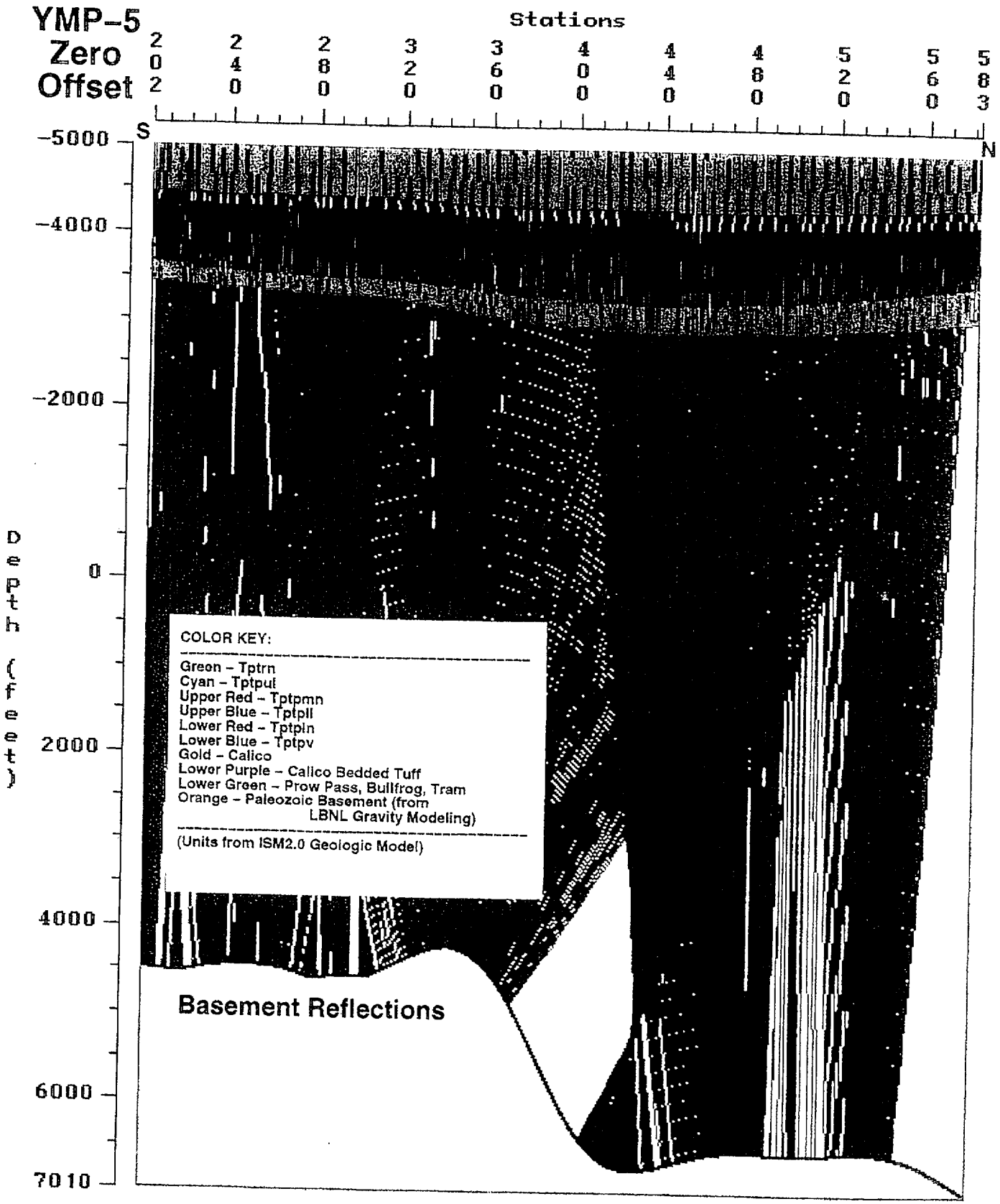

Figure 4 Raypaths for zero offset modeling of YMP-5.

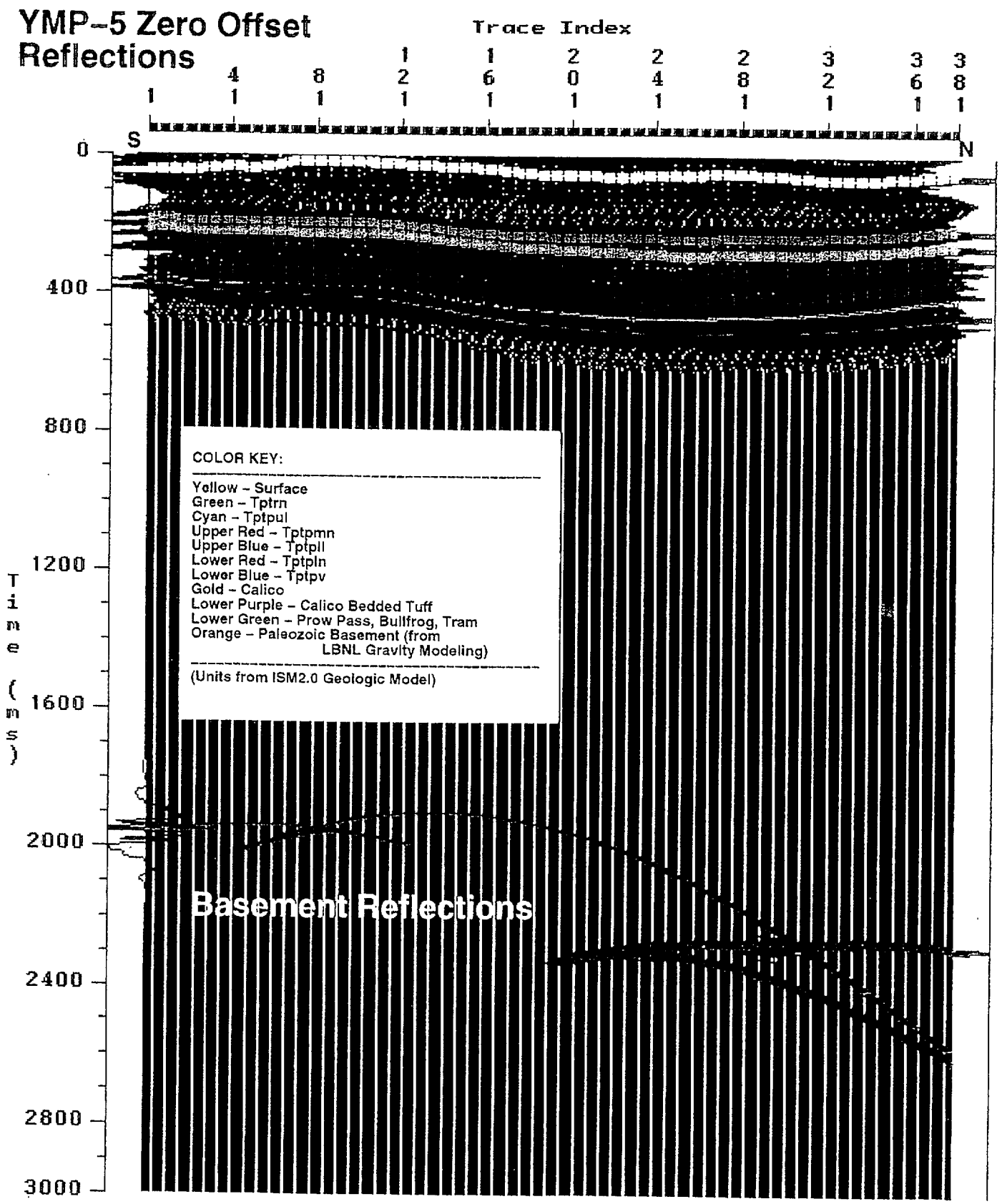

Figure 5 Reflection seismograms for zero offset modeling of YMP-5. All arrivals are color coded by the horizon generating the reflection. Note that the ground level surface is shown as a seismic reflector (yellow) for reference.

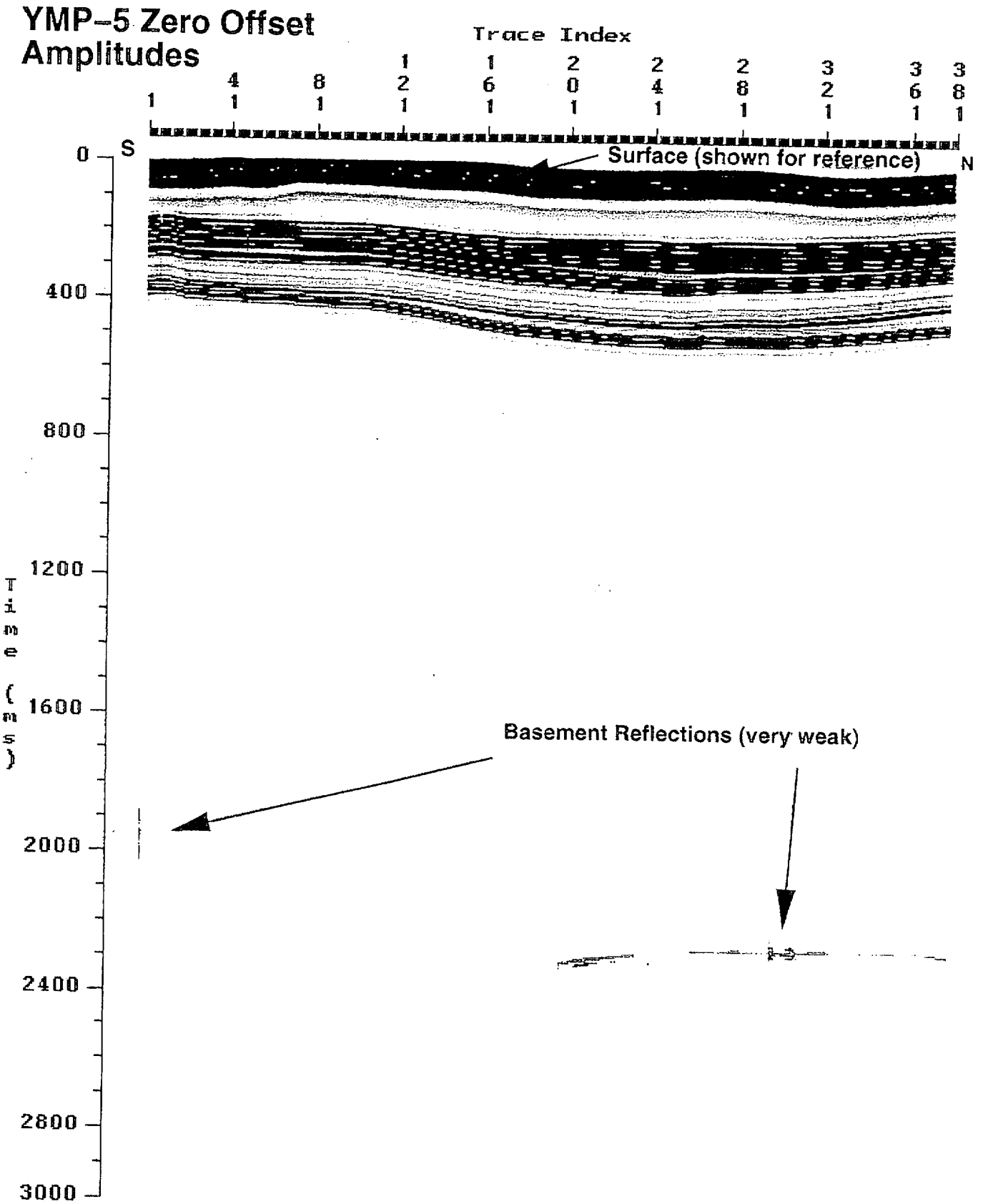

Figure 6 Reflection amplitudes for modeled seismograms from YMP-5.

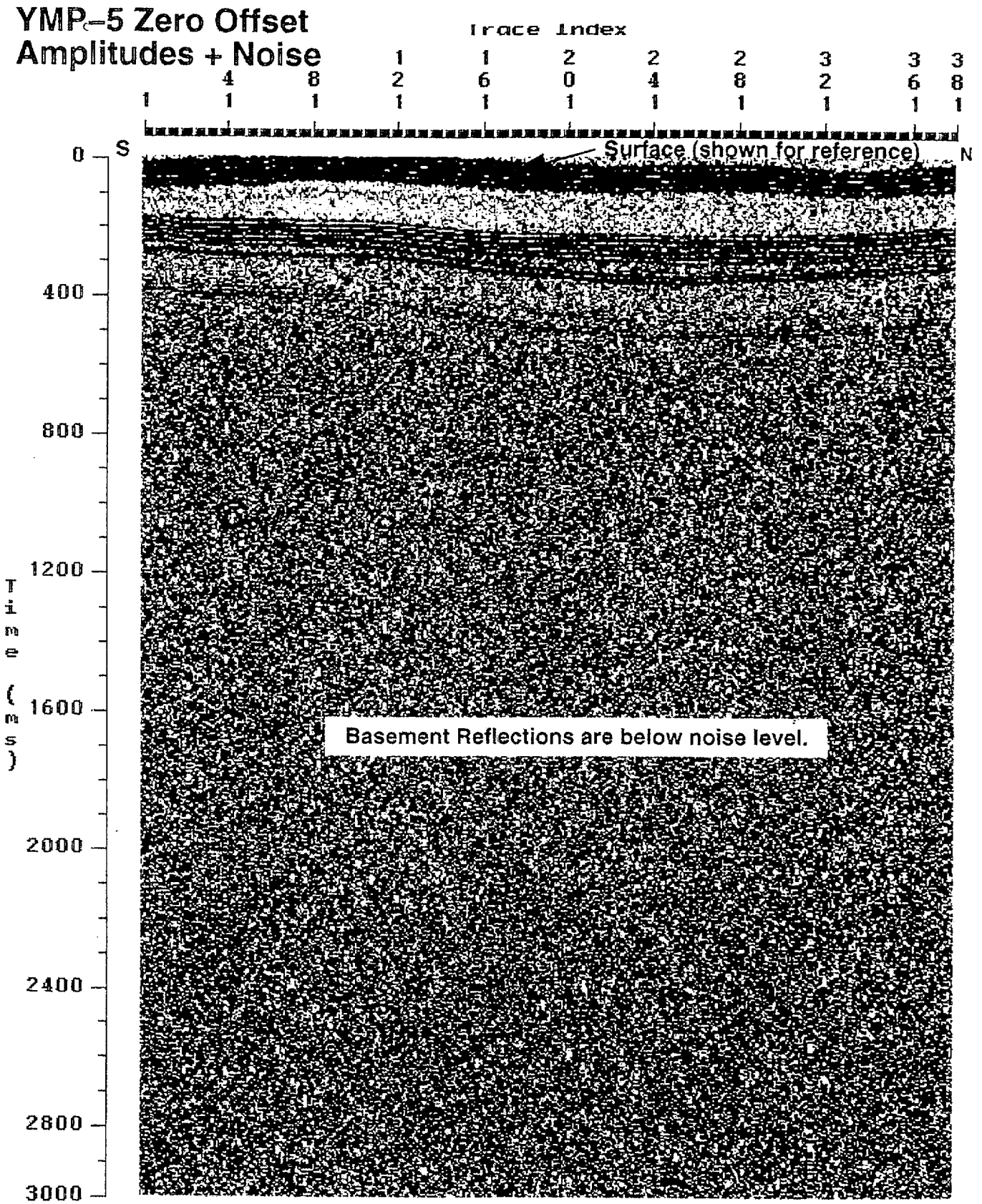

Figure 7 Reflection amplitudes plus random noise for YMP-5.

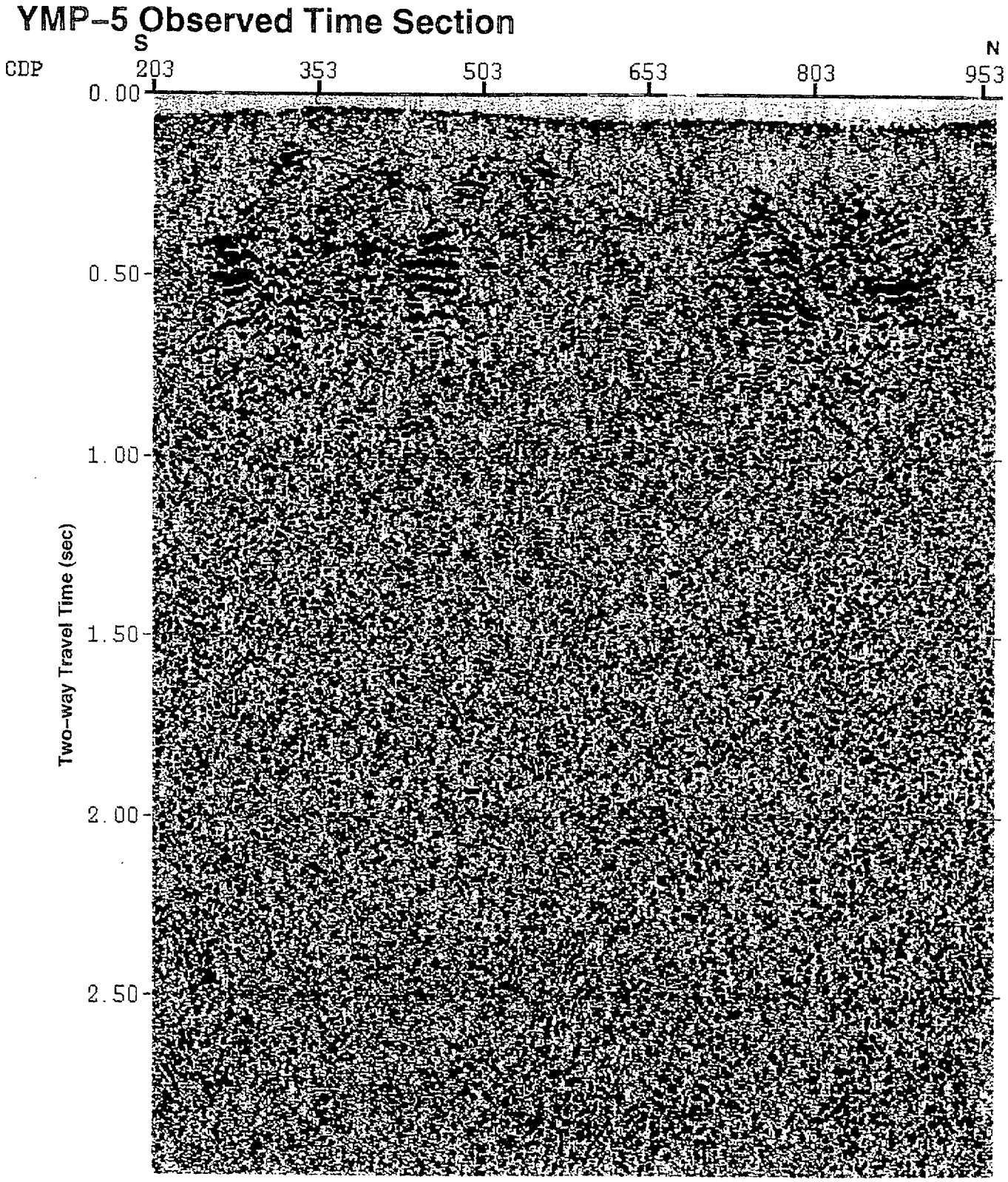

Figure 8 Field data CDP time section for YMP-5.

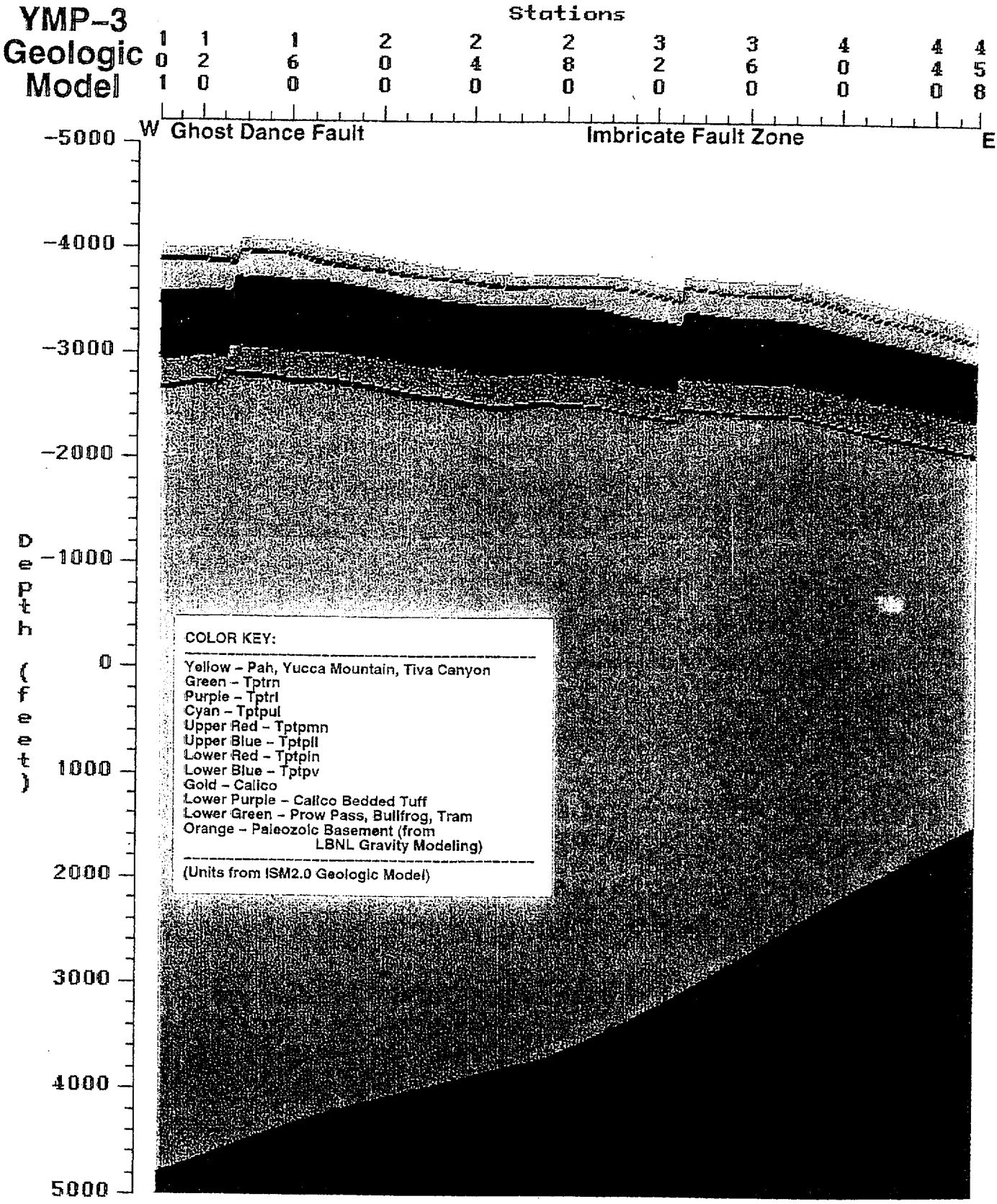

Figure 9 Geologic model for line YMP-3

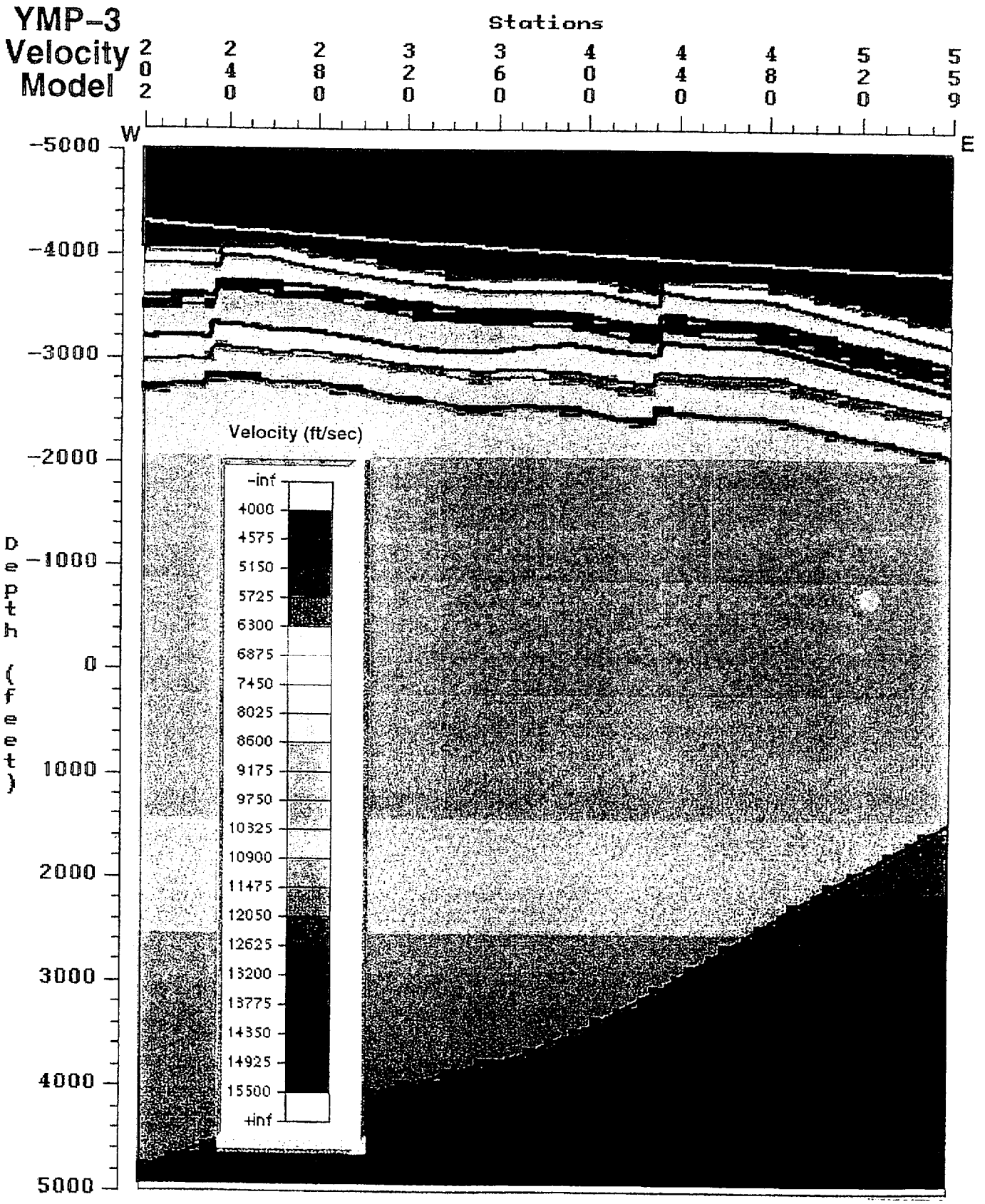

Figure 10 Velocity model for line YMP-3. The bottom two units have a linear vertical velocity gradient.

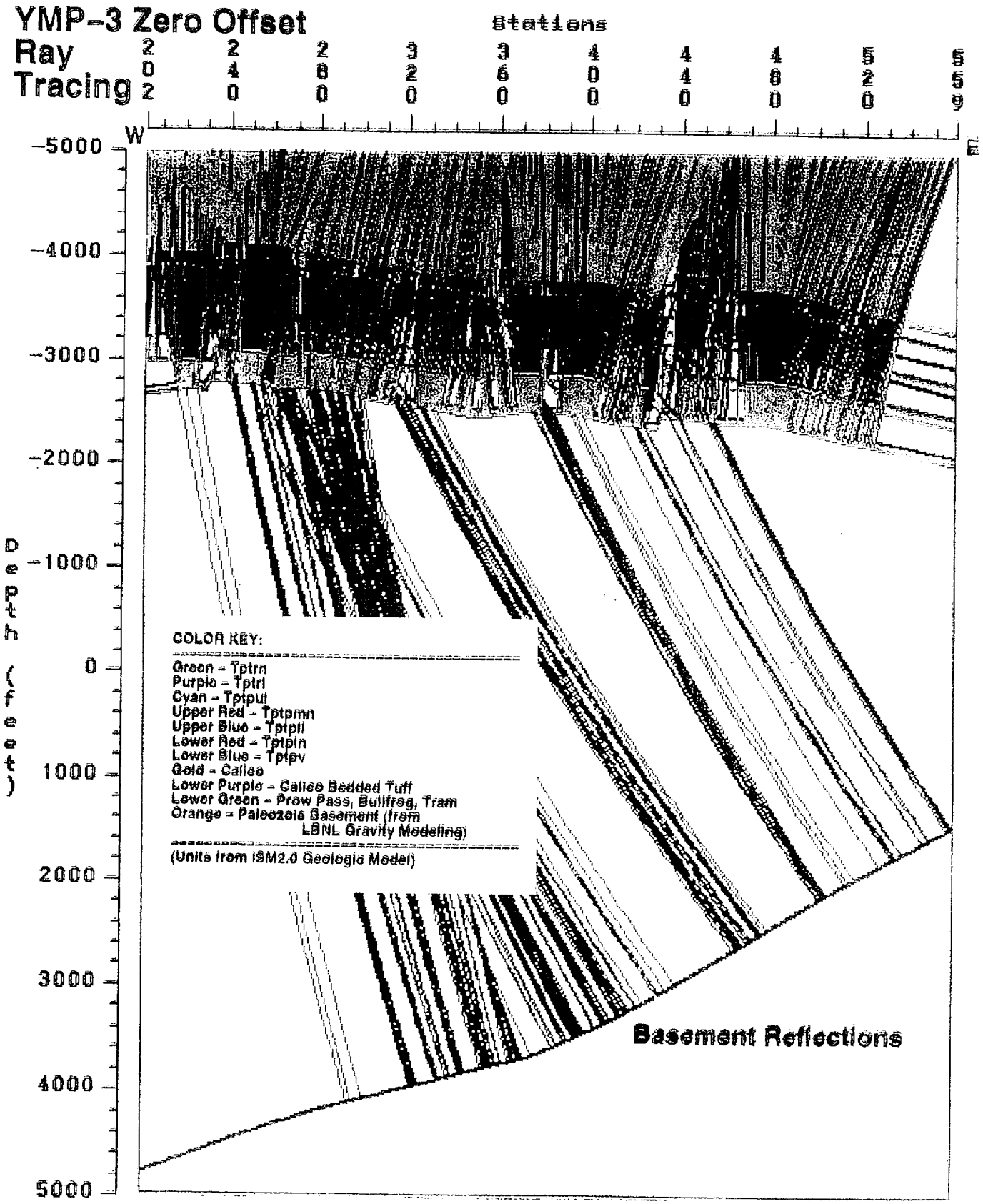

Figure 11 Raypaths for zero offset modeling of YMP-3. Rays are color coded to match the horizon generating reflection.

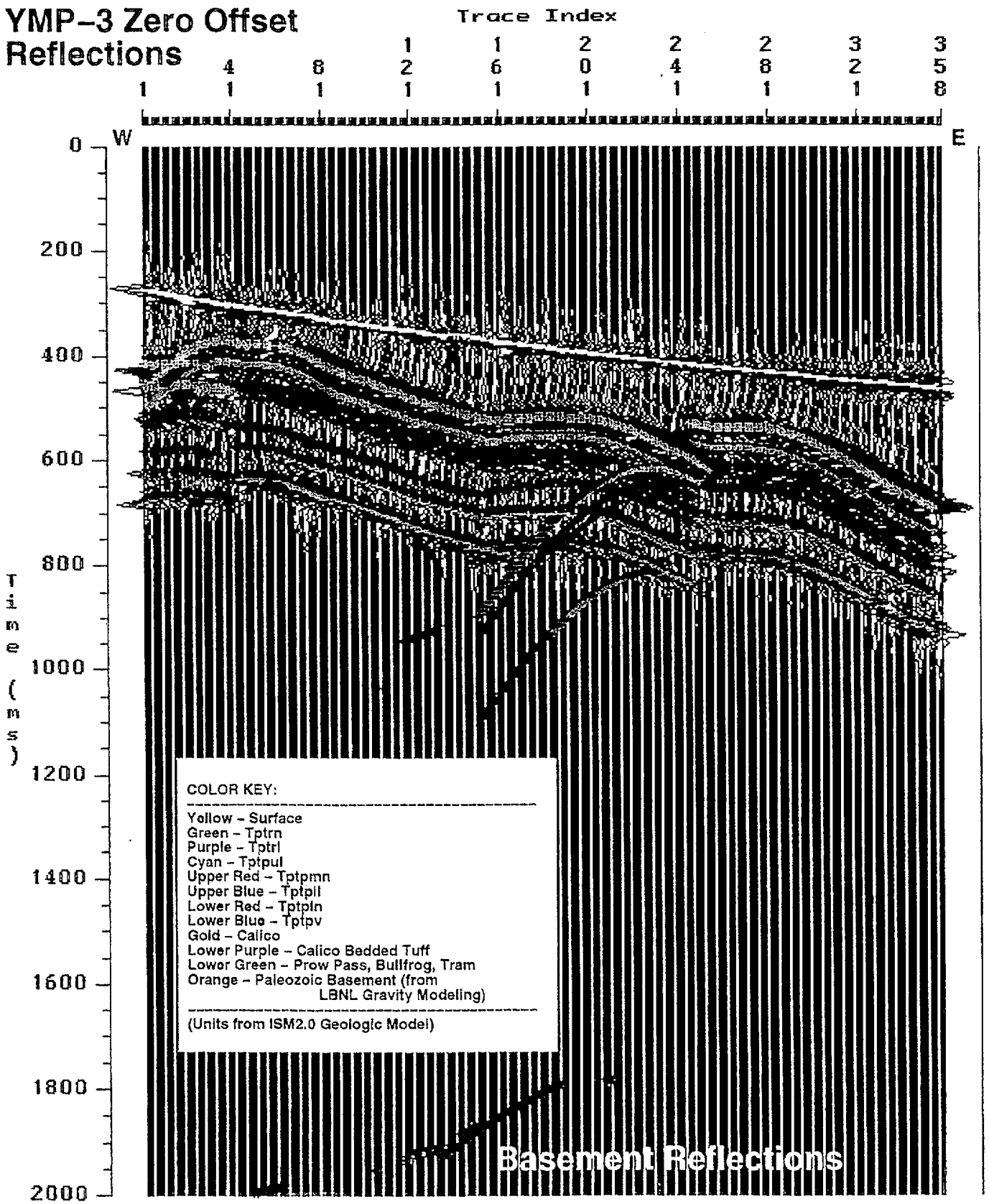

Figure 12 Reflection seismograms for zero offset modeling of YMP-3. All arrivals are color coded by the horizon generating the reflection. Note that the ground level surface is shown as a seismic reflector (yellow) for reference.

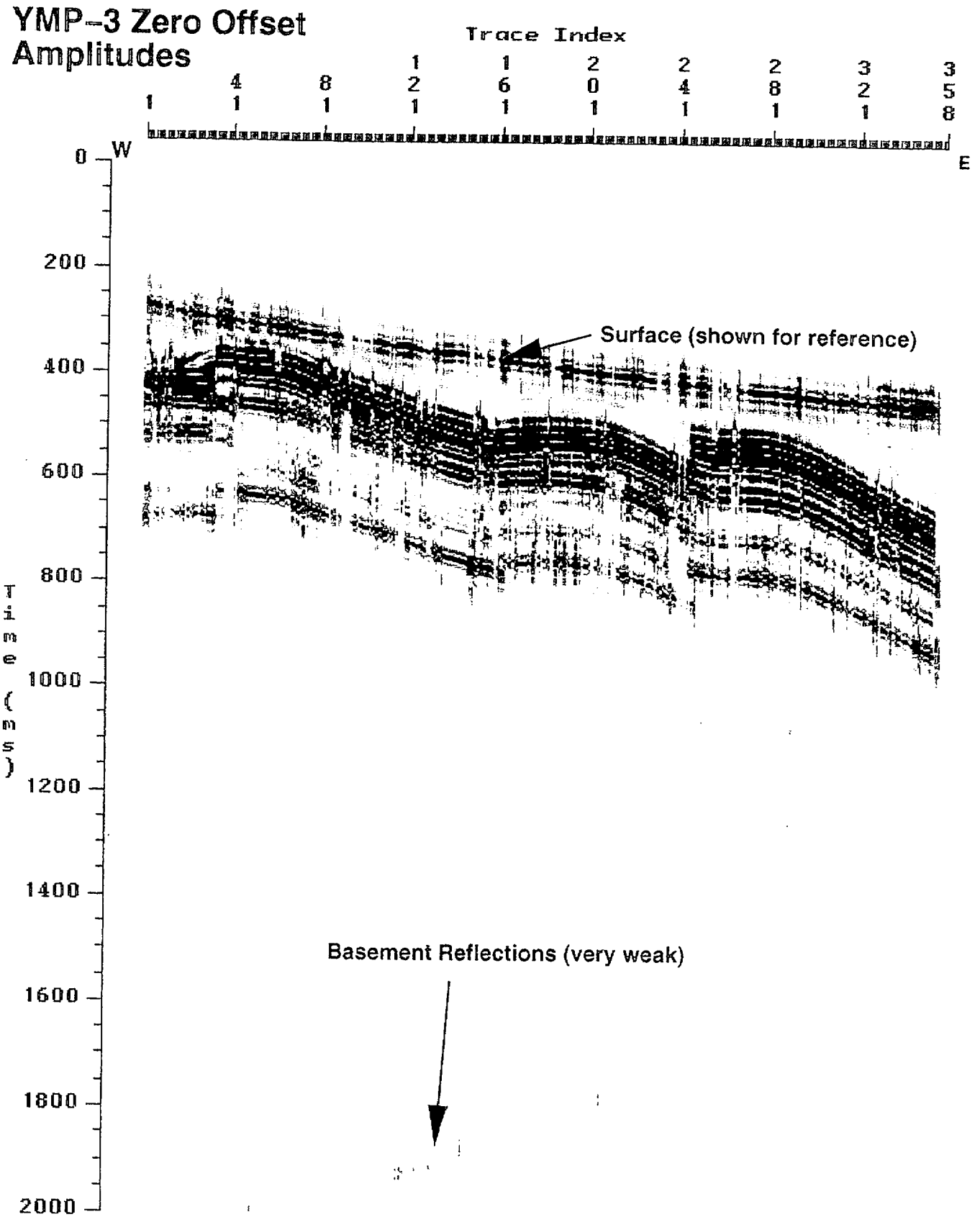

Figure 13 Reflection amplitudes for modeled seismograms from YMP-3.

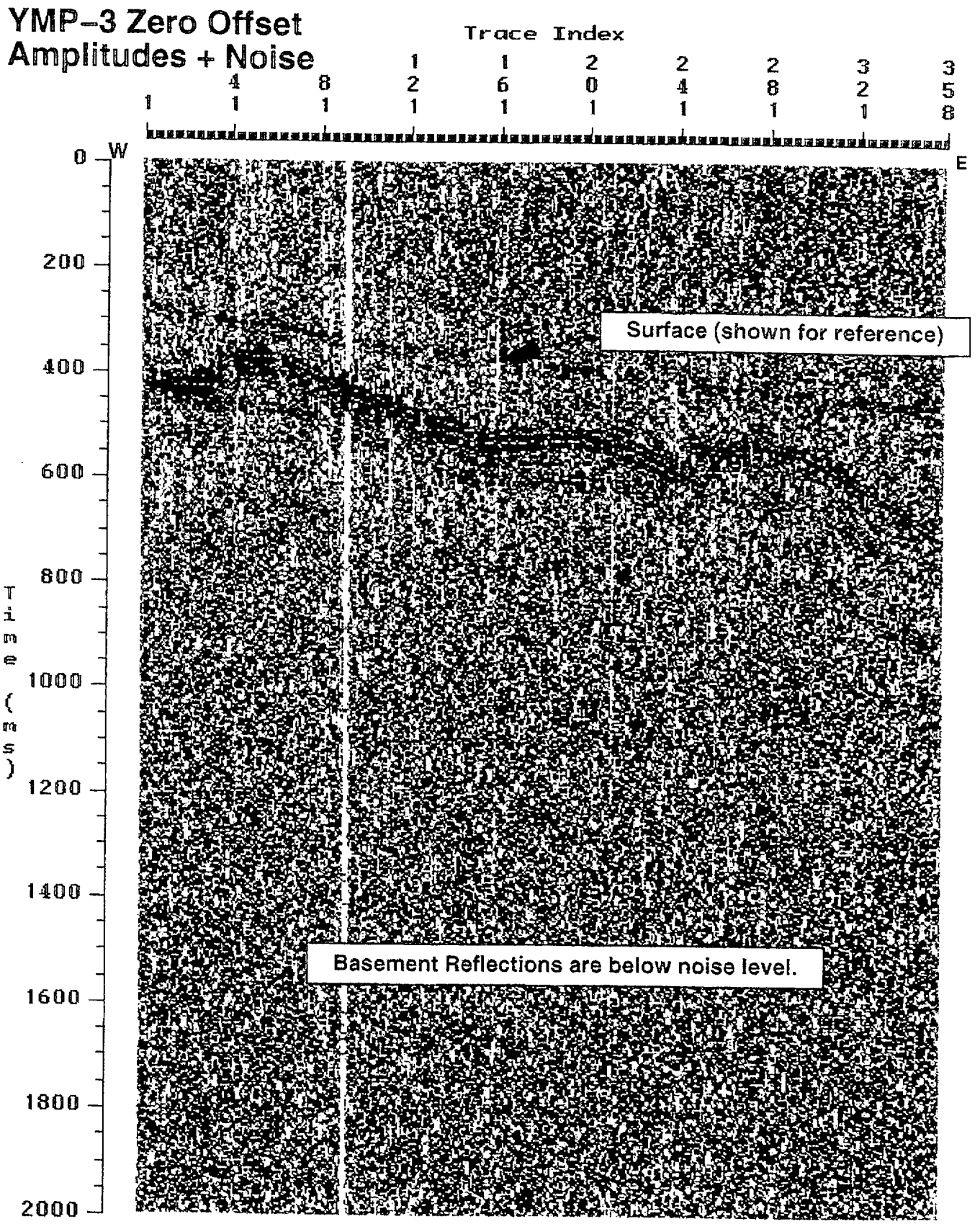

Figure 14 Reflection amplitudes for modeled seismograms from YMP-3 with addition of random noise.

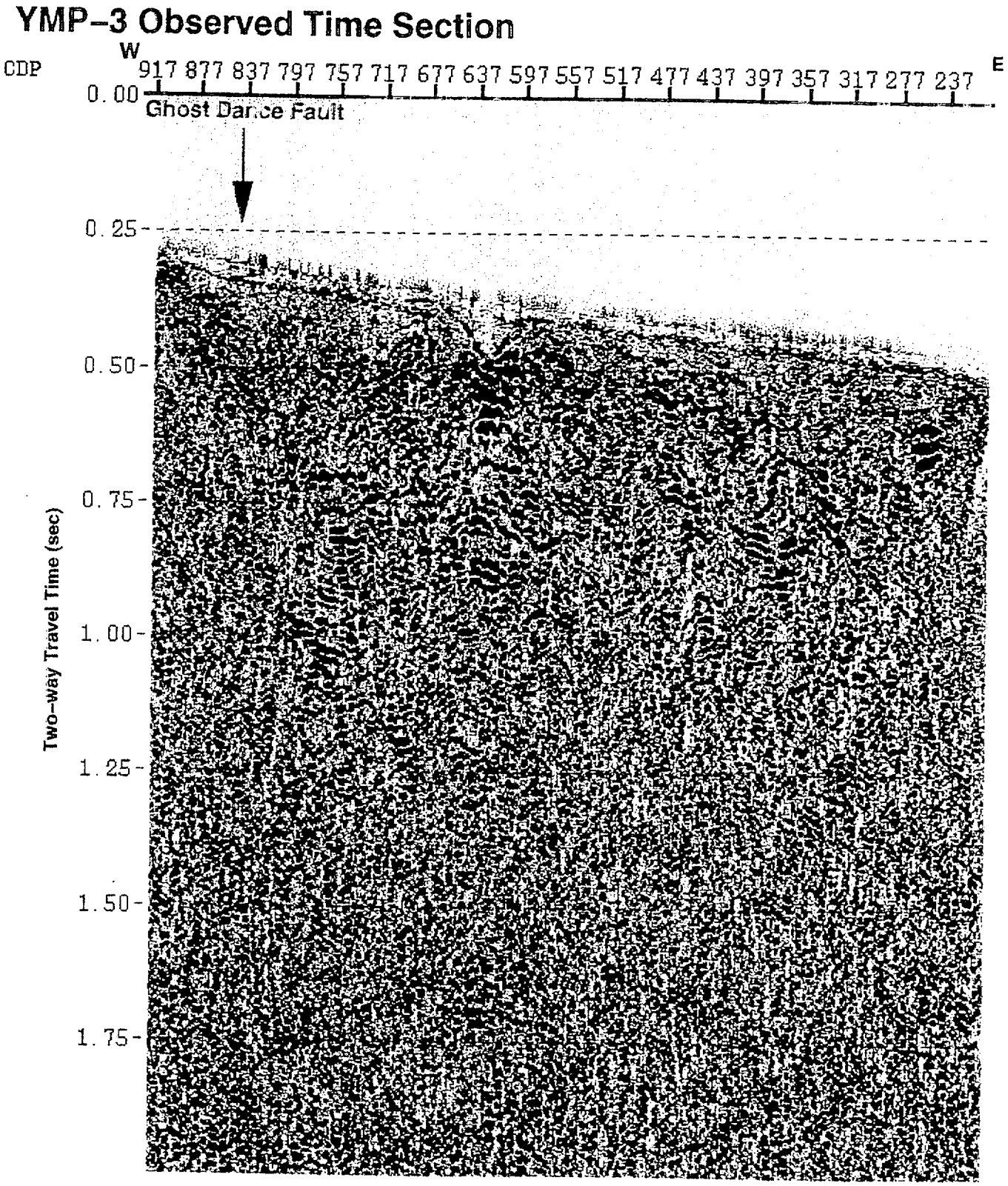

Figure 15 Field data CDP time section for YMP-3.

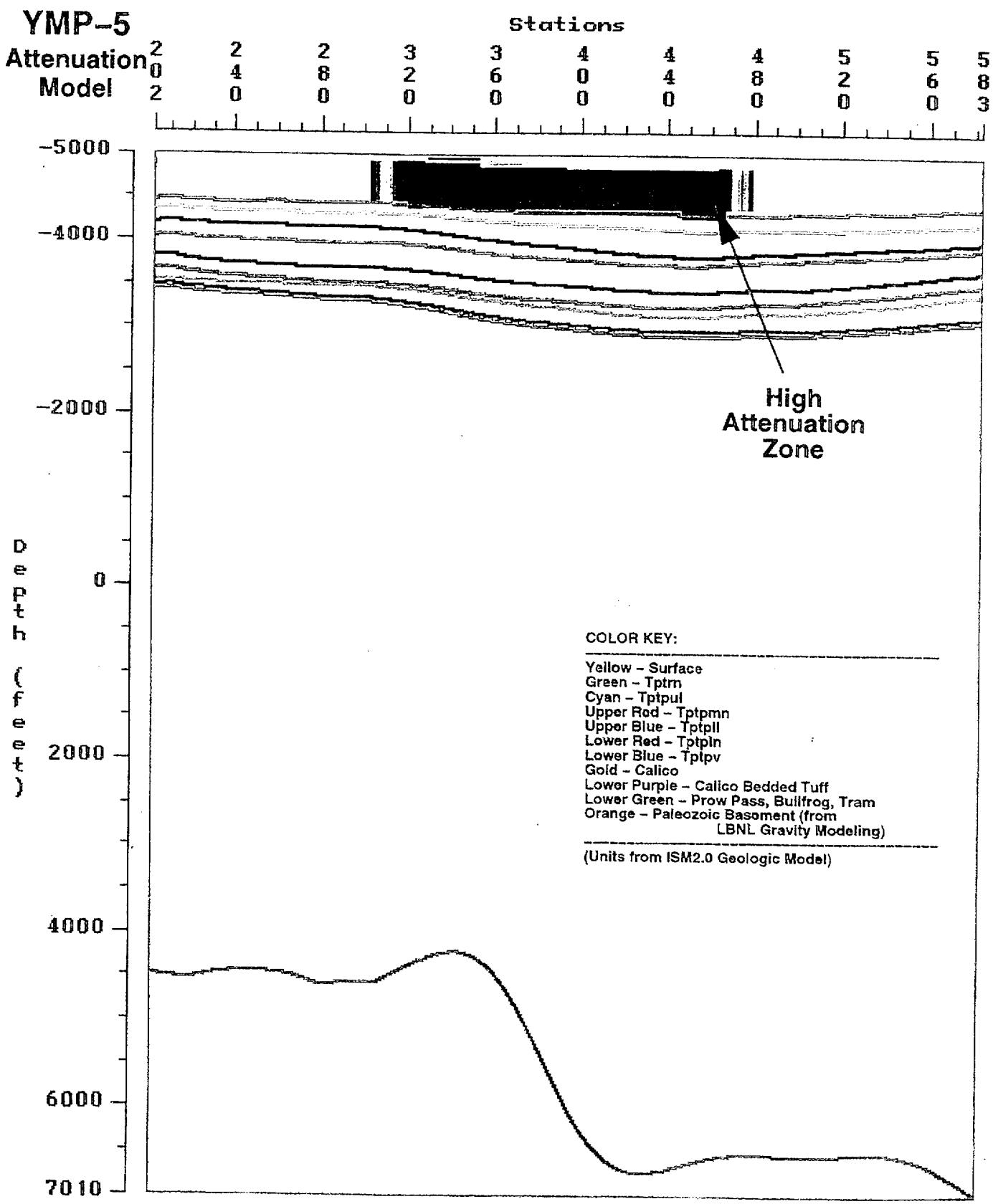

Figure 16 Geologic model for YMP-5 showing high attenuation (seismic Q = 10) zone location used for attenuation modeling.

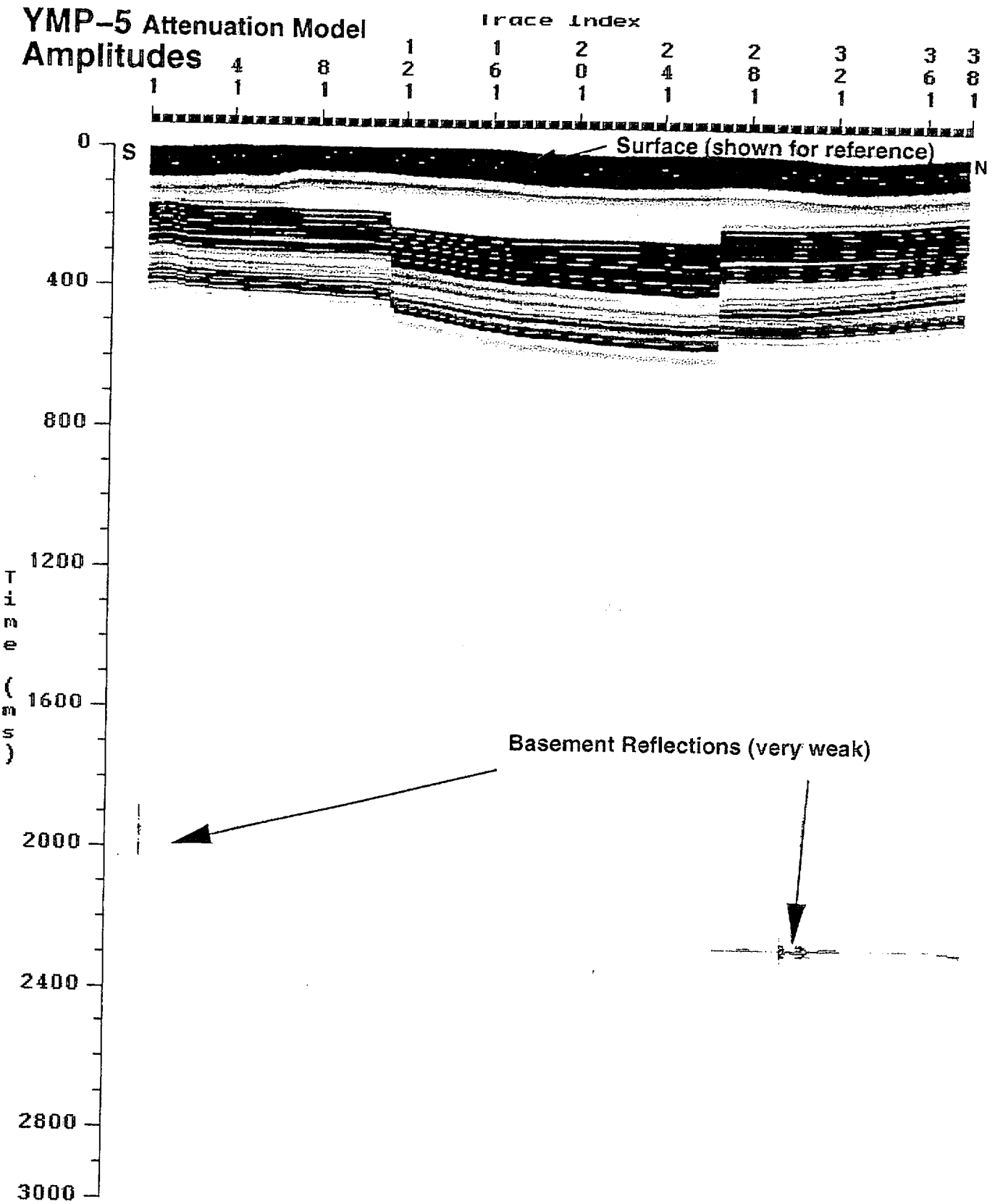

Figure 17 Reflection amplitudes for attenuation modeling of YMP-5. Velocity model is same as Figure 3.

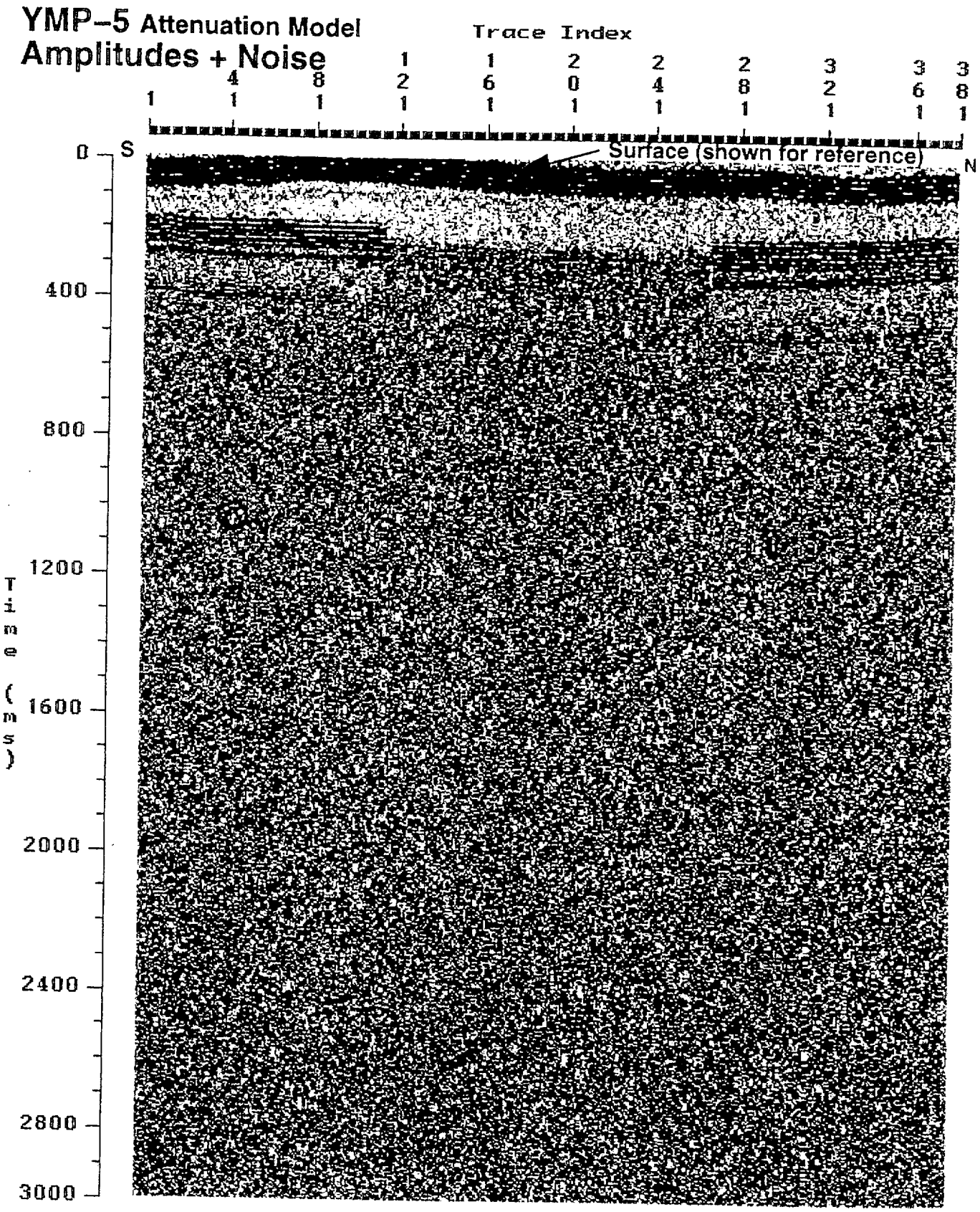

Figure 18 Reflection amplitudes from Figure 17 with random noise added.

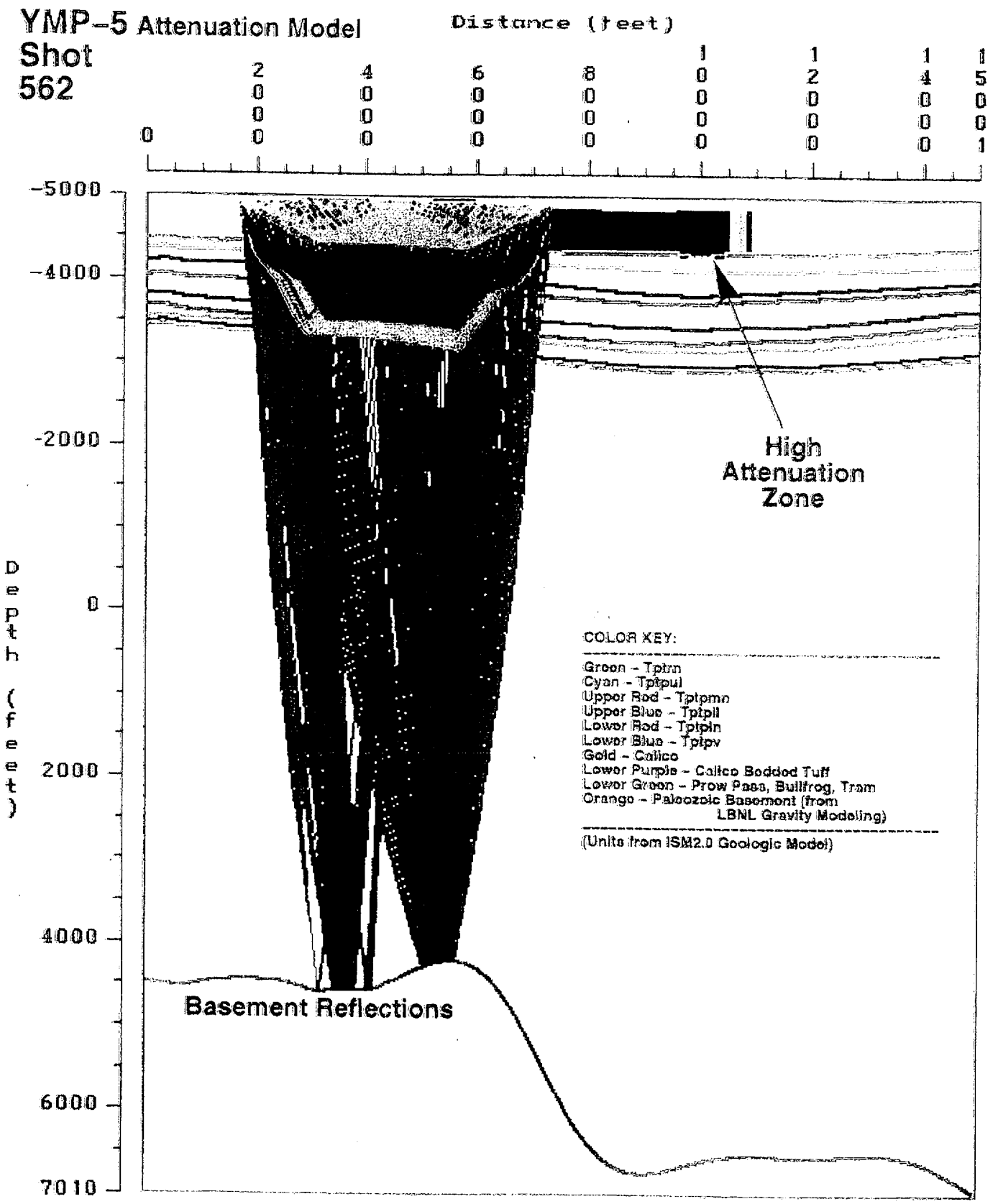

Figure 19 Rays from single shot gather (number 562) for the attenuation model of YMP-5.

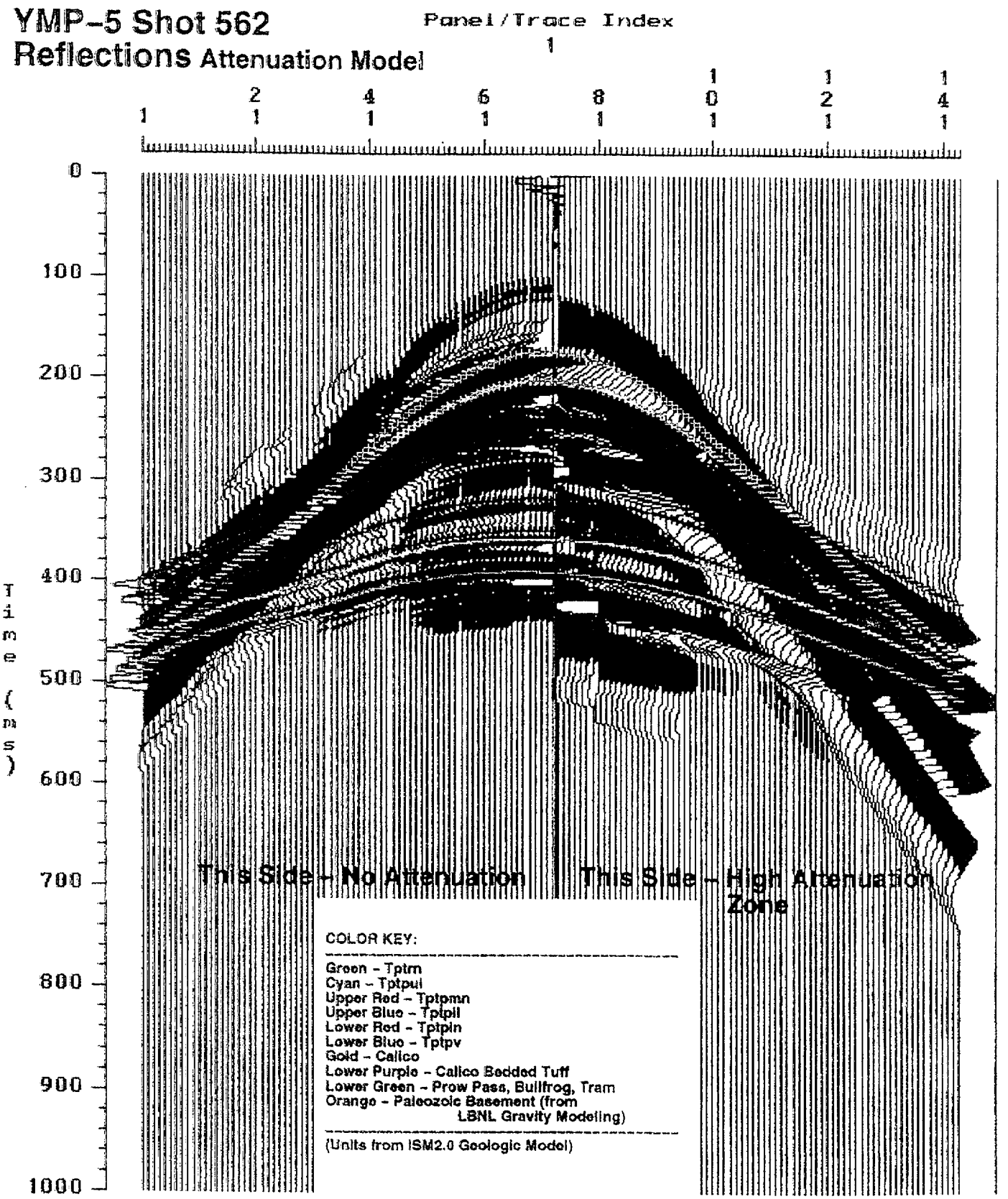

Figure 20 Seismograms for shot 562 from the YMP-5 attenuation model. All arrivals are color coded by the horizon generating the reflection.

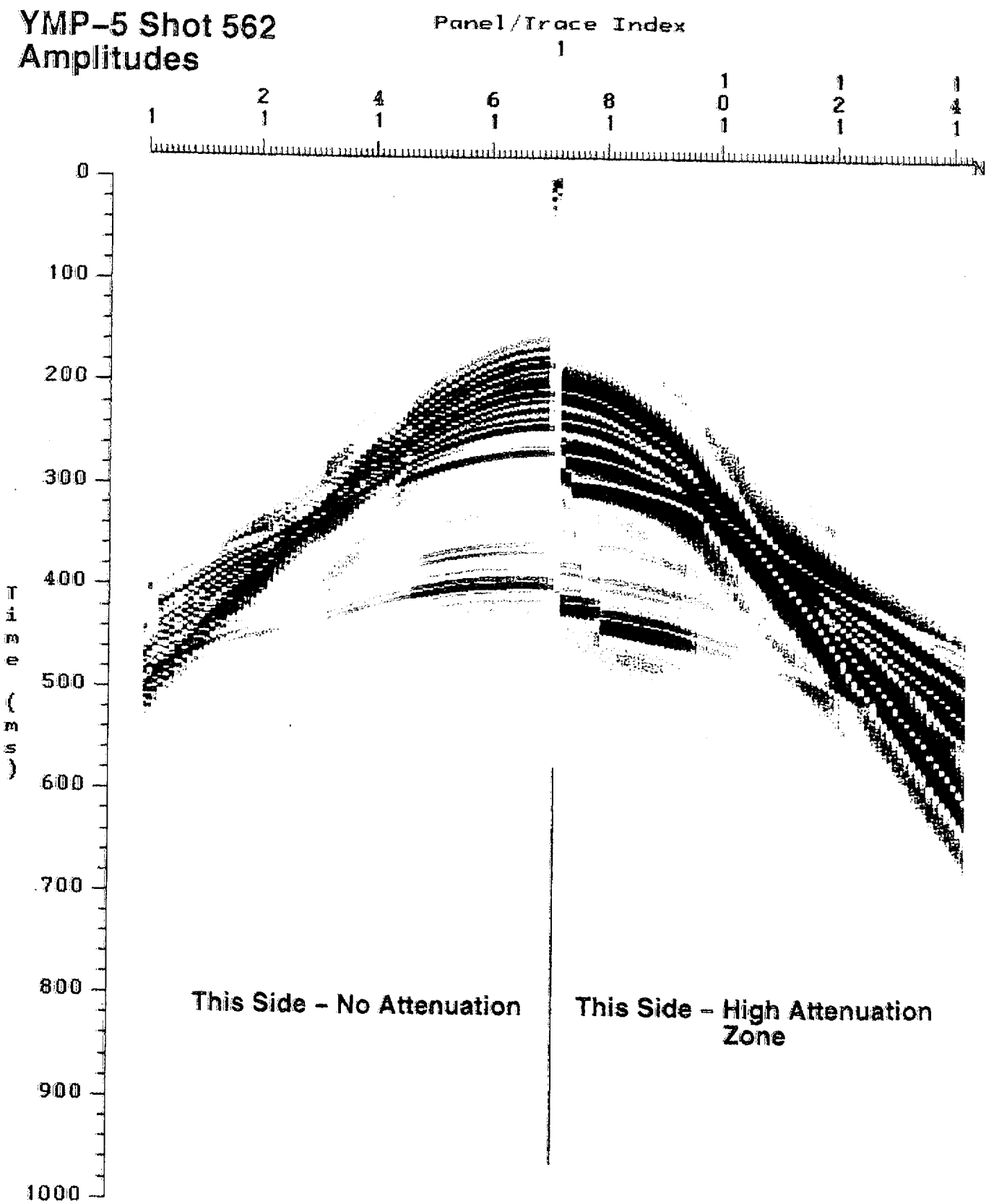

Figure 21 Reflection amplitudes for shot 562 from the YMP-5 attenuation model.

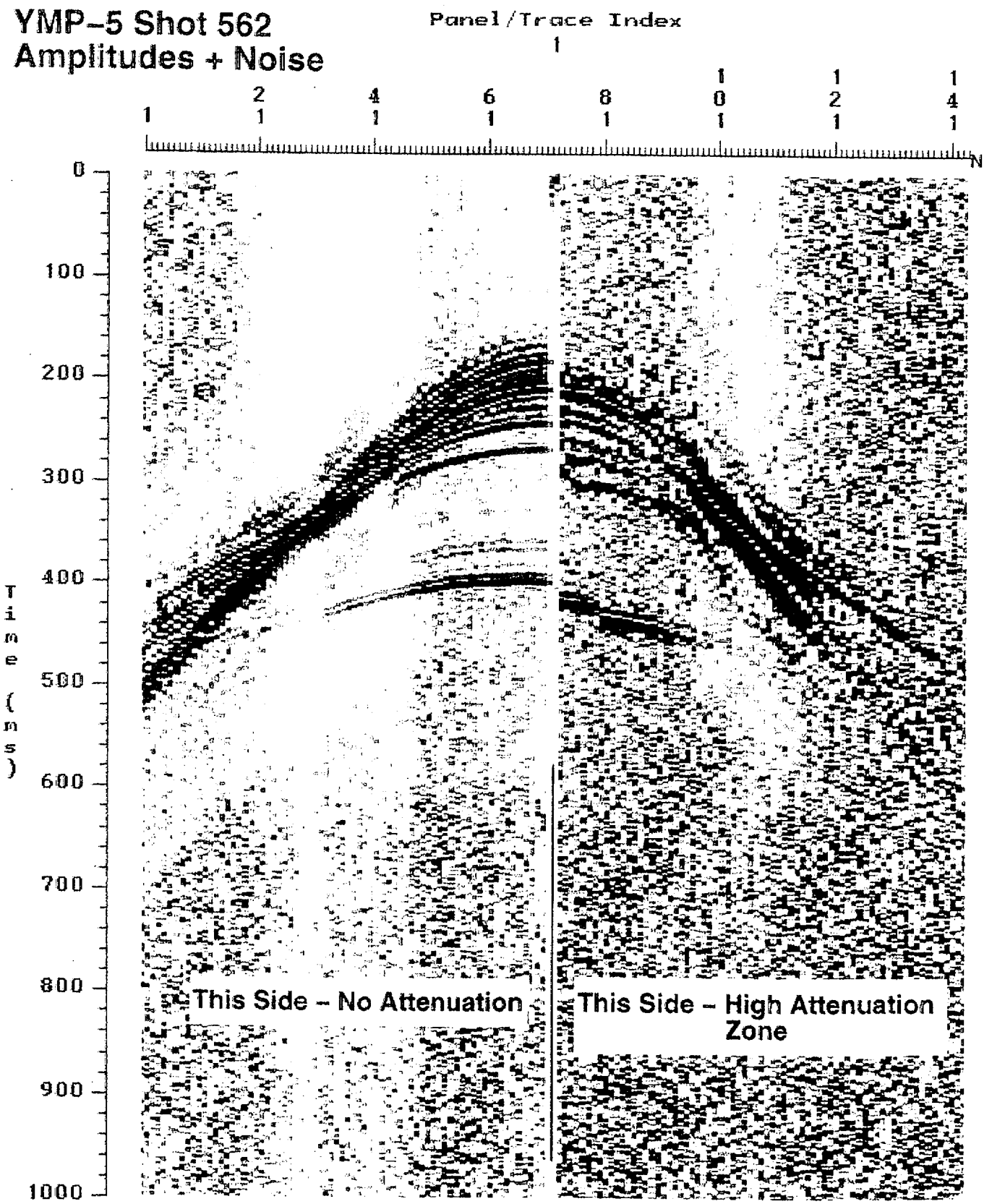

Figure 22 Reflection amplitudes for shot 562 from the YMP-5 attenuation model random noise added.

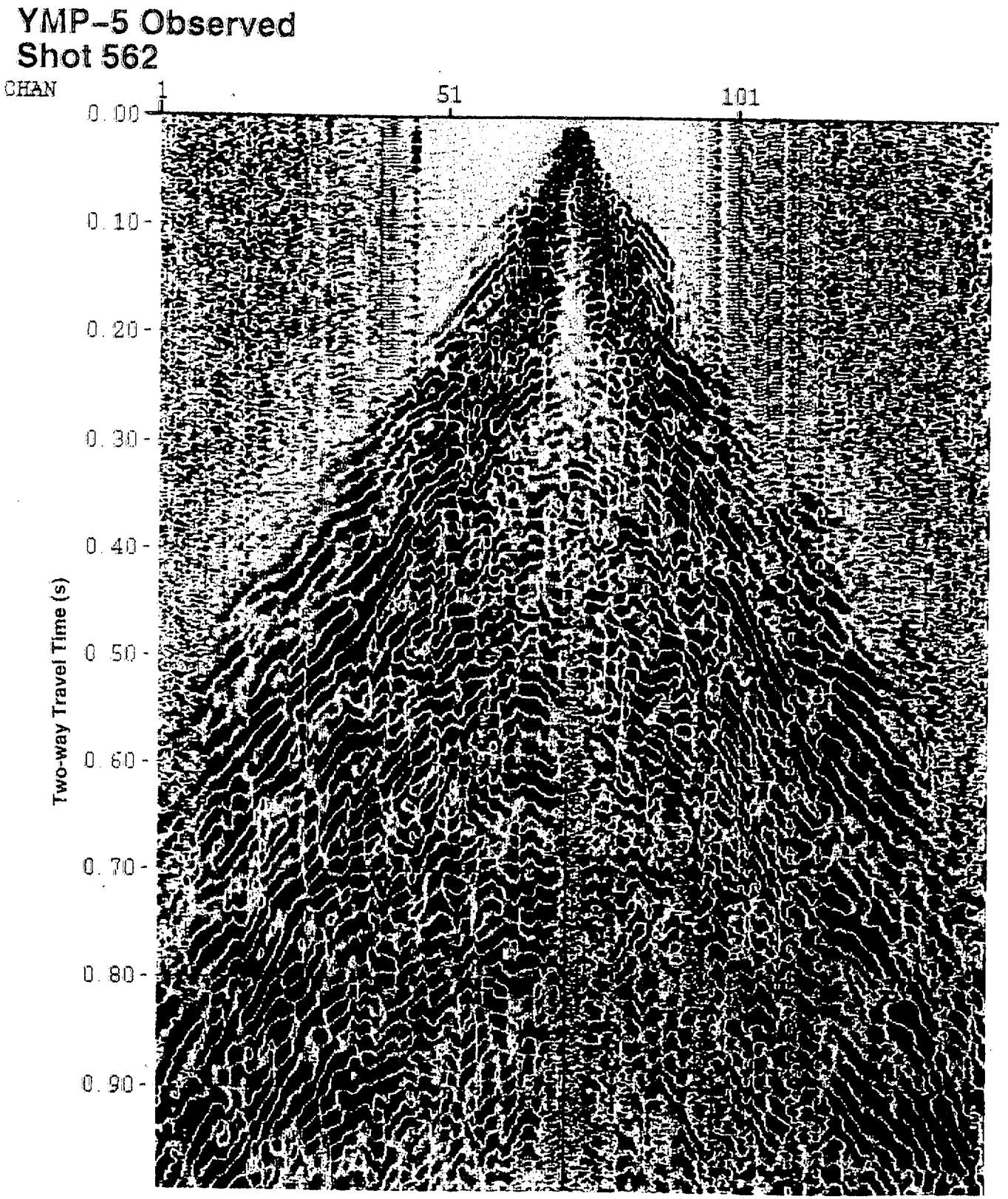

Figure 23 Field data for shot 562 from YMP-5.

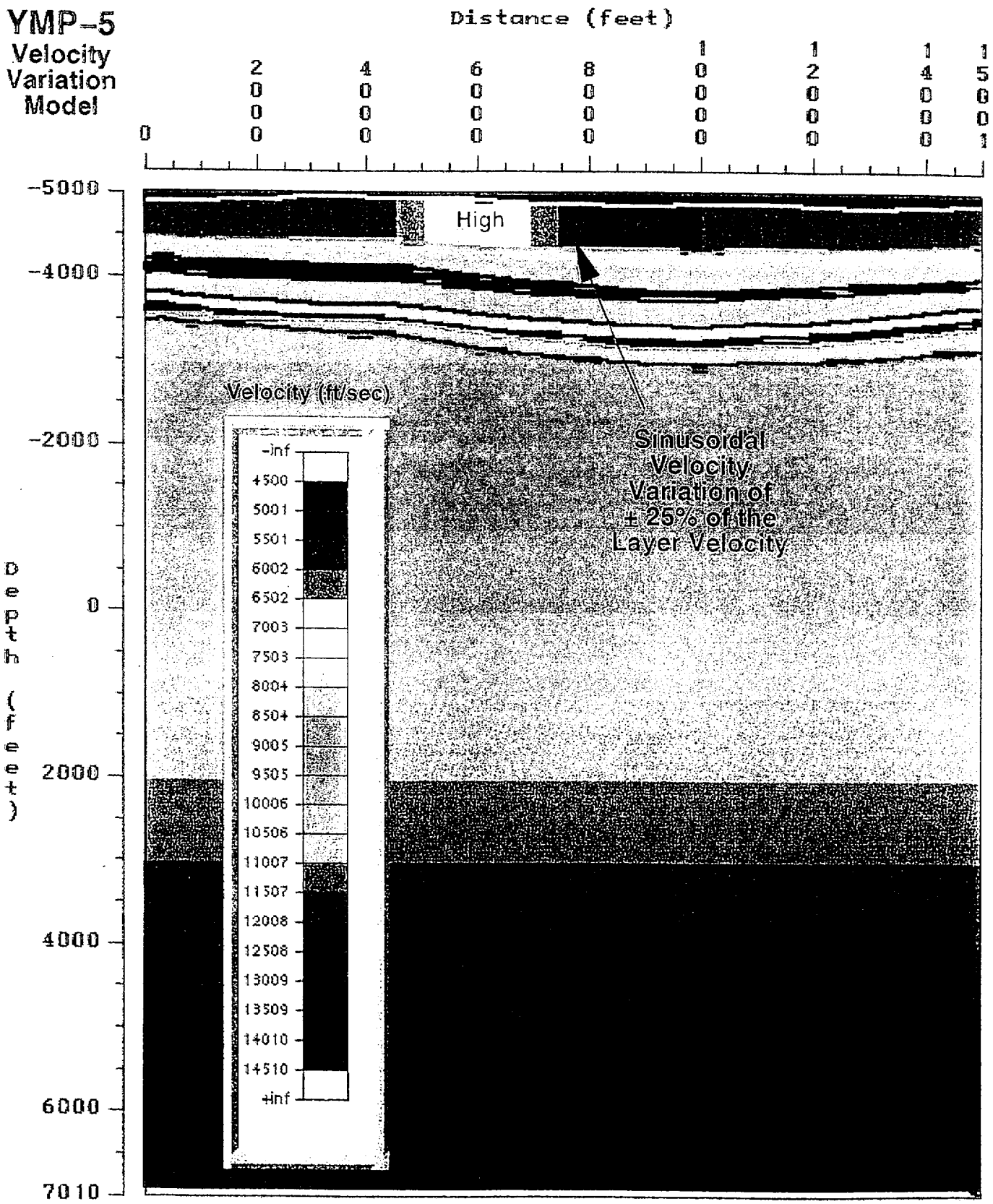

Figure 24 Lateral velocity variation model for YMP-5.

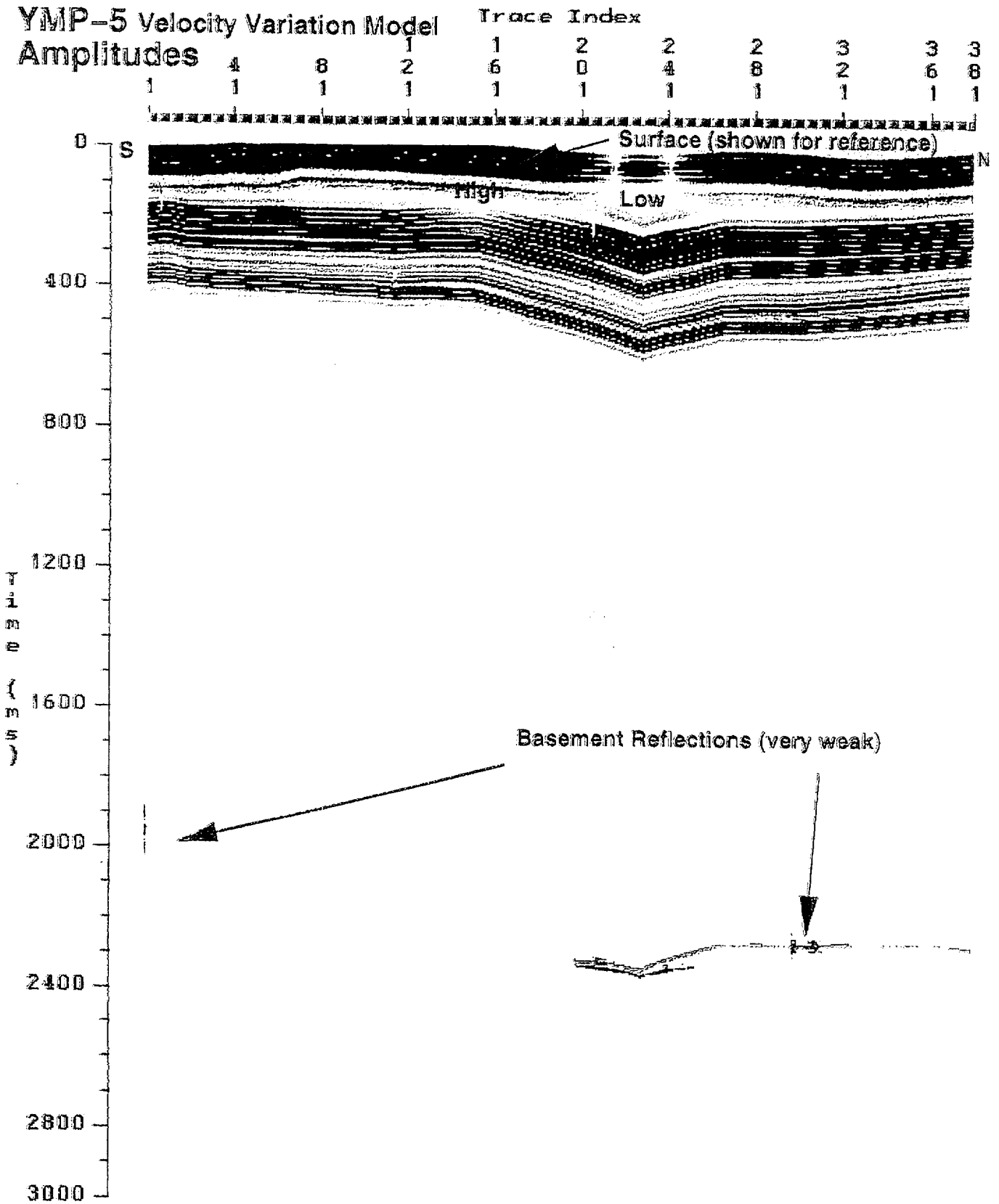

Figure 25 Reflection amplitudes for the lateral velocity variation model shown in Figure 24.

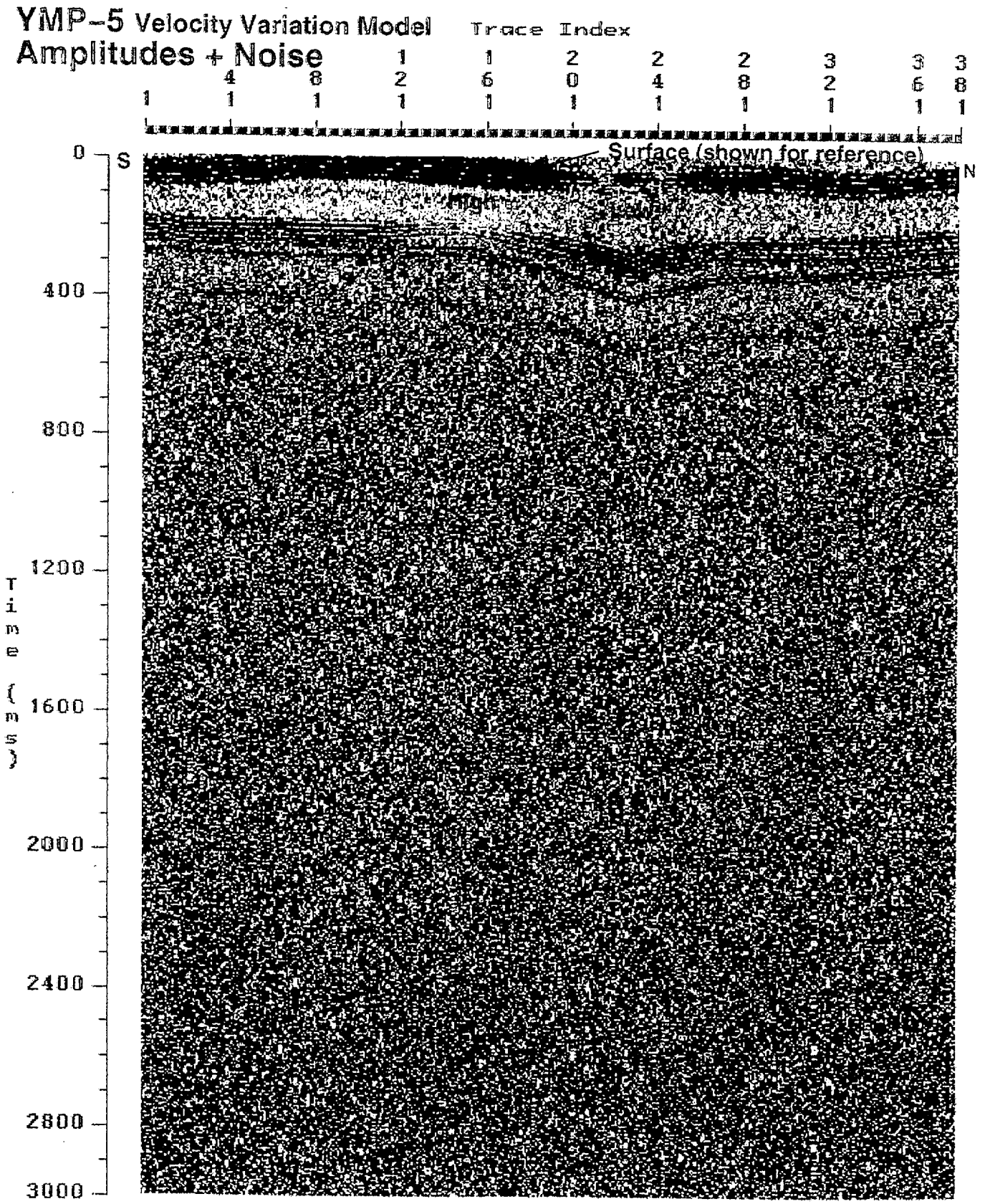

Figure 26 Reflection amplitudes for the lateral velocity variation model shown in Figure 24 with the addition of random noise. The ground level surface is shown as a seismic reflector for reference.

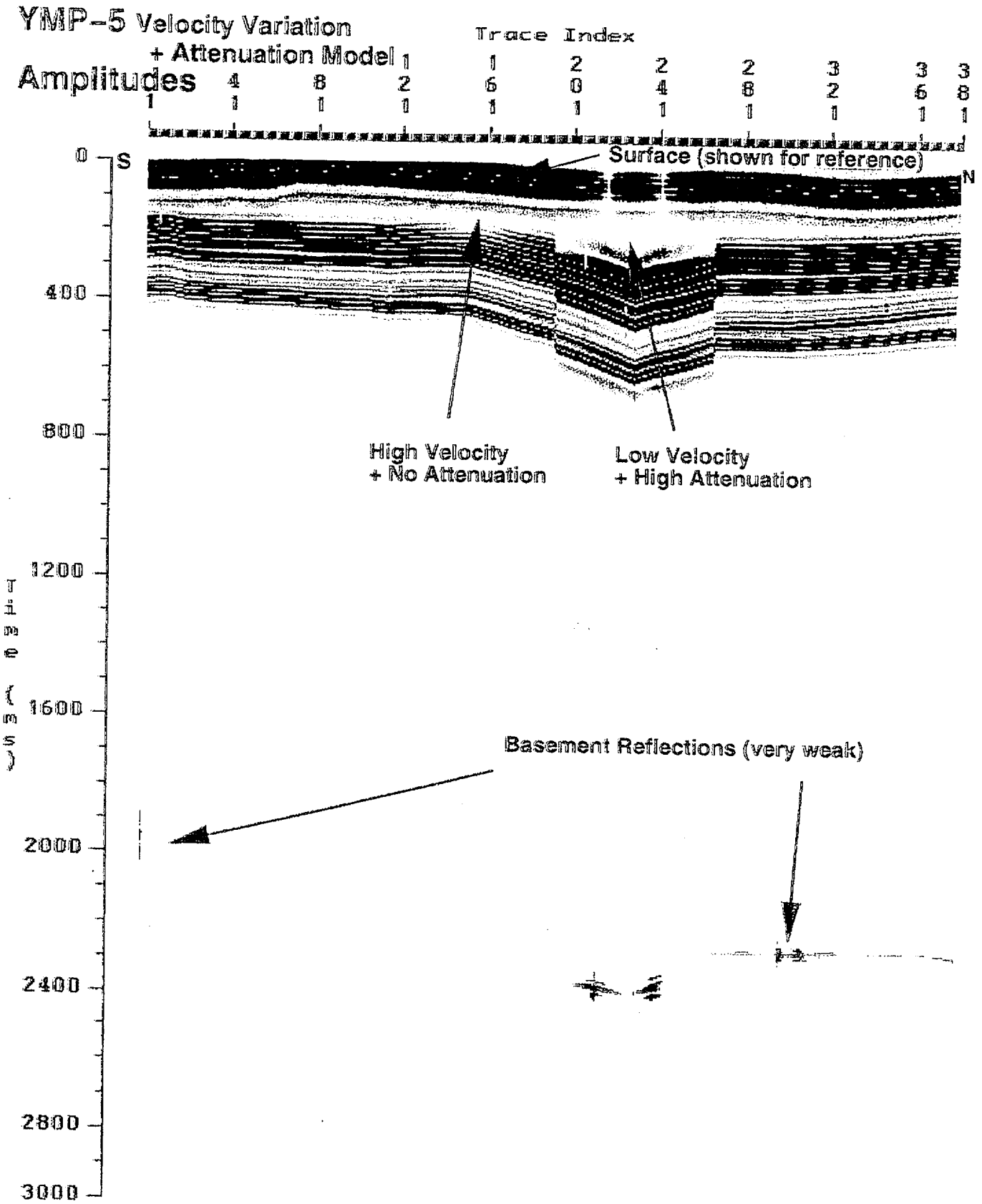

Figure 27 Reflection seismograms for a YMP-5 model which has both the high attenuation zone (see Figure 16) and the lateral velocity variation (Figure 24).

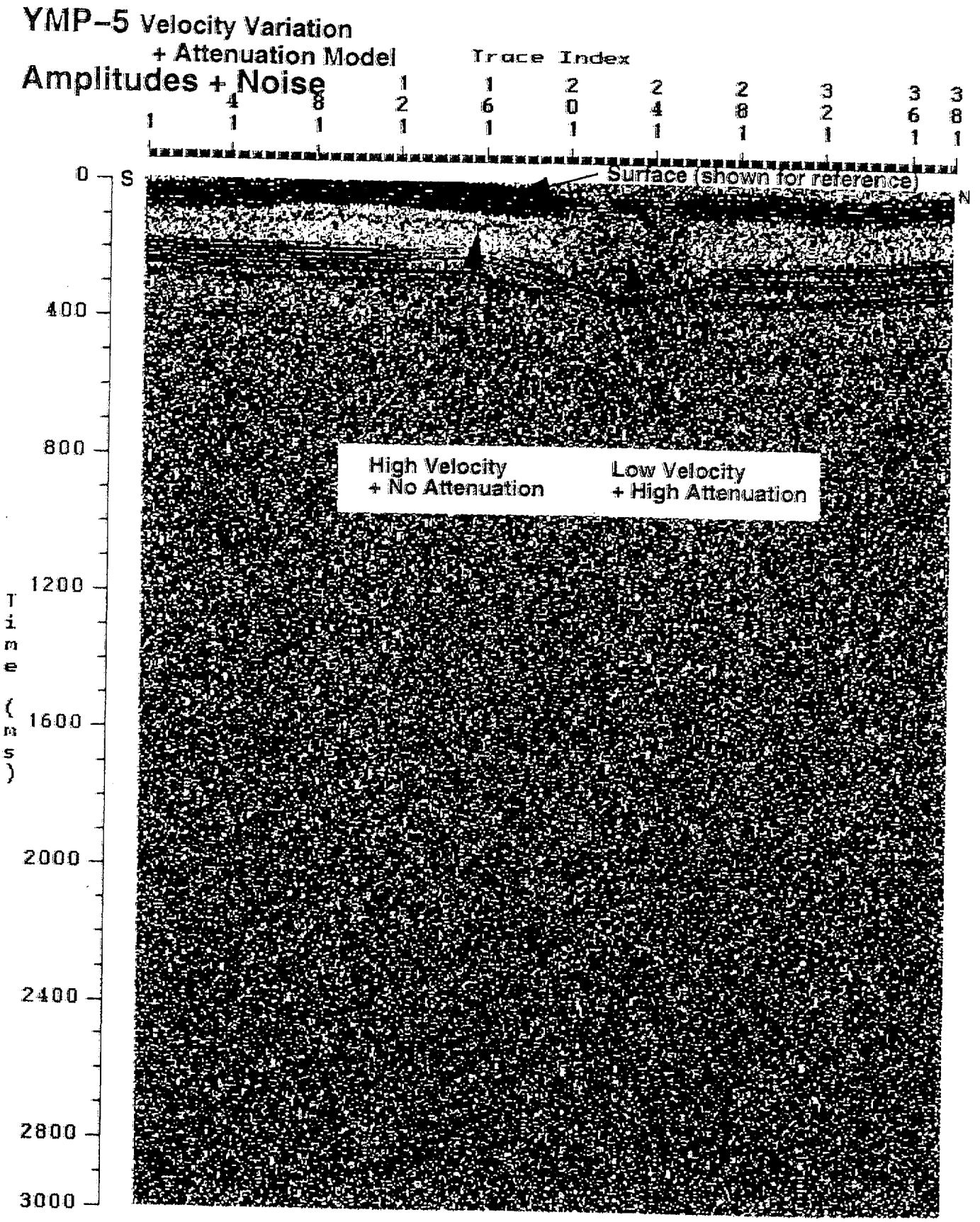

Figure 28 Reflection seismograms plus random noise for a YMP-5 model which has both the high attenuation zone (see Figure 16) and the lateral velocity variation (Figure 24).

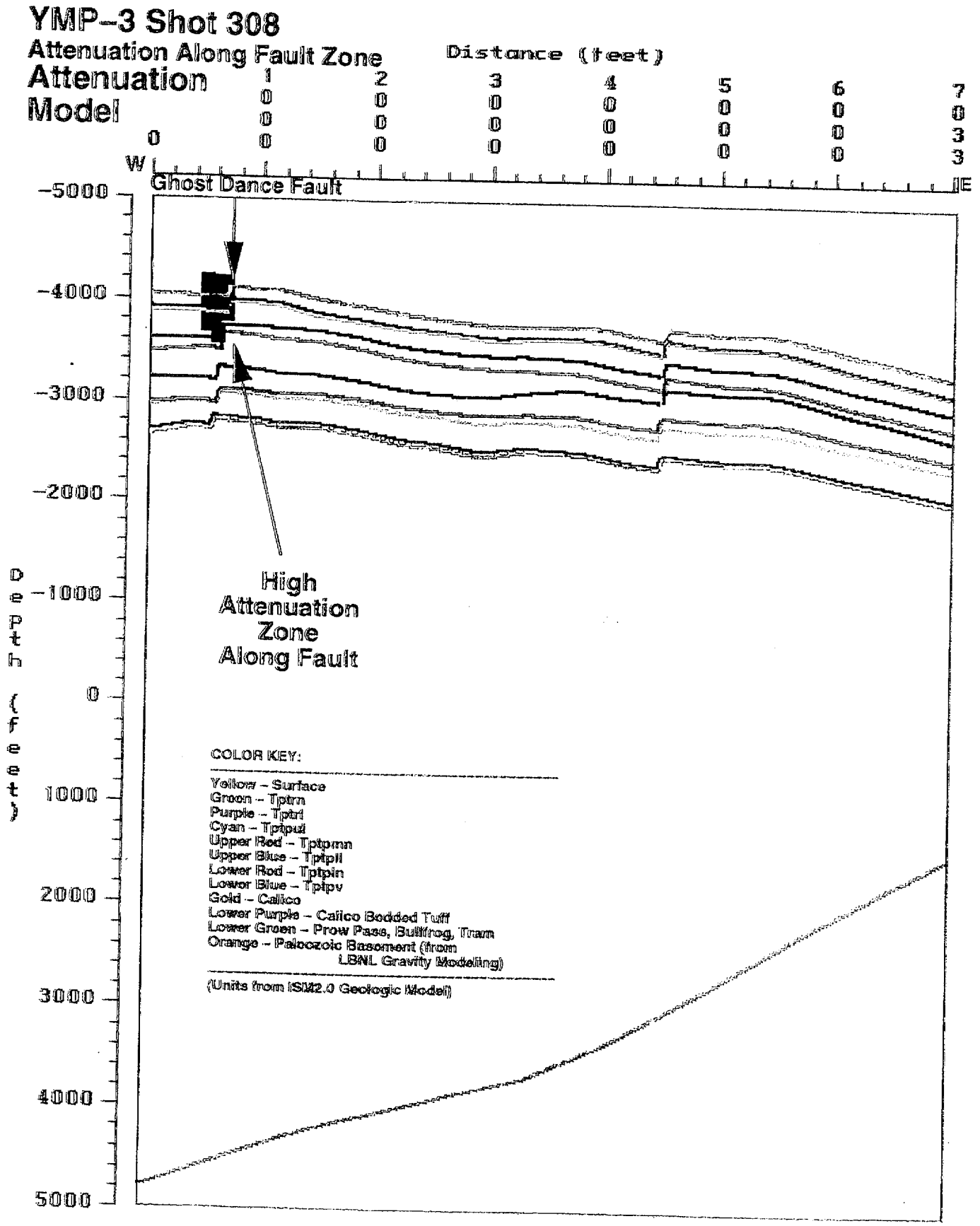

Figure 29 Geologic model of YMP-3 with a high attenuation zone superimposed on the shallow portion of the Ghost Dance Fault zone.

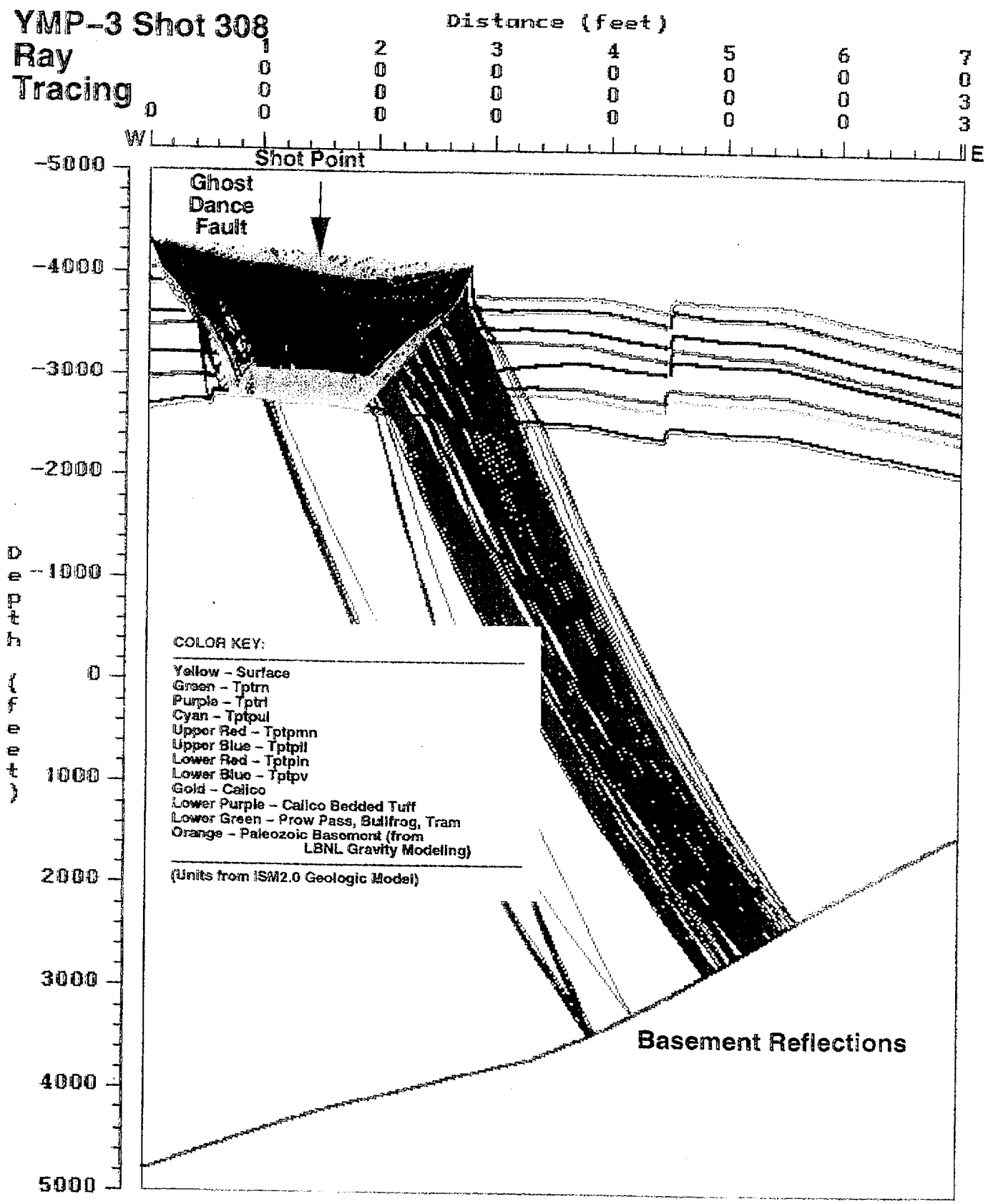

Figure 30 Raypaths for YMP-3 shot 308. The rays are color coded by the geologic horizon causing the reflection.

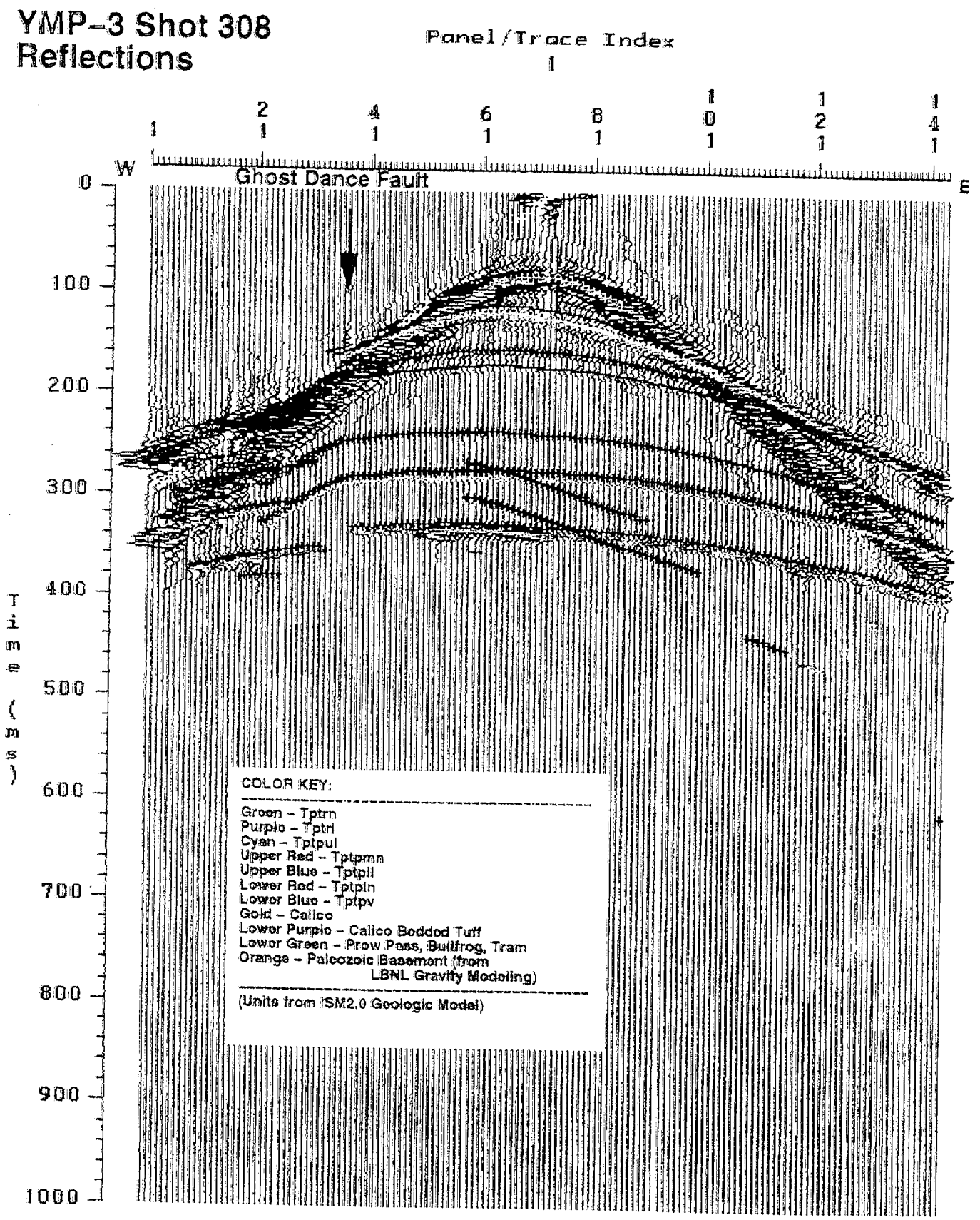

Figure 31a Reflection seismograms for the raypaths shown in Figure 30. All arrivals are color coded by the horizon generating the reflection.

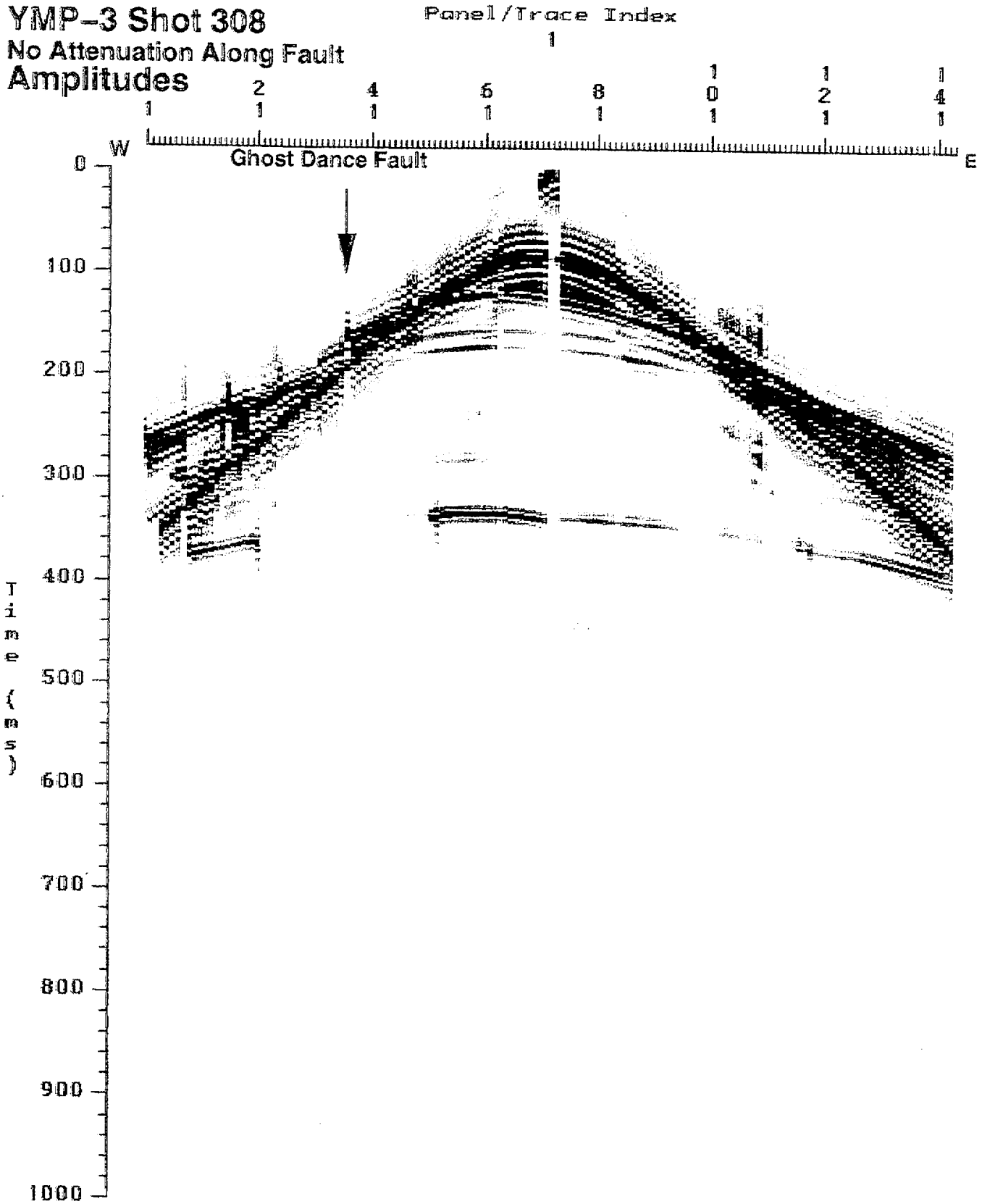

Figure 31b Reflection amplitudes for YMP-3 shot 308 for a model with no attenuation in the fault zone.

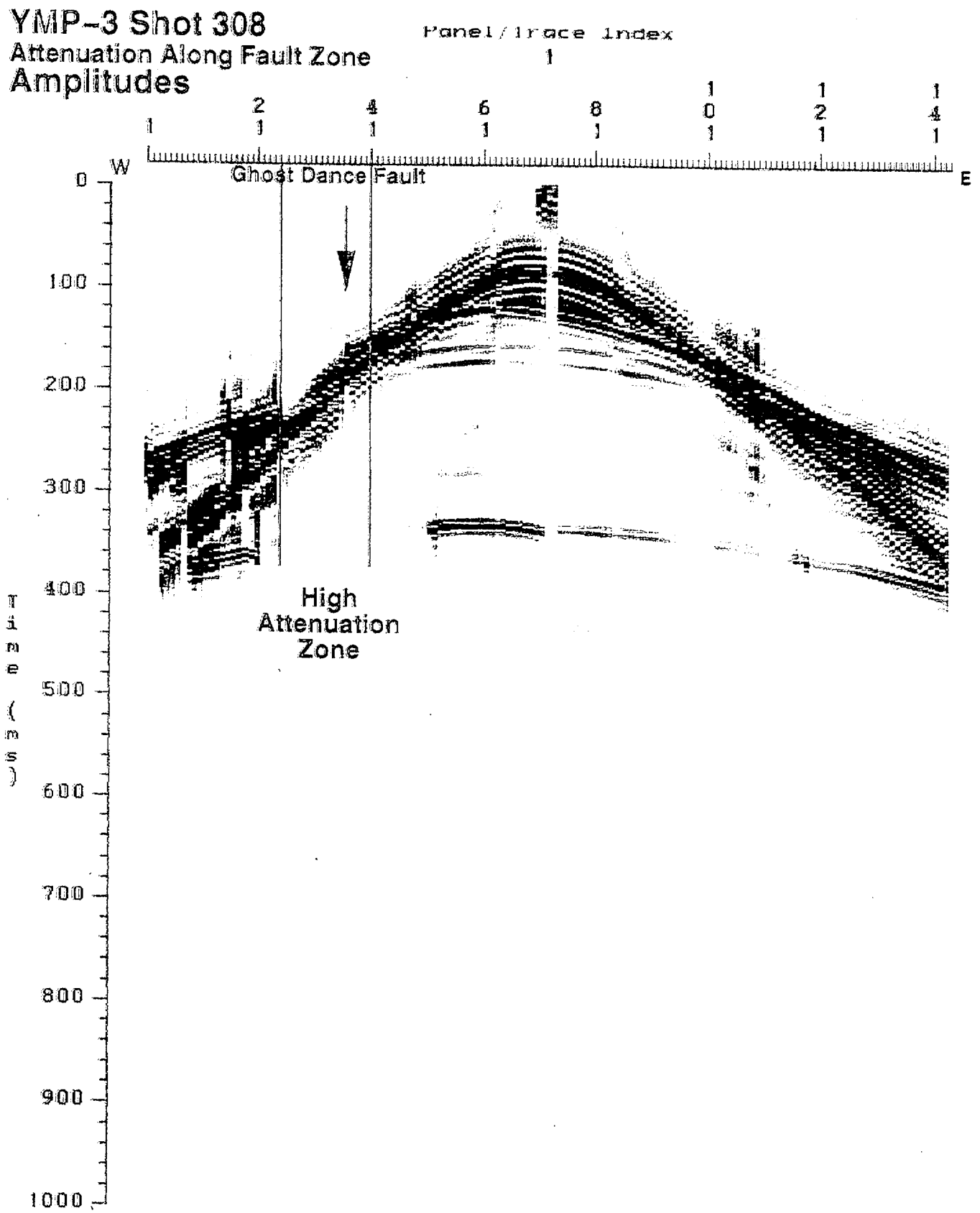

Figure 31c Reflection amplitudes for YMP-3 shot 308 for a model with high attenuation in the fault zone.

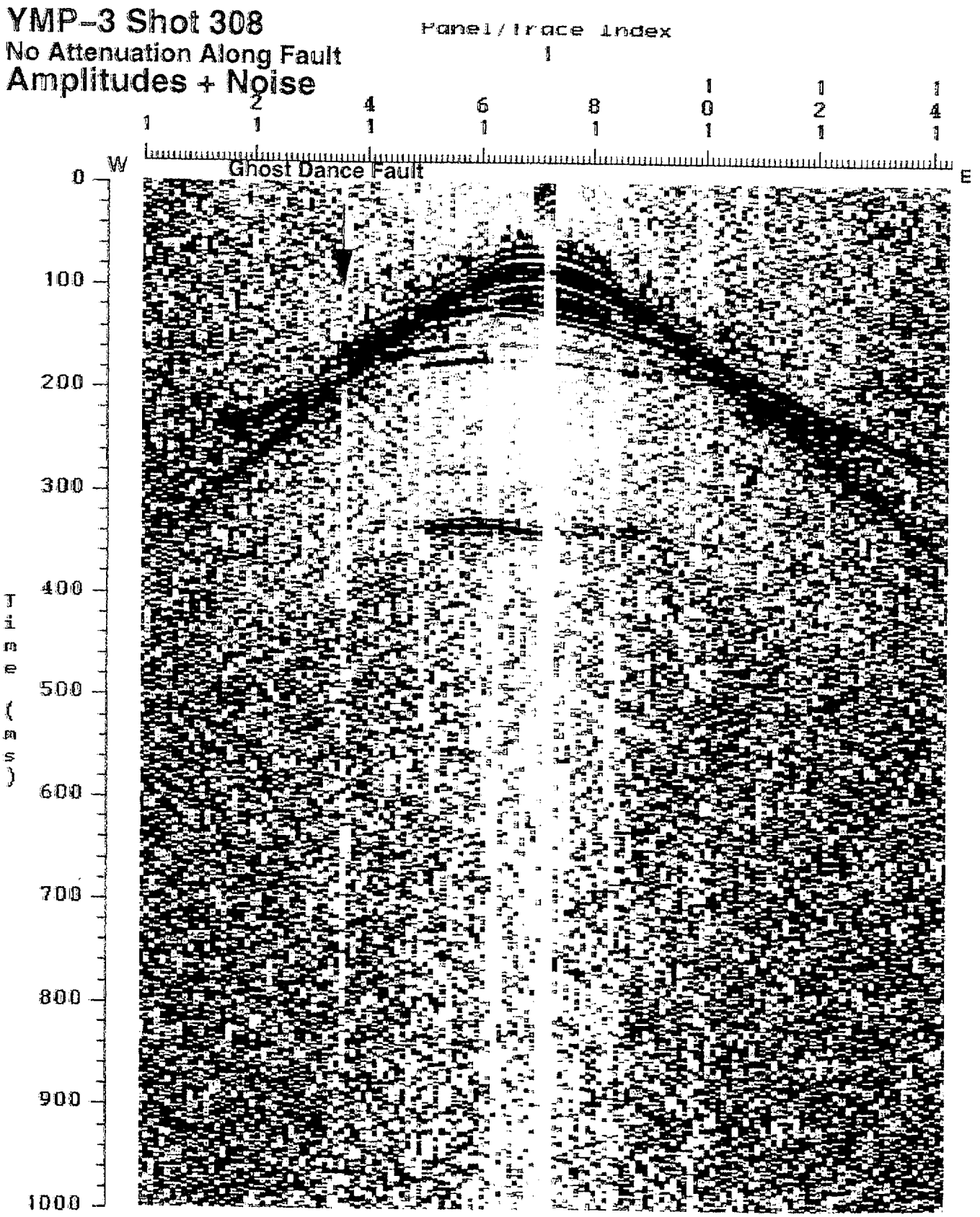

Figure 32a Reflection amplitudes plus random noise for YMP-3 shot 308 for a model no high attenuation in the fault zone.

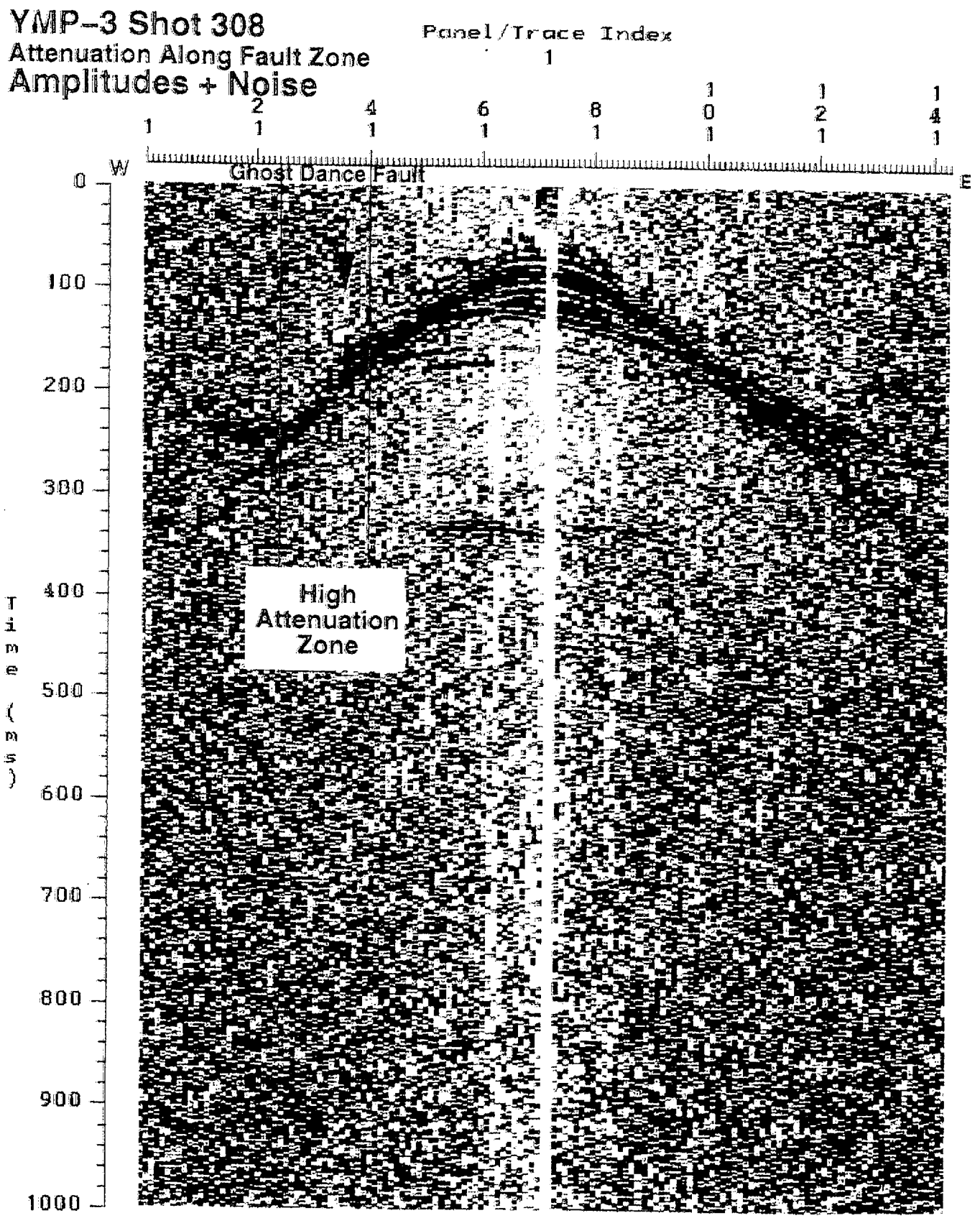

Figure 32b Reflection amplitudes plus random noise for YMP-3 shot 308 for a model with high attenuation in the fault zone.

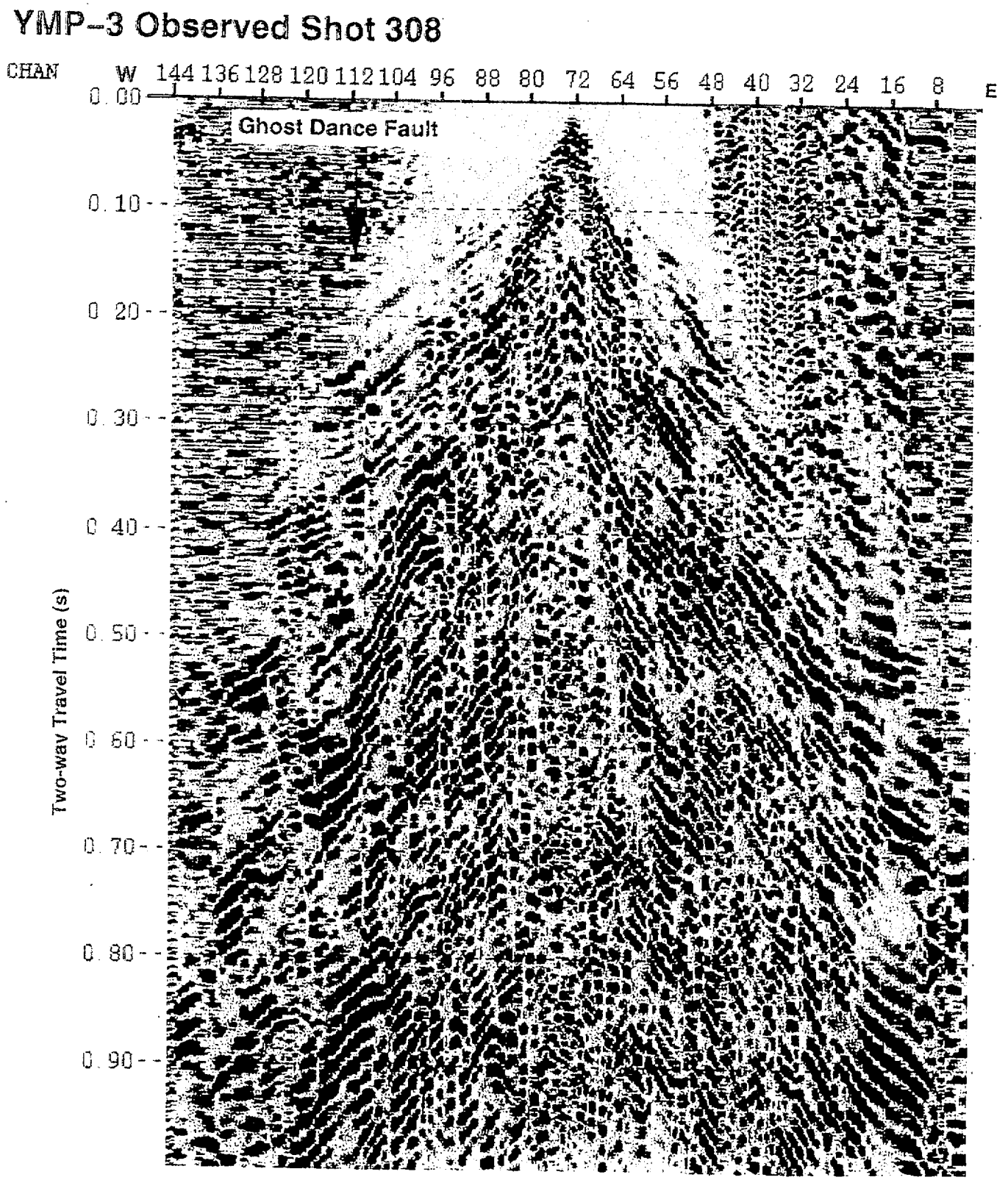

Figure 33 Field data for shot 308 from YMP-3.

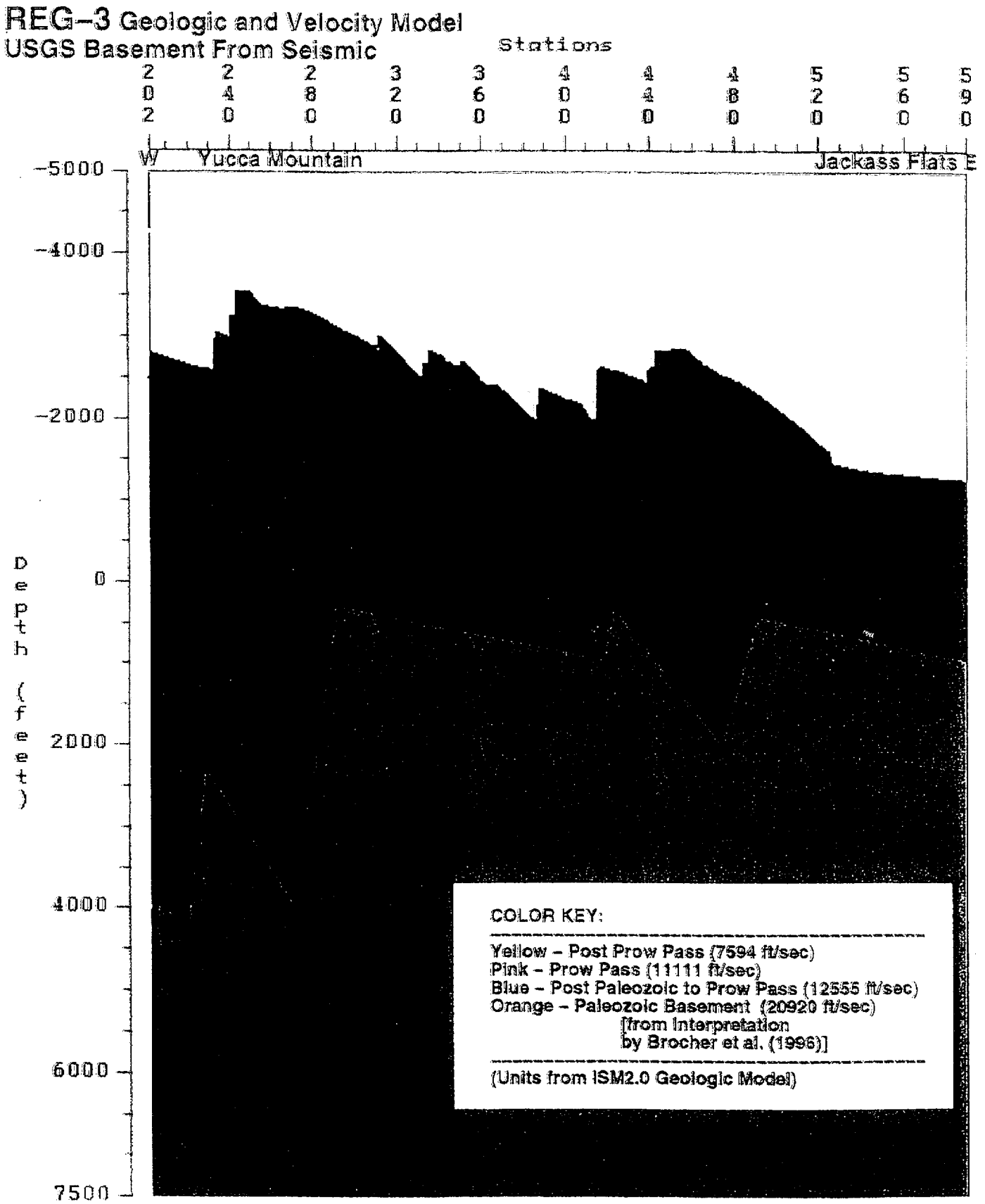

Figure 34 Geologic model for REG-3 showing a Paleozoic basement structure derived from USGS seismic interpretation. The velocities assigned to each unit are listed in the color key box.

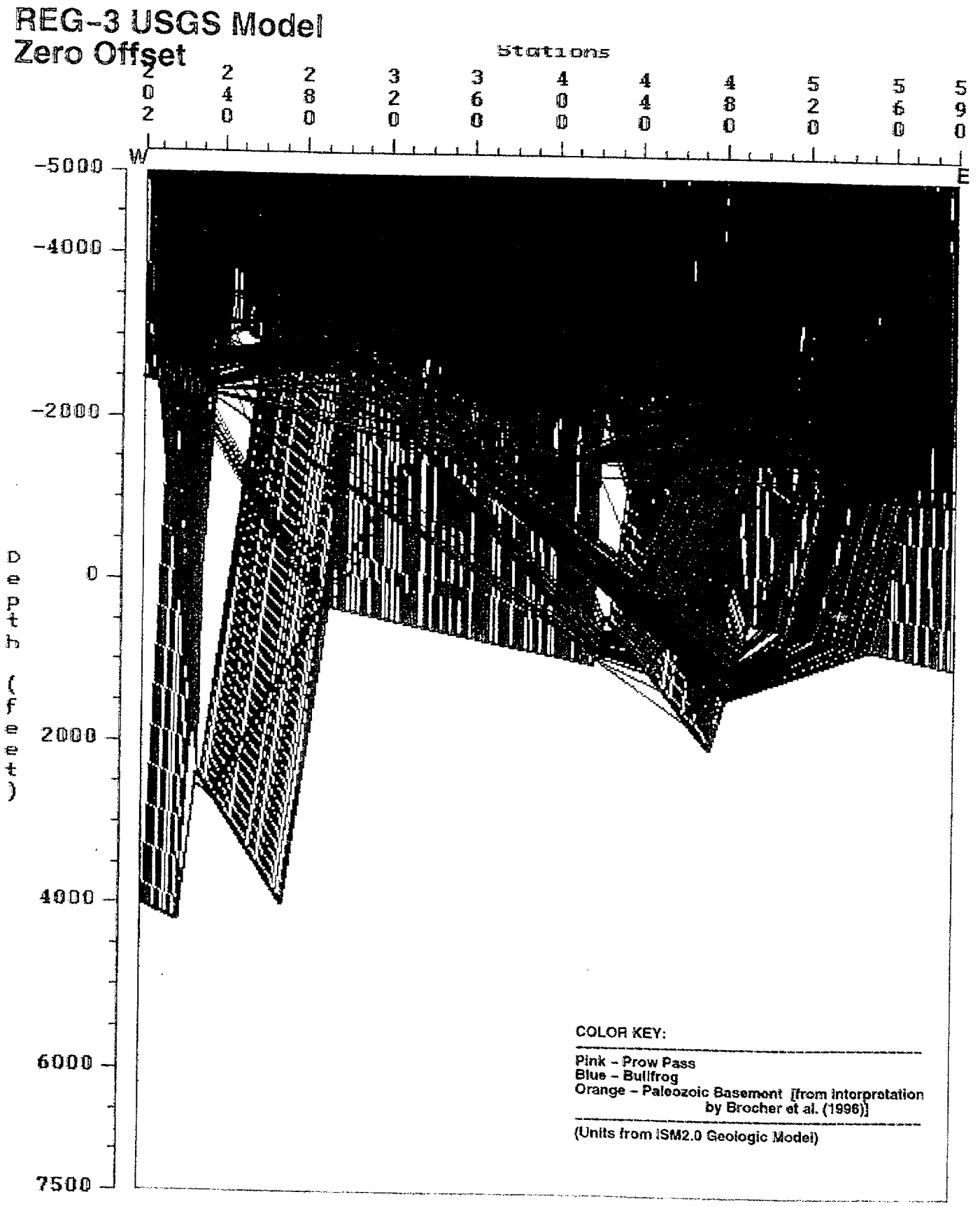

Figure 35 Raypaths for zero offset modeling of the model shown in Figure 34.

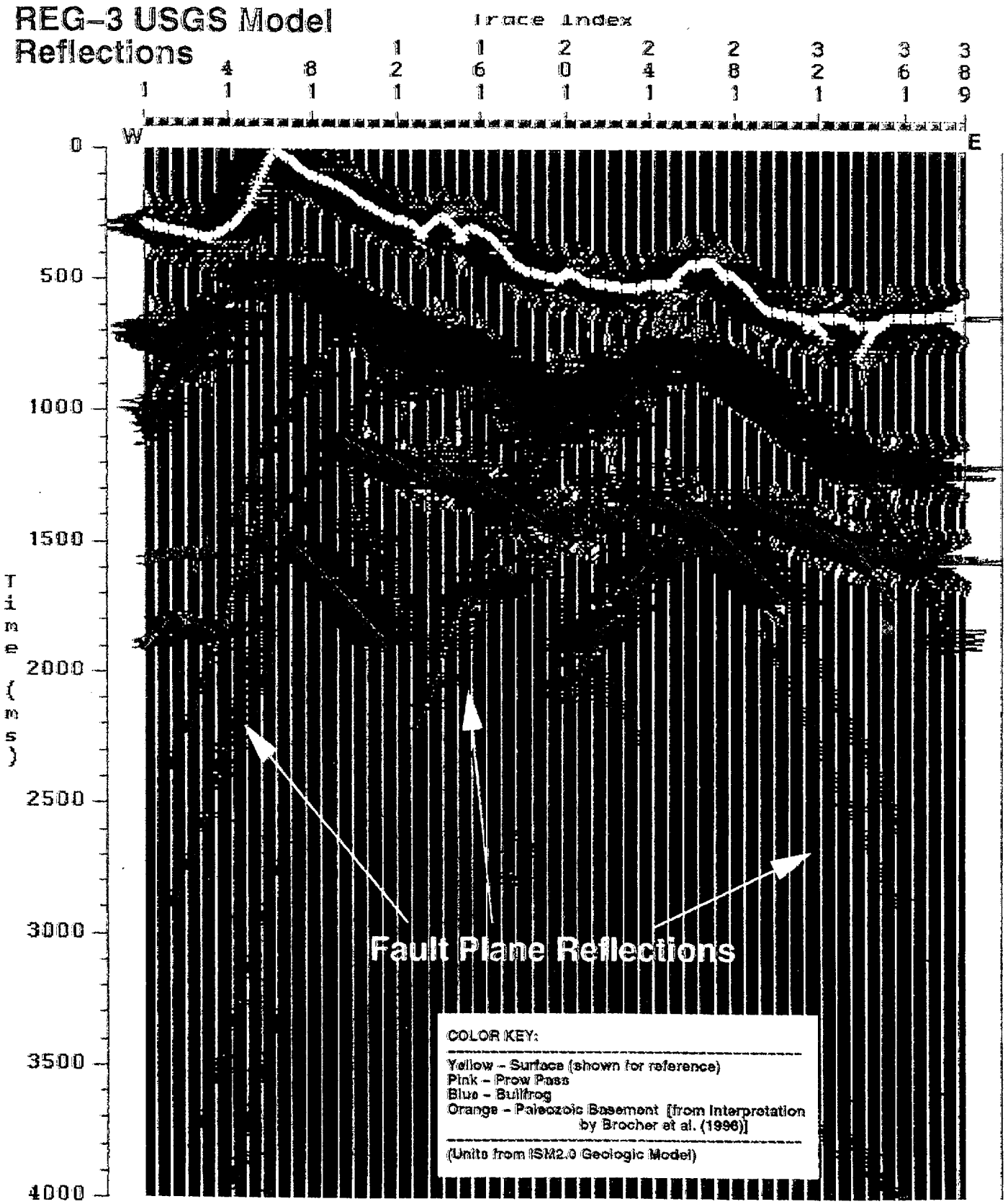

Figure 36 Reflection seismograms for the raypaths from Figure 35. All arrivals are color coded by the horizon generating the reflection. Many fault plane reflection events are observed.

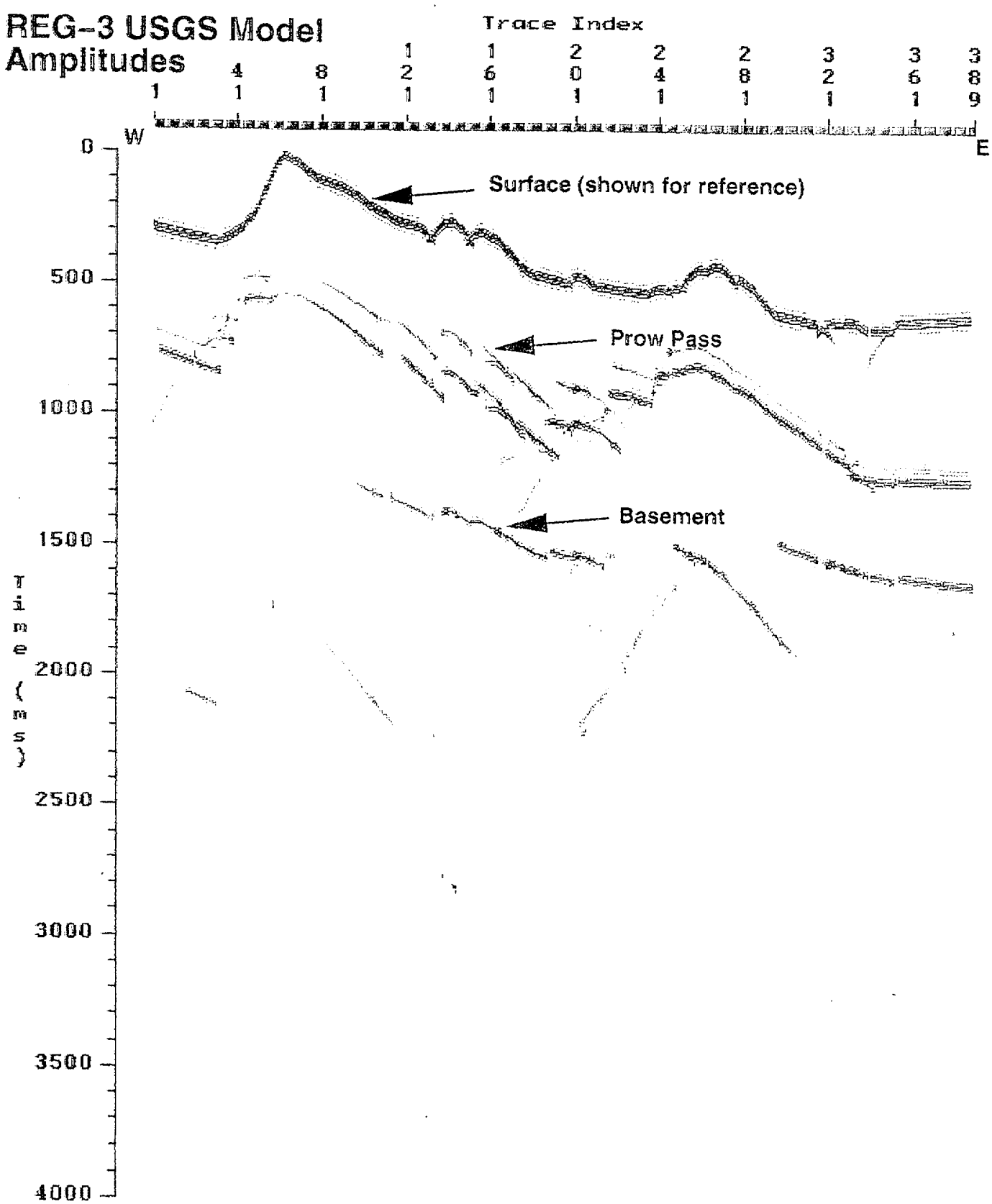

Figure 37 Reflection amplitudes for the raypaths from Figure 35. The ground level surface is shown as a seismic reflector for reference.

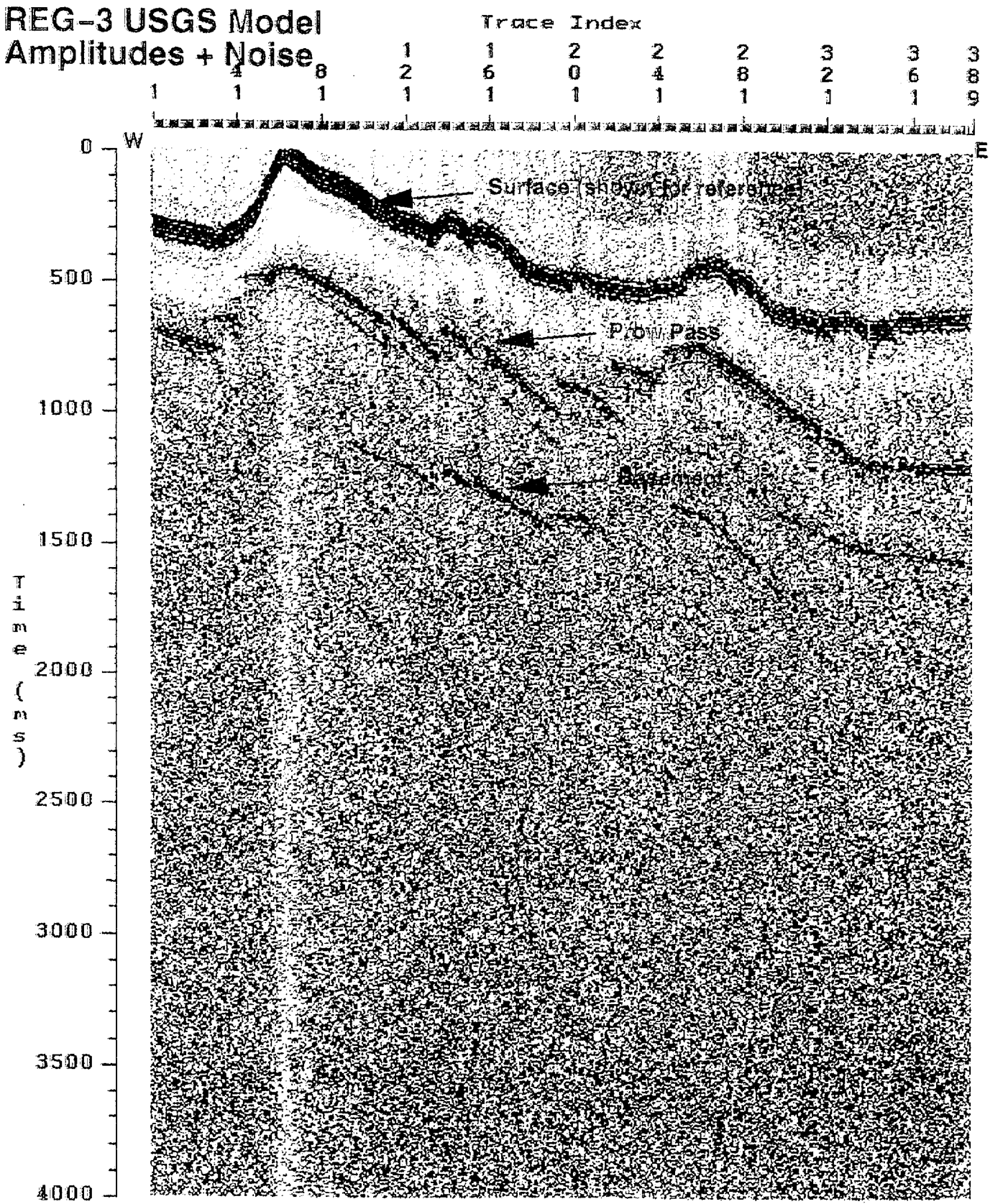

Figure 38 Reflection amplitudes plus random noise for the raypaths shown in Figure 35. The ground level surface is shown as a seismic reflector for reference.

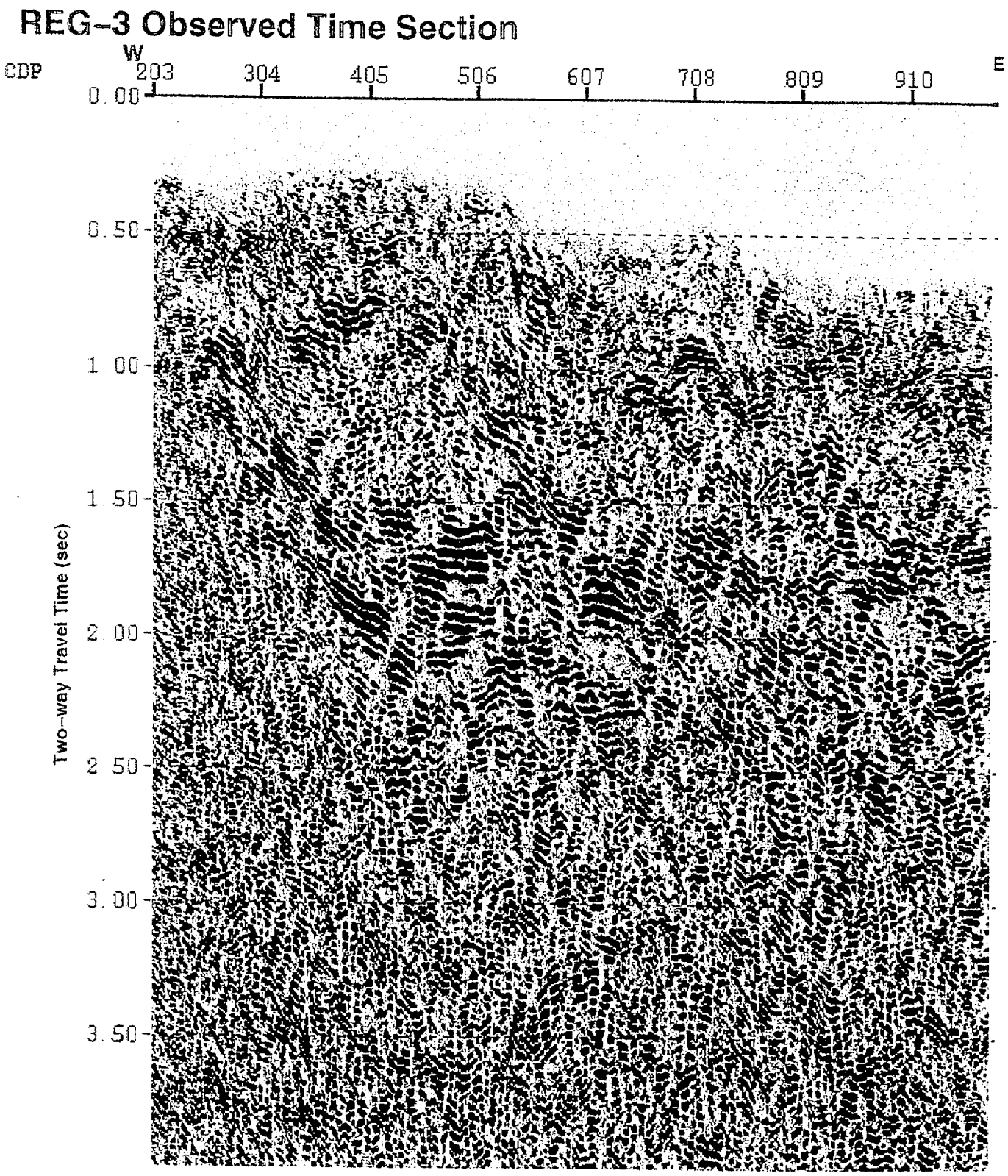

Figure 39 Field data in CDP time section for REG-3.

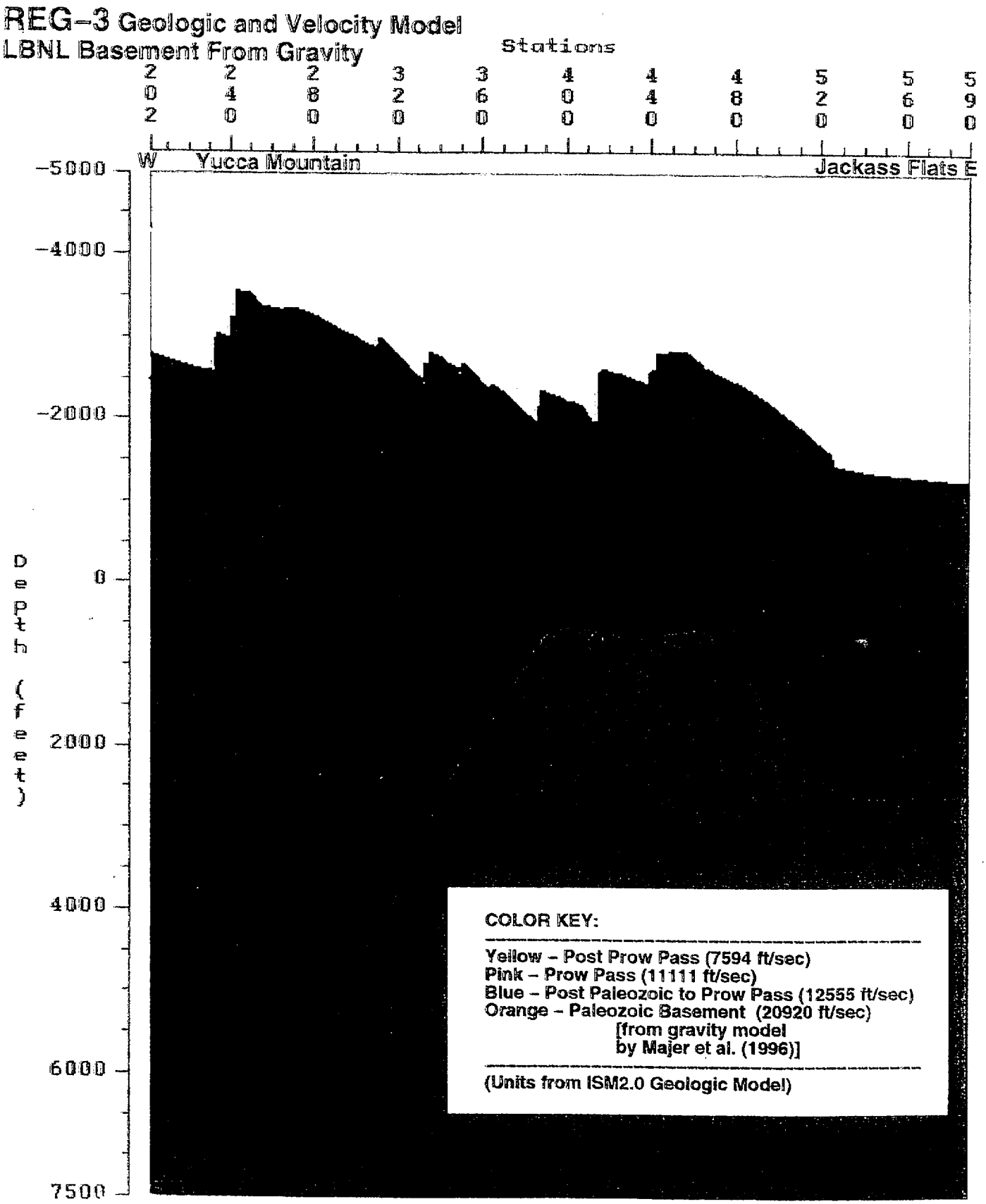

Figure 40 Geologic model for REG-3 showing a Paleozoic basement structure derived from LBNL gravity interpretation. The velocities assigned to each unit are listed in the color key box.

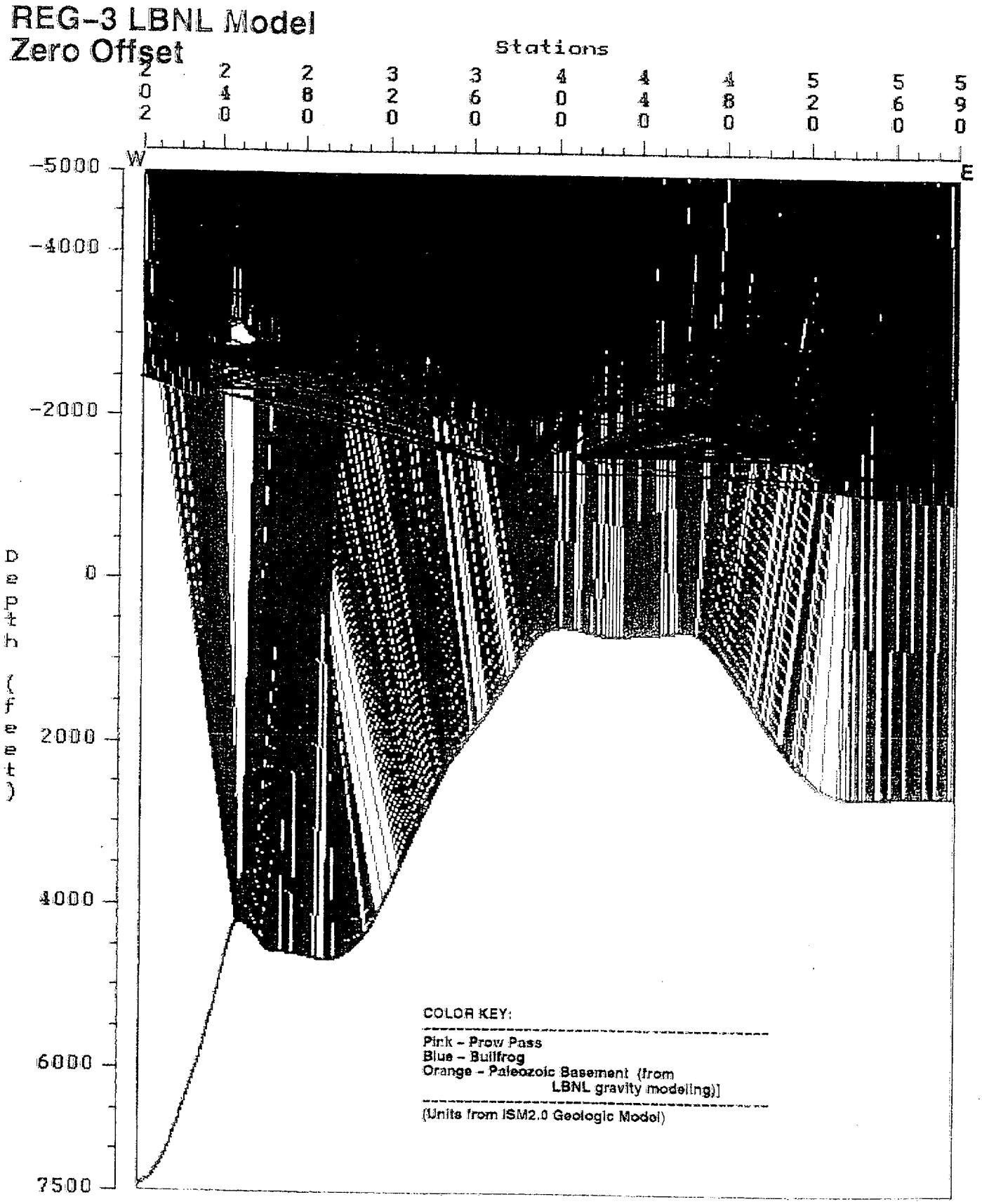

Figure 41 Raypaths for zero offset shooting of the model shown in Figure 40. All rays are color coded by the horizon generating the reflection.

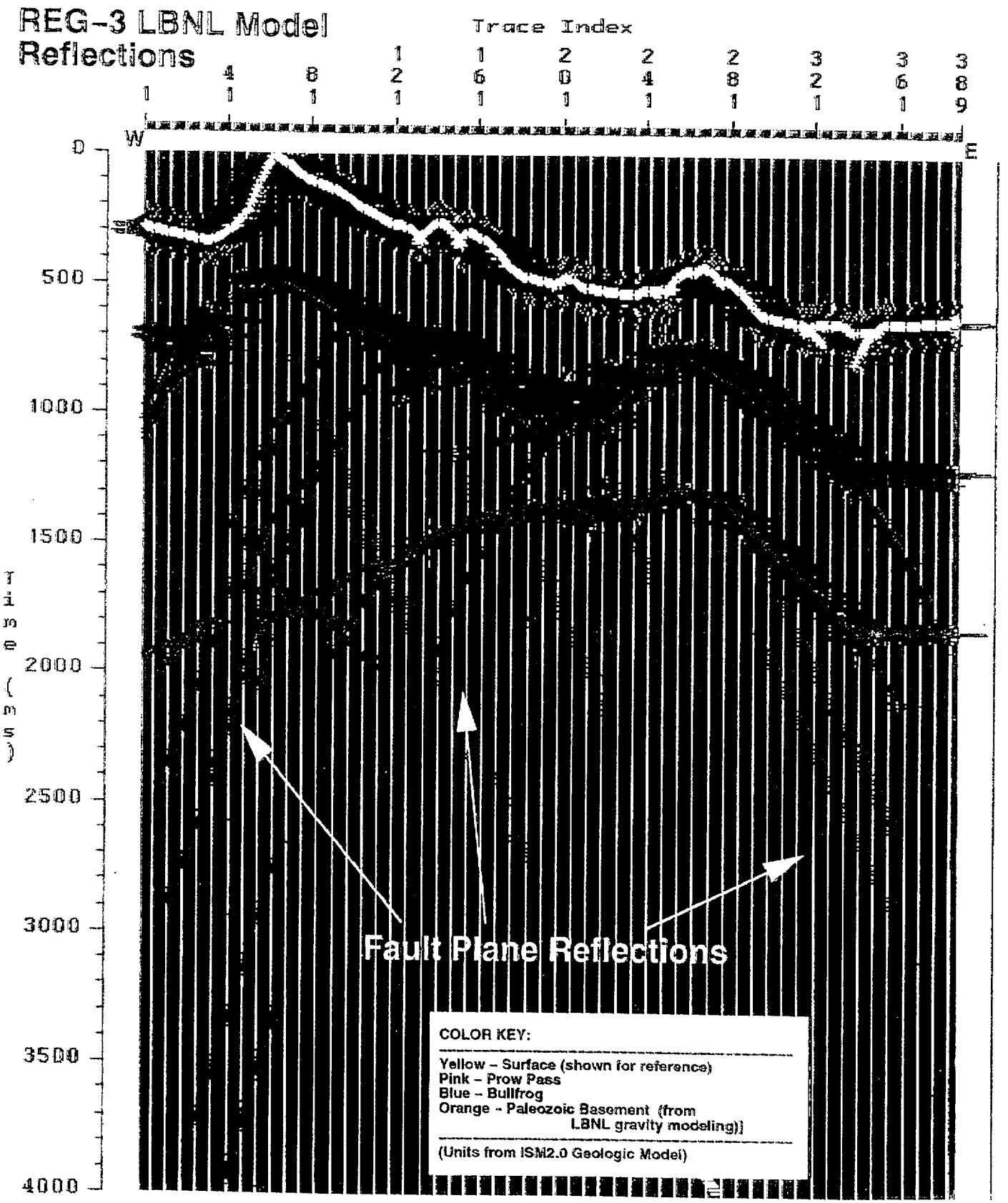

Figure 42 Reflection seismograms for the raypaths shown in Figure 41. All arrivals are color coded by the horizon generating the reflection.

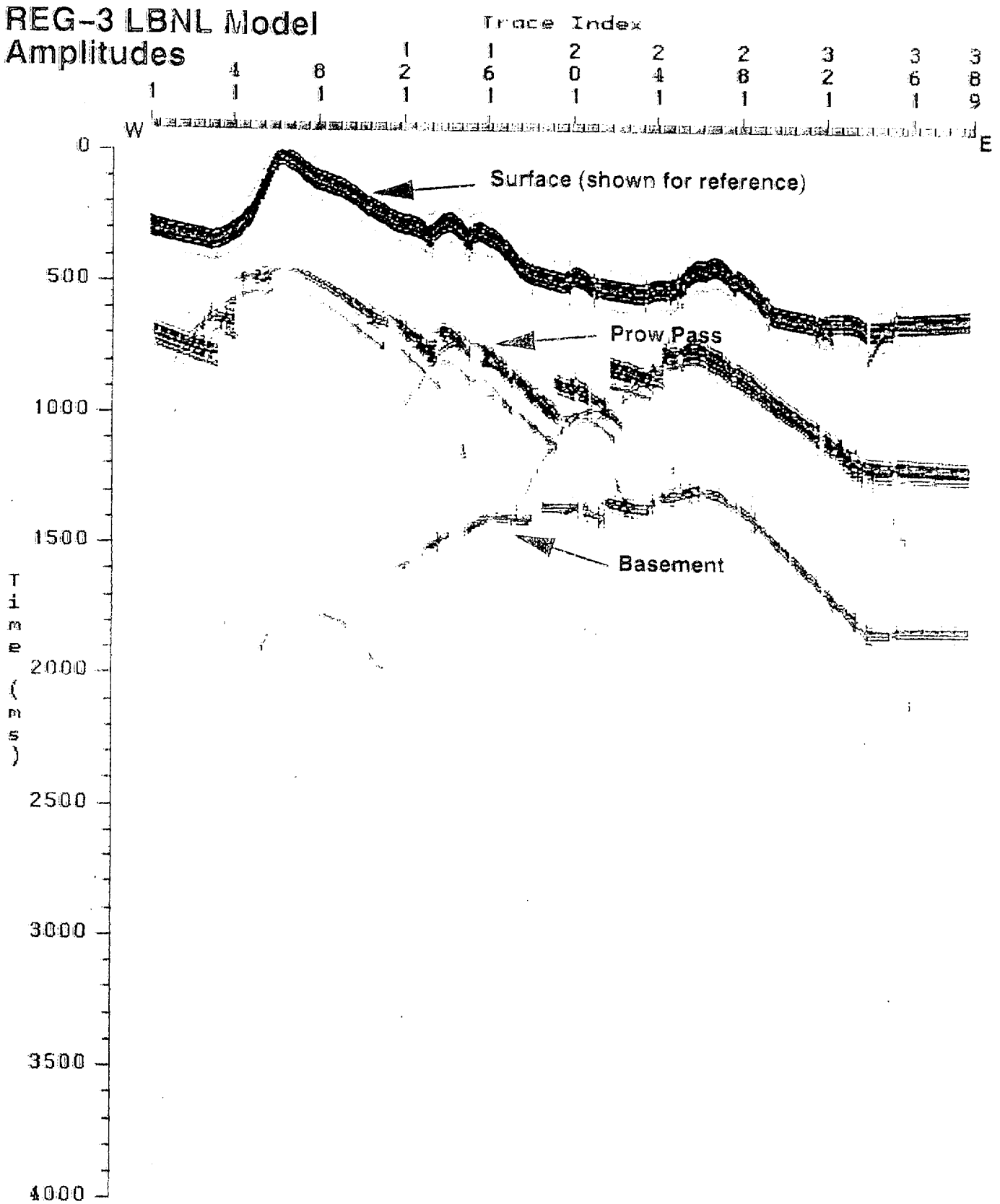

Figure 43 Reflection amplitudes for the seismograms shown in Figure 42. The ground level surface is shown as a seismic reflection for reference.

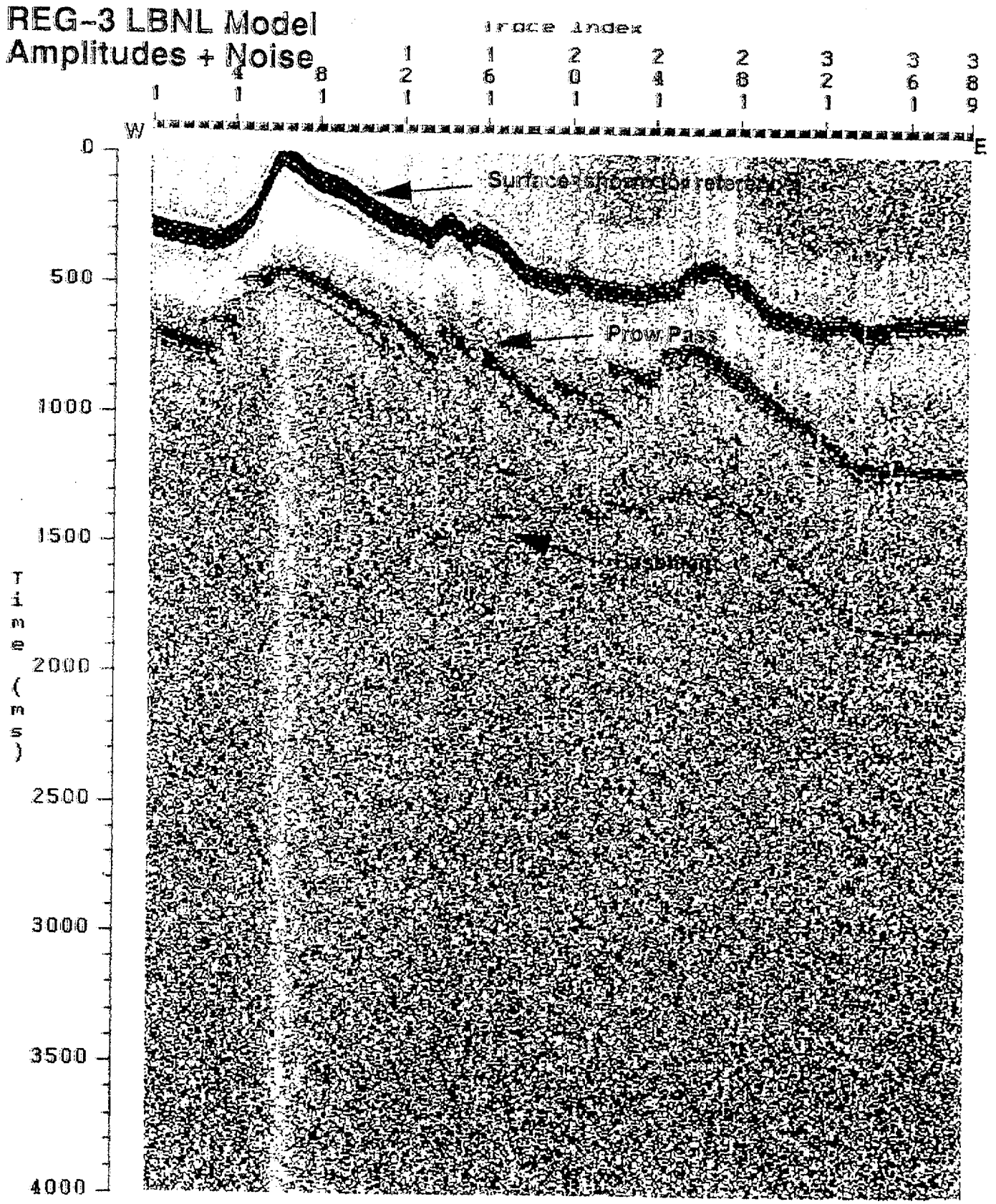

Figure 44 Reflection amplitudes plus random noise for the seismograms shown in Figure 42. The ground level surface is shown as a seismic reflection for reference.

Table 1. P-WAVE INTERVAL VELOCITIES USED IN MODELING

Geologic Unit	YMP-3 Velocity (ft/s)*	YMP-5 Velocity (ft/s)*	REG-3 Velocity (ft/s)+
Post-Tptrn	4000	6000	
Tptrn	7965	7965	
Tptrl	6713	very thin, not modeled	
Tptpul	10456	10456	
Tptpmn	13619	13619	
Tptpll	9909	9909	
Tptpln	10710	10710	
Tptpv3	12185	12185	
Calico	10367	10367	
Calico Bedded Tuff	14063	14063	
Pre-Calico Bedded Tuff	8218 with a gradient of 0.5 ft/s per foot to basement	8218 with a gradient of 0.5 ft/s per foot to basement	
	|	|	
Post-Prow Pass Tuff	|	|	7594 to surface
Prow Pass Tuff	|	|	11111
Bullfrog to Basement	| V	| V	12555
Paleozoic Basement	12000 with a gradient of 1 ft/s per foot	12000 with a gradient of 1 ft/s per foot	20920

*Kaelin and Johnson (1997) VSP data from well UZ-16, units Tptrn to Calico Bedded Tuff (smoothed averages from Figure 3).
+Brocher et al. (1996) VSP data from well UE-25 p#1 (Table 11).

Table II-1

Mineralogical composition of the rock matrix in UZ 16

	Fused Quartz	K-Feldspar	Glass	Zeolite
Alluvial Fill (0 - 47 ft.):	-	-	100 %	-
Tiva Canyon and Bedded Tuffs (47 - 195 ft.):	30 %	70 %	-	-
Topopah Spring Tuff (195 - 1111 ft.):	35 %	65 %	-	-
Vitric Zone (1111 - 1201 ft.):	35 %	10 %	55 %	-
Callico Hills Formation (1201 - 1485 ft.):	15 %	20 %	-	65 %
Prow Pass Tuff (1485 - 1640 ft.):	25 %	75 %	-	-

The single minerals have the following seismic properties:

	v_p (km/s)	v_s (km/s)	ρ (g/cm^3)	
Fused Quartz	5.60	3.60	2.20	(Carmichael, 1982)
K-Feldspar	5.88	3.05	2.57	(Anderson, 1989)
Glass	5.85	3.25	2.30	(Johnson & Plona, 1982)
Zeolite	6.11	3.53	2.30	(Carmichael, 1982)

Table II-2

Rock matrix properties used to match the VSP data

	v_p (km/s)	v_s (km/s)	ρ (g/cm^3)
Alluvial Fill	4.75	0.55	2.57
Tiva Canyon Tuff	4.50	0.87	2.46
Bedded Tuffs (*)	5.72	3.22	2.44
Topopah Spring Tuff	4.85 ± 0.26	1.74 ± 0.51	2.44
Vitric Zone	4.52 ± 0.20	1.28 ± 0.46	2.29
Callico Hills Formation	5.39 ± 0.34	2.54 ± 0.50	2.34
Prow Pass Tuff	5.13 ± 0.61	1.68 ± 1.15	2.48

(* Impossible to adjust for the high porosities)

Table II-3

Rock matrix properties used to match the VSP data

	v_p (km/s)	v_s (km/s)	ρ (g/cm^3)
Alluvial Fill	4.75	0.55	2.57
Tiva Canyon Tuff	4.50	0.87	2.46
Bedded Tuffs	4.98 ± 0.08	2.11 ± 0.14	2.44
Topopah Spring Tuff	4.85 ± 0.26	1.74 ± 0.51	2.44
Vitric Zone	4.52 ± 0.20	1.28 ± 0.46	2.29
Callico Hills Formation	5.39 ± 0.34	2.54 ± 0.50	2.34
Prow Pass Tuff	4.96 ± 0.38	1.56 ± 0.90	2.48

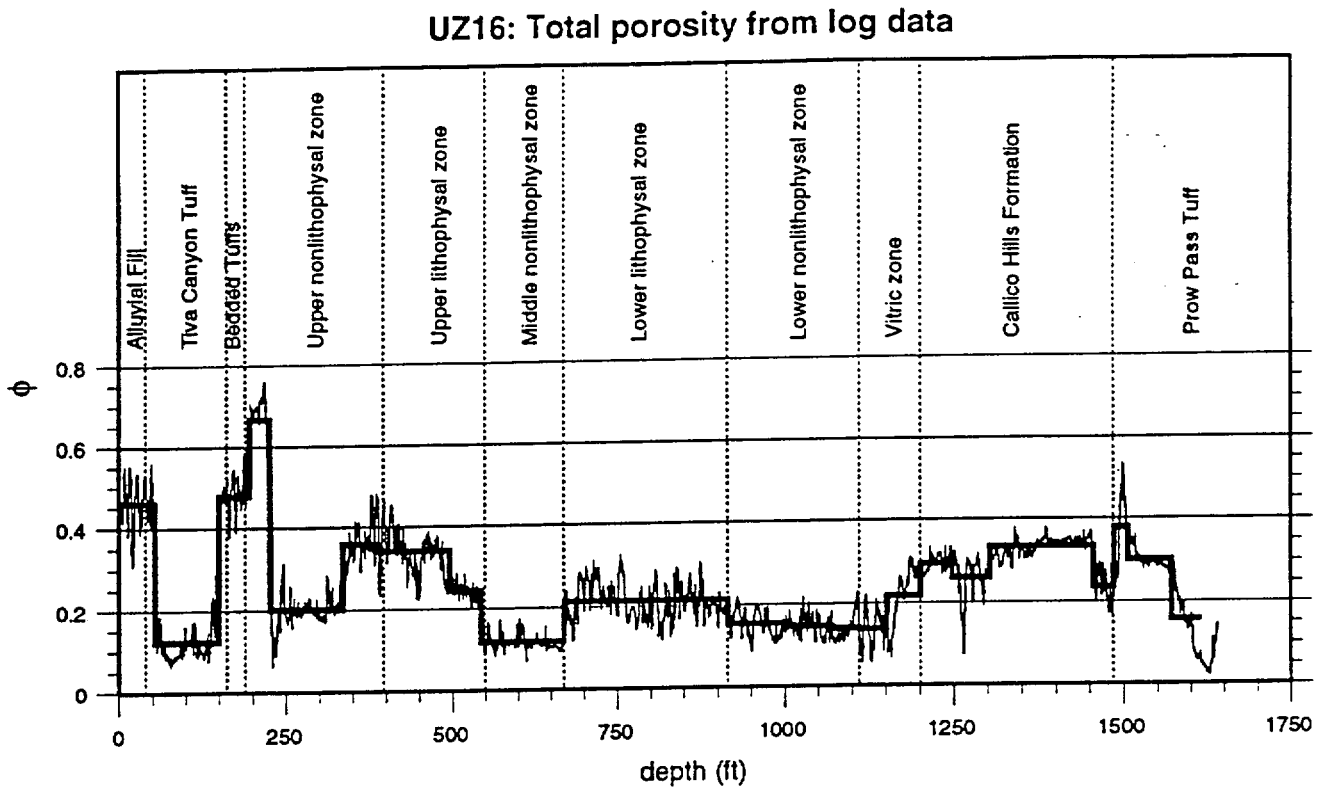

Fig. II - 1a Total porosity from the well log data in UZ 16.

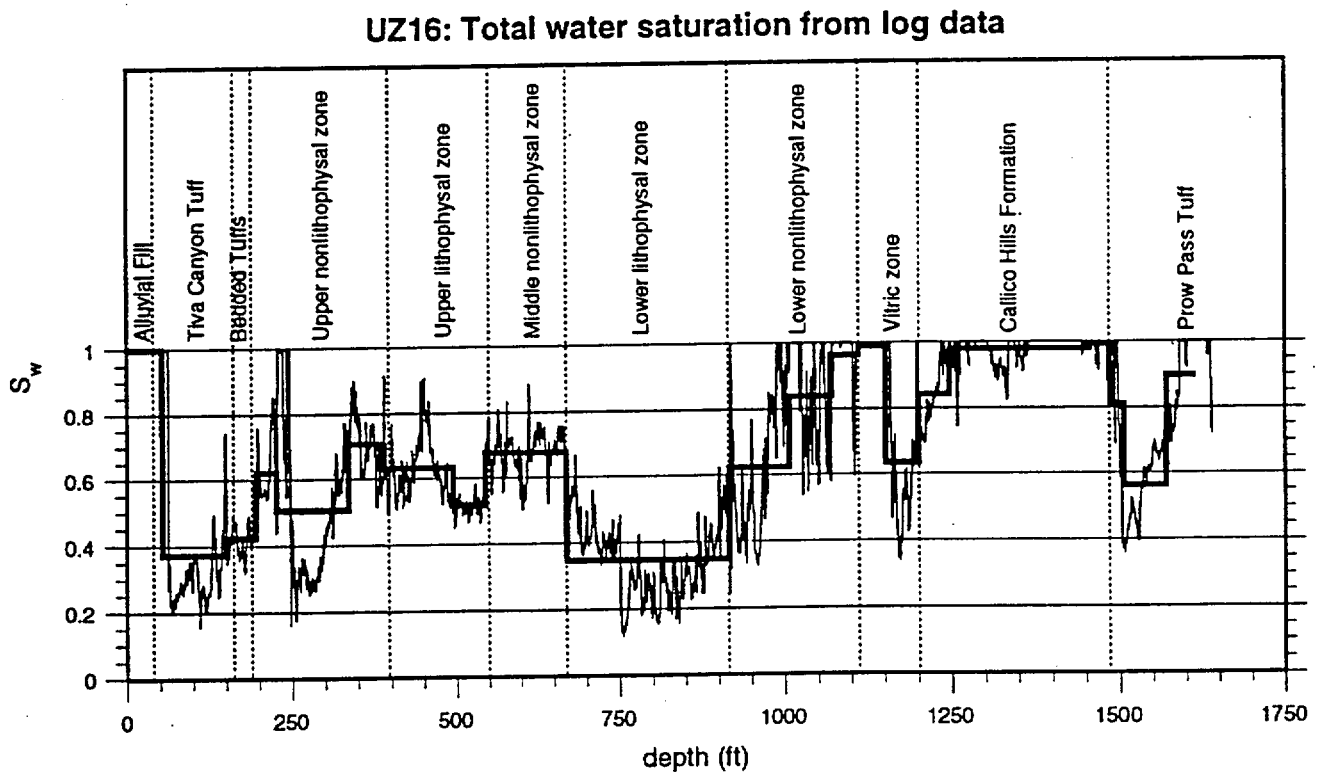

Fig. II - 1b Total water saturation from the well log data in UZ 16.

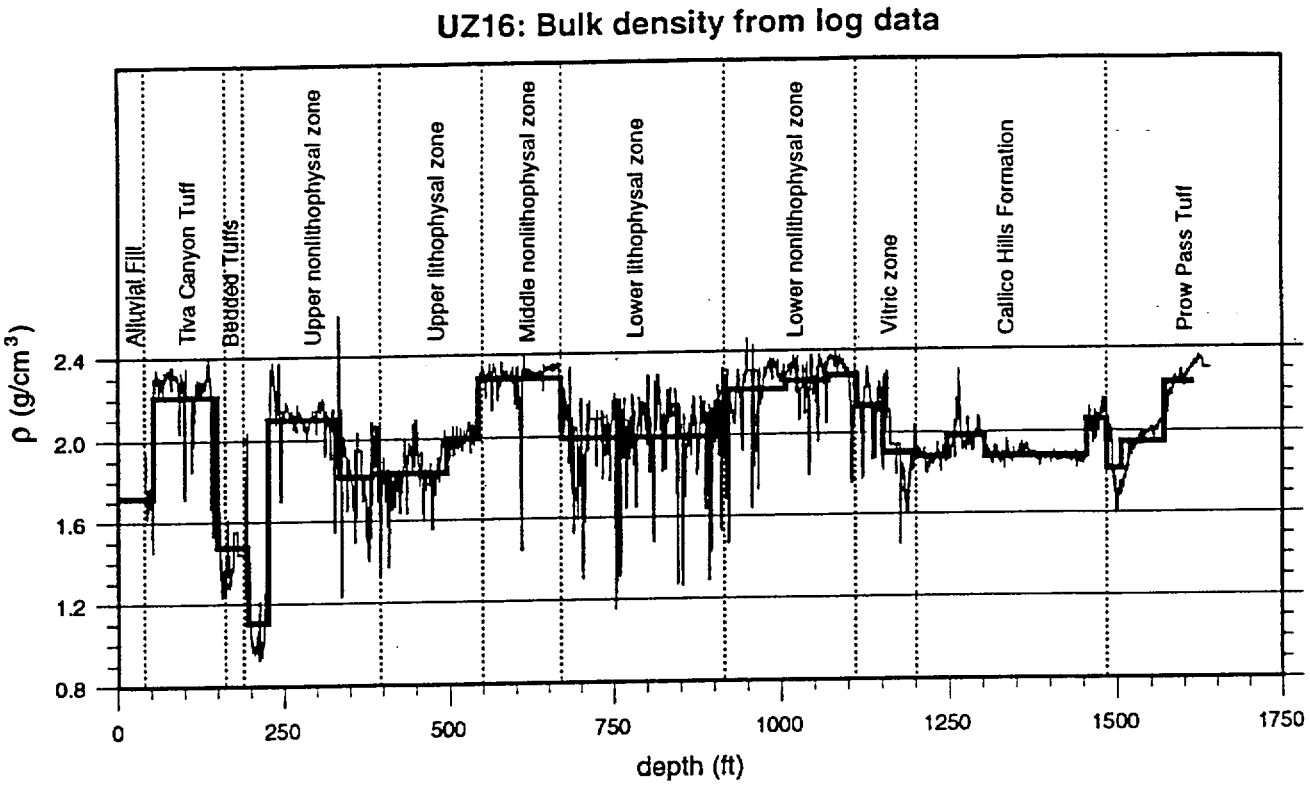

Fig. II - 1c Bulk density from the well log data in UZ 16.

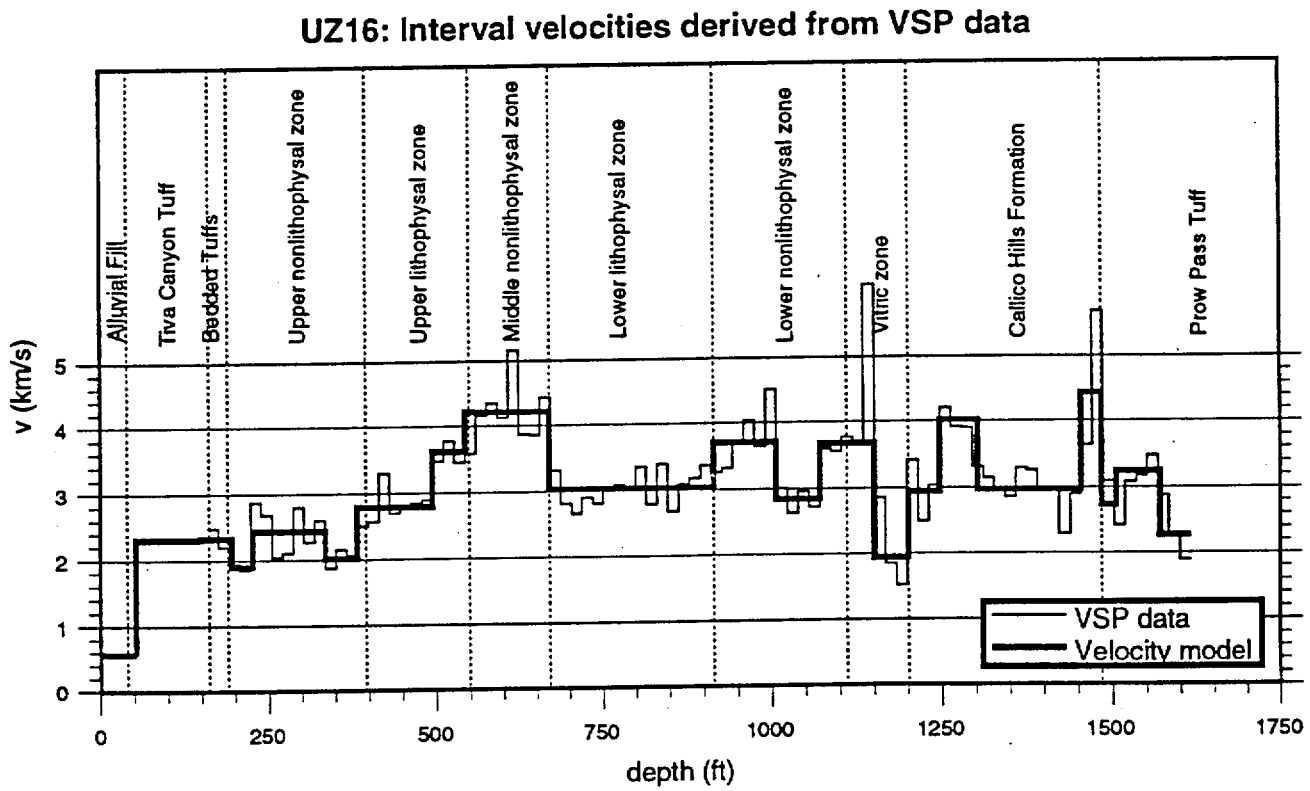

Fig. II - 2 Interval velocities derived from the VSP data in UZ 16.

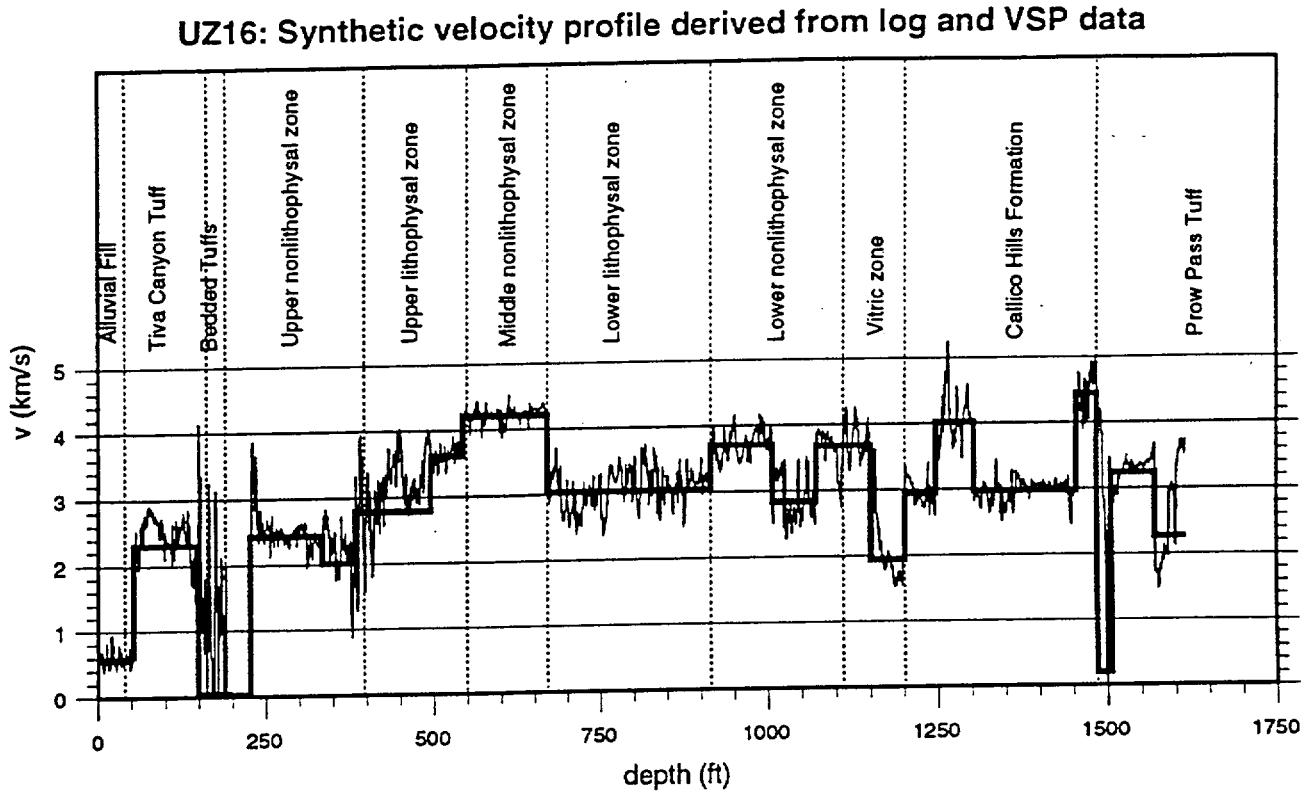

Fig. II - 3 Velocity profile computed with porosity, water saturation and the rock matrix properties.

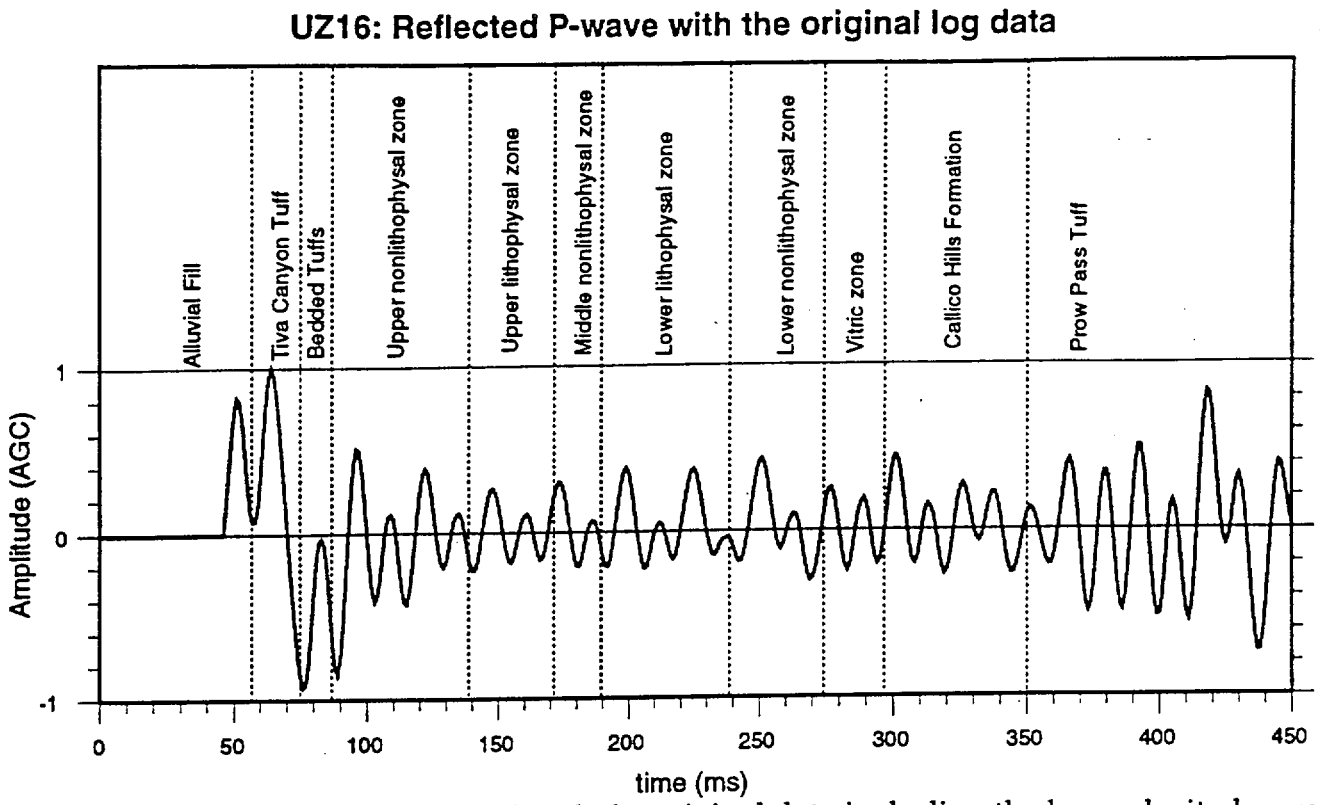

Fig. II - 4a Reflected P-wave computed with the original data including the low velocity layers but without any velocity variation within the layers.

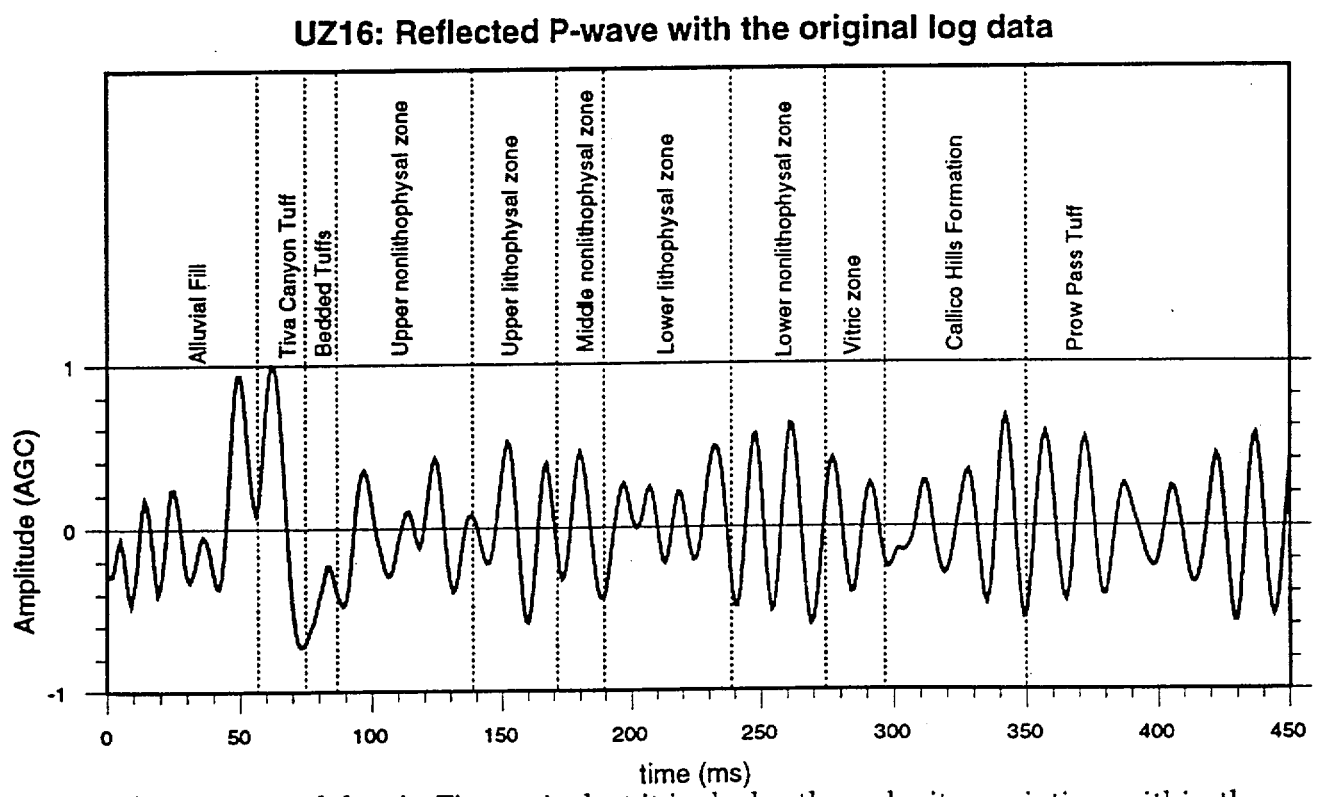

Fig. II - 4b The same model as in Figure 4a, but it includes the velocity variation within the layers.

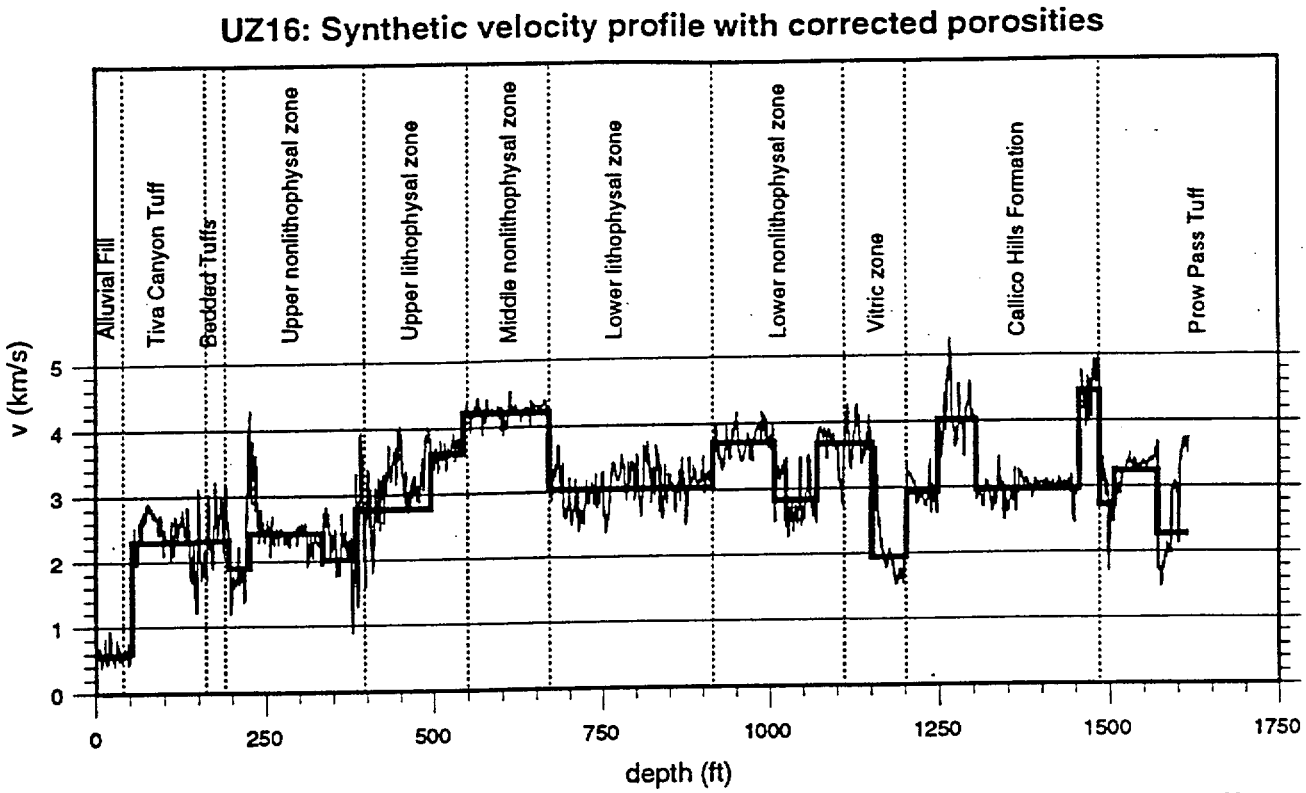

Fig. II - 5 Velocity profile computed with the corrected porosity values in the bedded tuffs and at the top of the Prow Pass Tuff.

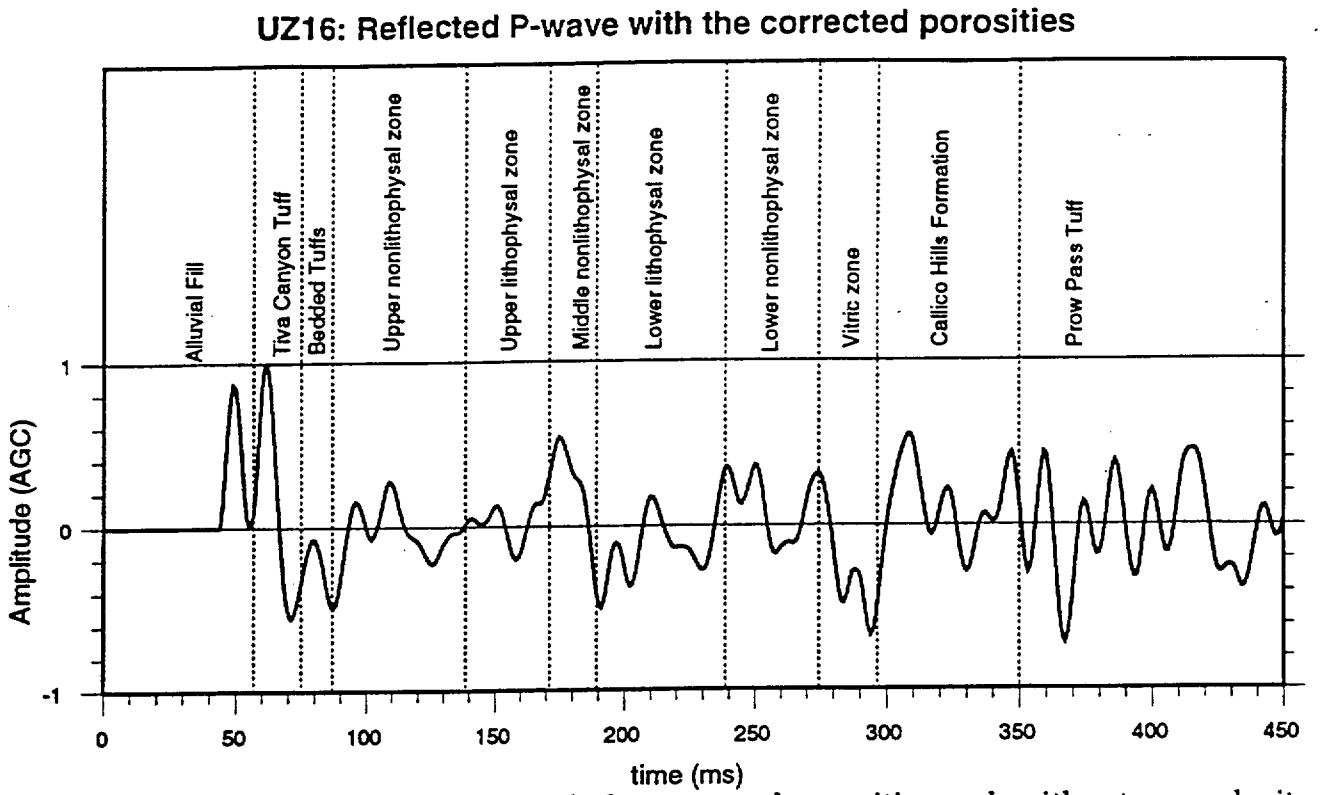

Fig. II - 6a Reflected P-wave computed with the corrected porosities and without any velocity variation within the layers.

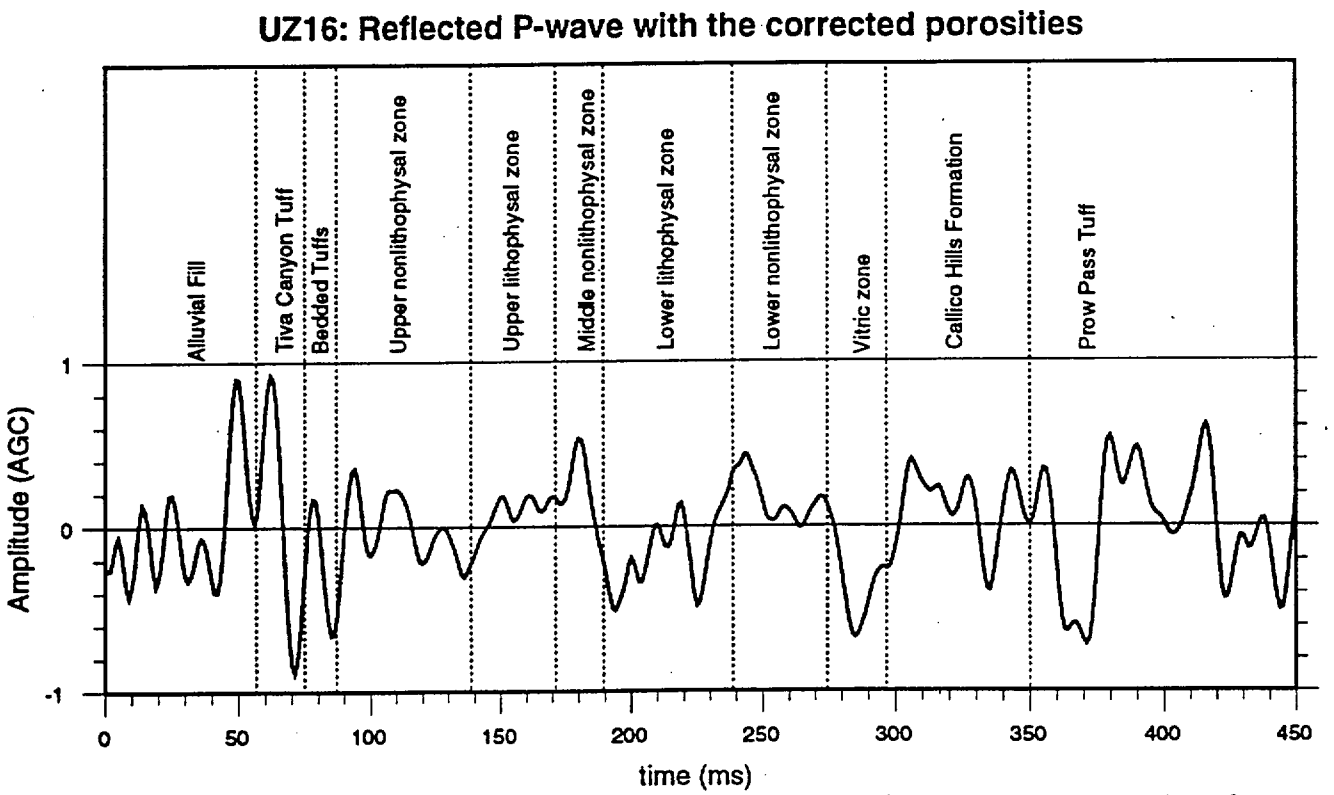

Fig. II - 6b The same model as in Figure 6a, but it includes the velocity variation within the layers.

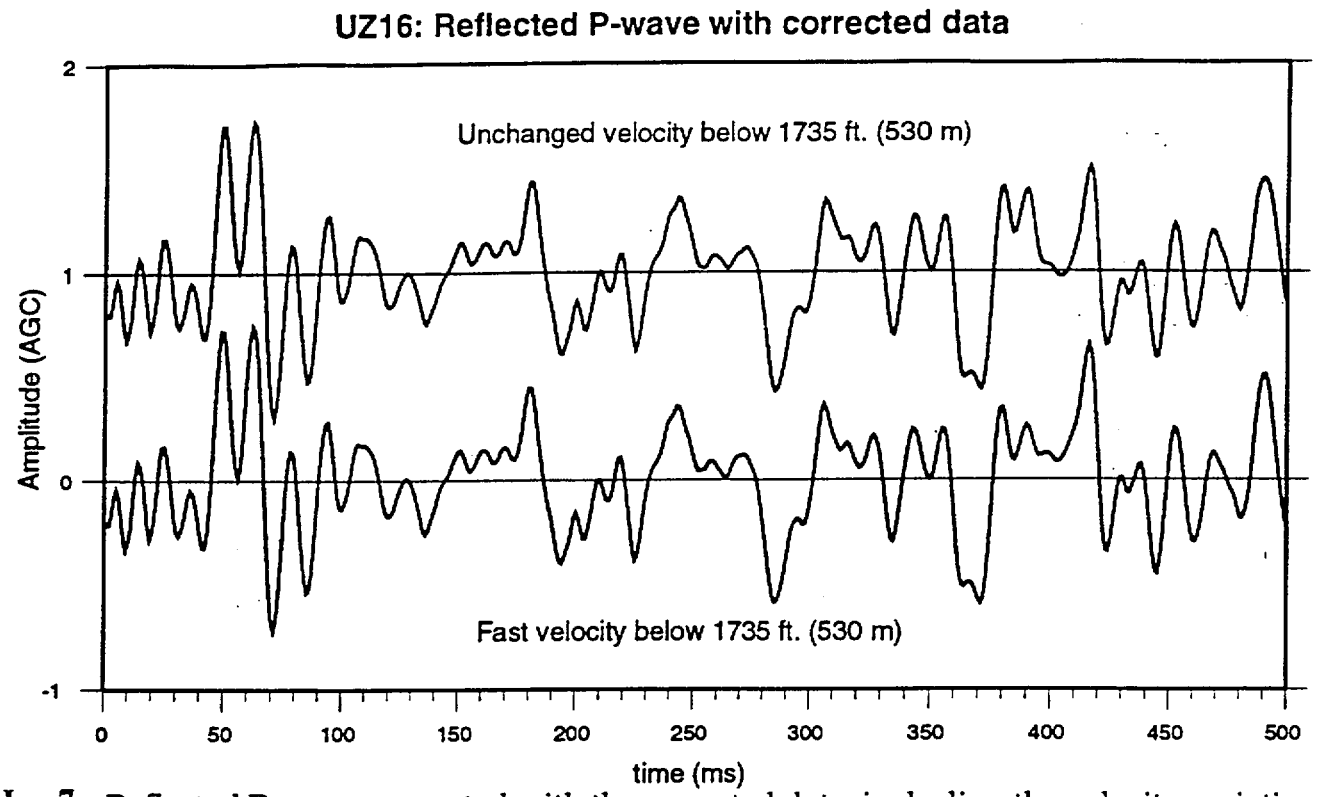

Fig. II - 7 Reflected P-wave computed with the corrected data, including the velocity variation within the layers (top) and with a hypothetical high velocity layer at the bottom of the Prow Pass Tuff..

11/26/96

DRAFT DISCLAIMER

This contractor document was prepared for the U.S. Department of Energy (DOE), but has not undergone programmatic, policy, or publication review, and is provided for information only. The document provides preliminary information that may change based on new information or analysis, and is not intended for publication or wide distribution; it is a lower level contractor document that may or may not directly contribute to a published DOE report. Although this document has undergone technical reviews at the contractor organization, it has not undergone a DOE policy review. Therefore, the views and opinions of authors expressed do not necessarily state or reflect those of the DOE. However, in the interest of the rapid transfer of information, we are providing this document for your information.

BERKELEY LAB

Earth Sciences Division

November 26, 1996

Larry R. Hayes
Scientific Programs Operations
M&O/TRW
MS 423/SU-427
101 Convention Center Drive
Las Vegas, NV 89109

QA:N/A

WBS: 1.2.3.11.2

SUBJECT: Level 4 Milestone SPT23KM4, "Results of the Analysis of the Timber Mt., Lathrop Wells, and Yucca Mt. Aeromagnetic Data" by M. A. Feighner, and E. L. Majer.

Enclosed, please find a copy of the above analysis report entitled "Results of the Analysis of the Timber Mt., Lathrop Wells, and Yucca Mt. Aeromagnetic Data." In accordance with YAP 5.1Q, this report fulfills Level 4 Milestone SPT23KM4 entitled "Geophysical Data Analysis," which describes the results of an analysis of aeromagnetic data to interpret the magnetic basement in the vicinity of Yucca Mountain.

Per YMP-LBNL-QIP 6. 1, technical reviews were performed by L. Johnson and N. Goldstein and a quality assurance review was performed by D. Mangold. No technical data have resulted from this deliverable.

Sincerely,

Joseph S. Wang
for
Gudmundur S. Bodvarsson
Head, Nuclear Waste Department
Earth Science Division

cc: GSB
Enclosure
J.Wang
N.E. Biggar
E. L. Majer
M. A. Feighner
RPC

Ernest Orlando Lawrence Berkeley National Laboratory
One Cyclotron Road | Berkeley, California 94720 | Tel: 510.486.7071 | Fax: 510.486.5686